

Politecnico di Torino

Master's degree programme in  
ENVIRONMENTAL AND LAND ENGINEERING



Urban Heat Island Mitigation in Turin: A Geospatial, 3D  
Modeling, and Climate Scenario Approach

Supervisor(s)

Dr. Matteo Bilardo

Candidate

Kiana Haghighatnejad Chobari

A.Y. 2023/2024



# Abstract

This thesis investigates the Urban Heat Island (UHI) effect in Turin, Italy, through an integrative approach that combines geospatial analysis, remote sensing, and 3D modeling to identify UHI-prone areas and propose mitigation strategies. The research employs advanced remote sensing techniques using Google Earth Engine to collect and analyze satellite imagery and temperature data, identifying regions susceptible to higher temperatures due to dense infrastructure and limited vegetation. Detailed 3D modeling using the Dragonfly plugin in Rhino software enables a comprehensive simulation of UHI dynamics under various climate scenarios. Future weather data projections, generated using the CCWorldWeatherGen tool, provide insights into the potential intensification of UHI effects by 2050 and 2080.

The study's case analysis of Turin reveals a potential increase in UHI intensity by up to 4.4°C in summer and 2.4°C in winter under a high-emission scenario. Mitigation strategies such as increasing vegetation coverage and utilizing high-albedo materials are simulated, demonstrating the ability to reduce peak surface temperatures by up to 3°C and improve thermal comfort by approximately 20%. The research framework includes a systematic comparison of multiple mitigation scenarios based on key performance indicators (KPIs) like the Universal Thermal Climate Index (UTCI), UHI intensity, Heating Degree Days (HDD), and Cooling Degree Days (CDD), offering actionable insights for urban planners and policymakers.

Overall, the findings of this study provide actionable insights for urban planners and policymakers, emphasizing the need for adaptive urban planning to mitigate UHI effects and enhance the resilience and sustainability of urban environments in the face of climate change. The study's

outcomes contribute valuable knowledge for developing effective strategies to address UHI challenges in urban settings worldwide.

**Keywords:** Climate change, Dragonfly, Mitigation, Remote sensing, Urban heat Islands (UHIs).

# Nomenclature

## Symbol

## Description

### Acronyms

UHI	Urban Heat Island
GIS	Geographic Information System
LST	Land Surface Temperature
UTCI	Universal Thermal Climate Index
EPW	EnergyPlus Weather
GEE	Google Earth Engine
RH	Relative Humidity
TIR	Thermal Infrared
CPR	Climate Prediction and Research
GCM	General Circulation Model
CC-WorldWeatherGen	Climate Change World Weather Generator
HVAC	Heating, Ventilation, and Air Conditioning

### Key Elements in Equations

T	Temperature ( $^{\circ}\text{C}$ )
RH	Relative Humidity (%)
Q	Heat quantity (J)
K	Coefficient of heat transfer ( $\text{W}/\text{m}^2 \cdot \text{K}$ )
V	Volume ( $\text{m}^3$ )
$\Delta T$	Temperature difference ( $^{\circ}\text{C}$ )
A	Area ( $\text{m}^2$ )
C	Heat capacity ( $\text{J}/\text{kg} \cdot \text{K}$ )
E	Emissivity
H	Heat flux ( $\text{W}/\text{m}^2$ )

I	Solar irradiance ( $\text{W/m}^2$ )
L	Latent heat flux ( $\text{W/m}^2$ )
R	Reflection coefficient
S	Sensible heat flux ( $\text{W/m}^2$ )
U	Wind speed ( $\text{m/s}$ )
Z	Elevation ( $\text{m}$ )
q	Specific humidity ( $\text{g/kg}$ )

# Table of content

Abstract .....	3
Nomenclature .....	5
Table of content .....	7
1 Introduction and research framework .....	12
1.1 Introduction .....	12
1.2 Research questions .....	14
1.3 Research objectives and structure .....	15
2 Literature review .....	19
2.1 Introduction to Urban Heat Islands (UHI) .....	19
2.1.1 Definition and types of UHIs .....	19
2.1.2 Factors contributing to UHIs formation .....	21
2.1.3 UHIs effects on urban environments .....	23
2.1.4 Advancements in UHIs detection methods .....	26
2.2 Remote sensing for UHI detection .....	30
2.2.1 Remote sensing and its applications .....	30
2.2.2 Key principles guiding remote sensing applications .....	32

2.3	UHI and climate change.....	34
2.3.1	Importance of climate change .....	34
2.3.2	UHI and climate change dynamics .....	35
2.3.3	Studies on UHIs effect in Italian cities .....	36
2.4	Mitigation strategies for UHIs .....	37
2.4.1	Urban planning.....	37
2.4.2	Transforming buildings.....	39
2.4.3	Vegetation and green infrastructure.....	41
2.4.4	Case studies: Cities battling UHIs and climate change .....	43
2.5	Conclusion .....	46
3	Methodology.....	48
3.1	Research design and framework .....	48
3.2	Data acquisition and software selection.....	50
3.2.1	Remote sensing data .....	50
3.2.2	Weather data .....	52
3.2.3	UHIs analysis data .....	56
3.3	UHI assessment indicators .....	58
3.3.1	Universal Thermal Climate Index (UTCI).....	58
3.3.2	Urban Heat Island Intensity (UHI Intensity) .....	60
3.3.3	Heating Degree Days (HDD) and Cooling Degree Days (CDD) .....	61



3.4	Challenges and limitations .....	62
3.5	Conclusion .....	63
4	Case study (Turin, Italy) .....	64
4.1	Geographic location and characteristics .....	64
4.2	Climate data and future trends .....	65
4.3	Turin UHI dynamics .....	73
4.4	Conclusion .....	74
5	Unveiling Urban Heat Islands in Turin .....	75
5.1	Spatially identifying UHI prone areas .....	75
5.2	In-depth analysis with Dragonfly.....	81
5.2.1	Modelling and parameterization of selected region.....	83
5.2.2	Future weather data generation.....	91
5.3	UHIs analysis result .....	91
5.3.1	Current UHIs analysis result.....	92
5.3.2	2050 UHIs analysis result .....	95
5.3.3	2080 UHIs analysis result .....	97
5.3.4	Comparison of current and future UHI effects in defined KPIs .....	99
5.4	Conclusion .....	108
6	Assessing mitigation strategies.....	110
6.1	Development of mitigation scenarios .....	110

6.2	Result of analysis .....	112
6.2.1	Scenario 1.....	112
6.2.2	Scenario 2.....	113
6.2.3	Scenario 3.....	115
6.2.4	Scenario 4.....	116
6.2.5	Scenario 5.....	118
6.3	Compare and define best scenario .....	119
6.3.1	Sensitivity analysis.....	123
6.3.2	Design explorer tool result.....	126
6.4	Conclusion .....	130
7	Conclusion .....	132
7.1	Summary of key findings.....	132
7.2	Addressing research questions .....	133
7.3	Future research directions .....	136
7.4	Limitations of the study .....	136
7.5	Final remarks .....	137
8	Appendix 1 – Script for GEE .....	139
9	Appendix 2 – Algorithm file of grasshopper.....	142
11	References.....	143



# 1 Introduction and research framework

## 1.1 Introduction

In recent years, the impacts of climate change have become increasingly undeniable, manifesting through more frequent and severe extreme weather events, rising global temperatures, and shifts in precipitation patterns (Masson et al., 2020). Among the many consequences of climate change, the Urban Heat Islands (UHIs) effect stands out as a major challenge for cities worldwide (Phelan et al., 2015a). UHIs are localized zones where temperatures are significantly higher than in surrounding rural areas, primarily due to human activities, dense urban infrastructure, and the exacerbating effects of climate change (Leal Filho et al., 2017).

The expansion of UHIs in rapidly developing cities has far-reaching negative consequences, including increased temperatures, higher energy demands, worsened air pollution, and serious public health risks ([Li 2010](#), [Santamouris 2019](#), [Grdenić 2018](#), [Vujović 2021](#)). This phenomenon is driven by a combination of factors: urban materials like concrete and asphalt that absorb and retain heat, reduced vegetative cover, and the generation of anthropogenic heat from vehicles and buildings (Deilami et al., 2018). As a result, mitigating UHI effects is not just a matter of enhancing comfort but an essential step toward creating sustainable, livable cities for the future (Z.-L. Li et al., 2020).

In this context, remote sensing emerges as a pivotal tool, offering a vantage point for monitoring and analyzing UHI phenomena. The utilization of remote sensing technologies enables the detection of temperature anomalies and facilitates the assessment of land cover characteristics that contribute to UHI effects.

Looking ahead, Climate change scenarios, derived from Climate Prediction and Research (CPR) models, play a pivotal role in projecting future climate conditions under various greenhouse gas emission trajectories. These scenarios offer plausible representations of future climatic variables such as temperature, precipitation, and humidity, essential for understanding the evolution of UHIs. Particularly the A2 and B1 SRES's future scenarios, have been shown to influence UHI formation and intensity, with the A2 scenario leading to a more pessimistic outlook (Morais et al., 2020). Such insights enable the development of targeted mitigation strategies tailored to different future climate scenarios, thereby enhancing the resilience of urban environments to the challenges posed by UHIs in a changing climate.

Turin, Italy, renowned for its historical significance and vibrant urban landscape, is no exception to the impact of UHIs. Like many other cities globally, Turin faces the detrimental effects of UHI, including increased energy consumption, elevated air pollution levels, and compromised public health. The absence of comprehensive strategies to address UHIs exacerbates these issues, posing risks to both the environment and residents (Garzena et al., 2019a).

This study seeks to address these challenges by examining the factors driving UHI formation in Turin and proposing effective mitigation strategies. By understanding the interactions between UHIs and climate change, policymakers can develop targeted interventions to mitigate their adverse effects. Additionally, the integration of remote sensing technologies enables precise identification of vulnerable areas, facilitating informed decision-making in urban planning and infrastructure development.

This research aims to contribute to urban sustainability and climate resilience efforts not only in Turin but also in similar urban settings worldwide. By elucidating the complexities of UHIs and

providing actionable insights, it strives to foster a more sustainable and resilient urban environment for current and future generations.

## 1.2 Research questions

The phenomenon of Urban Heat Islands (UHI) poses a significant challenge in urban environments, particularly as cities like Turin face increasing impacts from climate change and urbanization. This research aims to explore various aspects of UHI formation, detection, and mitigation strategies, focusing on the use of remote sensing technology and advanced modeling tools. The following key research questions have been formulated to guide the investigation:

1. **Which areas in Turin are most susceptible to UHI formation, and what are the key parameters contributing to this susceptibility?** This question explores the spatial distribution of UHI-prone areas and aims to identify critical factors such as urban morphology, land cover, and surface materials that make certain regions more vulnerable to heat accumulation.
2. **How can remote sensing technology and land cover analysis be effectively utilized to identify and characterize UHI-prone regions in Turin?** Here, we examine the role of remote sensing as a pivotal tool in detecting and analyzing UHI dynamics across the urban landscape, providing insights into temperature variations and land-use patterns.
3. **How does Dragonfly software, integrated within the Rhino environment, enhance the analysis of UHI effects and inform mitigation strategies in urban areas?** This question focuses on the utility of advanced 3D modeling and simulation software in assessing UHI impacts and evaluating potential intervention strategies within complex urban environments.

4. **What will be the impact of climate change, specifically under the GCM<sup>1</sup> Climate Change Scenarios, on UHI-prone areas in Turin across different time frames?**

Considering future climate projections, this question addresses how UHI effects may intensify or shift over time, providing a framework for long-term urban resilience planning.

5. **Which mitigation strategies are most effective in reducing UHI effects in Turin under current and future climate conditions, and what practical insights can this research provide to urban planners and policymakers?** This final question synthesizes the findings and evaluates practical solutions to reduce UHI intensity, offering actionable recommendations for sustainable urban planning.

These research questions form the foundation for a comprehensive analysis of UHI formation, detection, and mitigation in Turin. Section 7.2 will revisit these questions, offering detailed answers based on the research findings. By integrating the results from various stages of analysis, Section 7.2 will provide a conclusive assessment of the strategies and technologies that are most effective in addressing UHI challenges. This section serves as a critical point of reflection, where the theoretical inquiries raised here are systematically addressed using empirical data and modeling outcomes.

## 1.3 Research objectives and structure

This research is driven by the need to understand and mitigate the impacts of UHI in Turin, Italy. To achieve this, the study integrates various analytical tools and methods, combining remote

---

<sup>1</sup> It uses **Intergovernmental Panel on Climate Change (IPCC) Third Assessment Report** model summary data of the HadCM3 A2 experiment ensemble

sensing technologies, advanced modeling, and climate change projections. The following objectives outline the key goals of this research, which collectively aim to provide a detailed assessment of UHI dynamics and propose actionable solutions.

First, this study seeks to **identify UHI-prone areas** in Turin using remote sensing techniques. By leveraging satellite data and land cover analysis, it will be possible to map regions that are particularly susceptible to the formation of UHIs, thus establishing a foundation for further investigation.

Building upon this, the next objective is to **analyze the parameters contributing to UHI formation** in these identified regions. Using the Dragonfly plugin within Rhino software, the research will model critical factors such as urban morphology, surface materials, and heat transfer mechanisms, providing a comprehensive understanding of how and why UHIs emerge in specific areas.

Another important aim is to **assess the impact of climate change** on UHI-prone regions. By employing General Circulation Models (GCM) Climate Change Scenarios, the study will project how UHI effects are likely to evolve under different future conditions, focusing on three distinct time periods. This will enable the development of long-term strategies to combat the growing intensity of UHIs due to climate change.

To address the ongoing challenge, this research will also **propose mitigation strategies**. These solutions will encompass both qualitative and quantitative approaches, focusing on urban planning interventions, building modifications, and the enhancement of green spaces. The goal is to identify ways to reduce heat accumulation, improve thermal comfort, and increase the overall resilience of Turin's urban environment.



Finally, the research aims to **provide valuable insights for urban planners and policymakers**. By offering evidence-based recommendations, the study will inform decision-making processes related to UHI mitigation, ensuring that the solutions proposed are both practical and effective in enhancing urban sustainability and resilience.

Although the focus of this study is Turin, the findings and methodologies developed here can be applied to other urban settings facing similar UHI challenges. However, the research also acknowledges certain limitations, including data availability, technological constraints, and the inherent complexity of urban systems. Despite these challenges, the study endeavors to offer a robust analysis of UHI dynamics and mitigation strategies, contributing to both local and global efforts in climate resilience.

Regarding Thesis Organization Table 1 presents an organized overview of chapters, outlining important elements and subject areas.

*Table 1: Thesis organization*

<i>Chapter</i>	<i>Content</i>
<i>Chapter 1: Introduction</i>	Background, problem statement, research objectives and questions and significance of the study.
<i>Chapter 2: Literature Review</i>	Review of existing literature on UHIs dynamics, factors contributing to UHIs formation, remote sensing techniques, mitigation strategies, and climate change interactions.
<i>Chapter 3: Methodology</i>	Research design, data collection (remote sensing, modeling, projections), climate change scenarios, tools (Dragonfly, Rhino, CCWorldWeatherGen), limitations, and challenges.
<i>Chapter 4: Case Study (Turin)</i>	Detailed analysis of Turin, geographic and climatic characteristics, future climate trends, UHI dynamics, and a spatial analysis of UHI-prone areas.
<i>Chapter 5: Results and Discussion</i>	Presentation of UHI analysis results, current and future UHI projections, comparative evaluation of UHI mitigation strategies based on key performance indicators (UTCI, HDD, CDD), and recommendations.

<i>Chapter 6: Assessing Mitigation Strategies</i>	Development of various mitigation scenarios (vegetation, high-albedo materials, mixed strategies), analysis, and effectiveness comparison for the present and future periods (2050 and 2080).
<i>Chapter 7: Conclusion</i>	Summary of key findings, addressing research questions, policy implications for UHI mitigation, suggestions for future research, and final remarks.

Also, worth mentioning that as shown in Figure 1, at first, this research methodology primarily utilizes remote sensing to detect high-temperature areas. Subsequently, it analyzes a selected area to identify UHIs. Following this, future scenarios, particularly the worst-case scenario for the year 2050 and 2080, will be examined. Finally, several scenarios aimed at mitigating the effects of climate change will be proposed and analyzed again to arrive at a final decision.

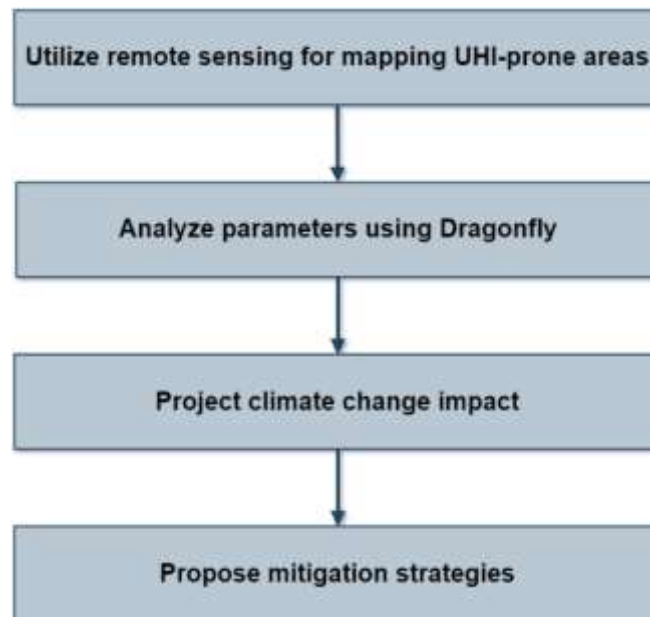


*Figure 1: Research overall framework*

## 2 Literature review

This chapter explores the UHIs effect and its growing significance due to urbanization and climate change. It begins by defining UHIs and explaining their importance in the context of urban environments. The literature review distinguishes between **surface UHIs**, related to heat absorbed by urban materials, and **atmospheric UHIs**, which involve elevated air temperatures due to human activities and city infrastructure.

The chapter further examines the **factors contributing to UHI formation**, including urban materials, reduced vegetation, and city layout. It also highlights the use of **remote sensing technologies** for detecting UHI-prone areas, which is crucial for planning mitigation strategies.

The connection between **climate change and UHI dynamics** is discussed, emphasizing how climate change intensifies UHI effects, particularly in Italian cities like Turin. Finally, the review evaluates **mitigation strategies** such as green infrastructure, building designs, and urban planning interventions, with insights drawn from global case studies of cities addressing UHIs.

### 2.1 Introduction to Urban Heat Islands (UHI)

#### 2.1.1 Definition and types of UHIs

UHIs refer to the phenomenon where urban areas experience higher temperatures compared to their surrounding rural regions due to human activities, urban infrastructure, and climate change (Garzena et al., 2019a). The definition of UHIs has evolved, encompassing not only temperature differentials but also variations in air quality, energy consumption, and ecosystem health within urban environments (Mirzaei & Haghighat, 2010).

Historical context reveals that UHIs research gained momentum in the late 20th and early 21st centuries as urbanization accelerated and its impacts on climate and environment became more pronounced (Ulpiani, 2021). Studies by SARRAT et al. (2006) laid the groundwork for understanding UHIs dynamics, emphasizing the role of surface materials, urban morphology, and land use patterns in exacerbating heat accumulation in cities. Today, UHIs are recognized as a global environmental challenge, with cities across the world facing the consequences of elevated temperatures and associated impacts on human health, energy consumption, and urban ecosystems (Masson et al., 2020).

There are two main types of UHIs:

**Surface Urban Heat Island:** Surface UHI occurs when urban surfaces such as roads, buildings, and pavements absorb and retain heat during the day and release it slowly at night, leading to elevated surface temperatures within the city compared to nearby rural areas. The materials used in urban infrastructure, such as concrete and asphalt, have higher heat-absorbing capacities than natural surfaces like vegetation and soil, exacerbating the heat island effect (Mohajerani et al., 2017). Remote sensing, particularly using data from satellites like Landsat, is commonly employed to detect this type of UHIs (Kwofie et al., 2022).

**Atmospheric Urban Heat Island:** Atmospheric UHI refers to the elevated air temperatures experienced within urban areas due to various factors such as emissions from vehicles and industrial activities, reduced vegetation cover, and the presence of tall buildings that obstruct airflow. These factors can lead to the formation of urban heat domes, where warm air becomes trapped within the city, further raising atmospheric temperatures (Deilami et al., 2018).

Surface temperatures vary more than air temperatures during the day but are more pronounced after sunset due to the slow release of heat from impervious surfaces. This phenomenon contributes to the persistence of the surface UHIs effect, as urban surfaces continue to emit stored heat into the surrounding environment during the night, maintaining elevated temperatures compared to rural areas (Phelan et al., 2015a) (Phelan et al., 2015b). Recognizing this, the research also focused on analyzing UHI effects during nighttime to capture the full extent of urban heat retention.

### 2.1.2 Factors contributing to UHIs formation

UHIs form due to various influences, including urbanization and changes in land use, the arrangement of built structures, weather patterns, and atmospheric conditions. These factors, collectively, contribute to the increased temperature and heat intensity experienced in urban areas (RIZWAN et al., 2008).

**Urbanization and Land Use Changes:** The expansion of urban areas alters the landscape, replacing natural vegetation with impermeable surfaces like concrete and asphalt. This transformation reduces vegetation cover, which plays a crucial role in regulating temperatures by providing shade and evaporative cooling (Phelan et al., 2015a).

The design and layout of buildings, roads, and other urban infrastructure affect the exchange of heat within cities. Urban structures can trap heat, restrict airflow, and create localized warm pockets, contributing to the intensification of UHIs effects (Andoni & Wonorahardjo, 2018). This has implications for building energy consumption, particularly during heatwaves (Heaviside et al., 2017). Additionally, the role of haze pollution in enhancing the UHI in China has been highlighted, with potential co-benefits of reducing heat stress through haze mitigation (Cao et al., 2016).

**Weather Conditions and Atmospheric Factors:** Meteorological elements such as clear skies, low wind speeds, and high humidity exacerbate UHIs effects by enhancing the absorption of solar radiation and impeding the dispersion of heat. These conditions create favorable environments for the amplification of temperature differentials between urban and rural areas (Sangiorgio et al., 2020).

**Heat Waves:** Periods of prolonged heatwaves and extreme heat events further magnify UHIs effects, exacerbating temperature disparities between urban and rural regions. Such events pose significant health risks to urban populations, particularly vulnerable groups, by increasing the likelihood of heat-related illnesses and heat-related mortality (Ulpiani, 2021).

The combination of these factors intensifies the heat retained in urban environments, making cities much warmer than their rural surroundings. Recognizing how these elements interact is key to crafting solutions that can help cool cities and improve the well-being of their residents. The Summary of factors contributing to UHI formation is provided in Table 2.

*Table 2: Summary of factors contributing to UHI formation*

<b>Factor</b>	<b>Description</b>	<b>Implications</b>	<b>Potential Solutions</b>
<b>Urban Materials</b>	Impervious surfaces like concrete and asphalt absorb and retain heat.	Leads to increased surface temperatures, especially in dense urban areas.	Use of cool materials, high-albedo surfaces, and green infrastructure (e.g., green roofs).
<b>Anthropogenic Heat</b>	Heat generated from human activities such as transportation, industrial processes, and HVAC systems.	Adds to overall urban heat, increasing energy demand and worsening air quality.	Promote energy-efficient systems, reduce traffic congestion, and encourage public transport.
<b>Reduced Vegetation</b>	Less greenery results in lower evapotranspiration, leading to higher surface temperatures.	Loss of natural cooling mechanisms increases discomfort and energy consumption for cooling.	Increase green spaces, urban tree planting, and vertical gardens.
<b>City Layout</b>	Urban design can trap heat (heat islands) and restrict airflow, exacerbating heat retention.	Reduced airflow increases heat stress and reduces outdoor comfort.	Incorporate natural ventilation in urban planning, design for wind corridors, and provide shade.

### 2.1.3 UHIs effects on urban environments

Exploring the multifaceted impacts of UHIs, this section delves into their profound implications across health, environment, economics, and society. From exacerbating heat-related illnesses to reshaping ecosystems and straining social cohesion, UHIs pose complex challenges demanding comprehensive solutions.

**Health Impacts of UHIs:** Elevated temperatures in urban areas can exacerbate heat-related illnesses such as heat exhaustion, heatstroke, and respiratory problems. Vulnerable populations, including the elderly, children, and individuals with pre-existing health conditions, are particularly susceptible to these adverse health effects. In Shanghai, the UHI effect has led to more hot days and heat waves, contributing to increased heat-related mortality (Tan et al., 2010). Therefore, it is crucial to implement heat-mitigation and adaptation strategies in urban planning to protect public health and improve overall well-being in cities (Dong et al., 2020).

**Environmental Consequences:** UHIs contribute to changes in local ecosystems, leading to alterations in biodiversity, vegetation patterns, and wildlife habitats. Additionally, higher temperatures can exacerbate air and water pollution levels, further degrading environmental quality and impacting ecosystem health (Phelan et al., 2015).

One consequence is the alteration of biodiversity, vegetation patterns, and wildlife habitats within urban areas. Higher temperatures associated with UHIs can disrupt the natural balance of ecosystems, leading to shifts in the types and distribution of plant and animal species. This can result in changes to the composition and diversity of local flora and fauna, potentially leading to the displacement or decline of certain species (Maggiotto et al., 2021; Ulpiani, 2021).

Moreover, UHIs can exacerbate air and water pollution levels, further compromising environmental quality and ecosystem health. Elevated temperatures can enhance the formation of ground-level ozone and other air pollutants, which can have detrimental effects on human health and ecological systems (Di Sabatino et al., 2020; Noro & Lazzarin, 2015a). Additionally, increased temperatures can accelerate chemical reactions that contribute to the production of pollutants such as smog and particulate matter. In water bodies, higher temperatures can reduce oxygen levels and promote the growth of harmful algae blooms, impacting aquatic ecosystems and biodiversity (Leal Filho et al., 2017).

**Economic Implications:** UHIs generate several economic burdens, including heightened energy consumption for cooling, which escalates bills and operating expenses for households and businesses (RIZWAN et al., 2008b).. Additionally, extreme heat events decrease labor productivity due to worker discomfort and health issues, thereby reducing efficiency and output (Guattari et al., 2018).. The rise in heat-related illnesses as a result of UHIs imposes additional costs on healthcare systems and individuals for treatment and management (Leal Filho et al., 2017). Moreover, UHI-affected areas experience decreased property values due to discomfort and health risks, leading to diminished demand and declining real estate values (Battista et al., 2020). Finally, UHIs inflict damage on infrastructure like roads and buildings, incurring increased maintenance and repair costs due to the expansion and contraction caused by extreme temperatures (Phelan et al., 2015).

**Social and Community Considerations:** Social and community considerations related to (UHIs) encompass several key aspects.

In terms of social life, UHIs can exacerbate social inequalities by disproportionately impacting vulnerable populations with limited access to cooling resources and healthcare services.



Marginalized communities, including low-income neighborhoods and elderly individuals, often bear the brunt of UHIs effects, facing greater risks of heat-related illnesses and discomfort. Additionally, during extreme heat events, social cohesion and community resilience may be strained as residents struggle to cope with the challenges posed by high temperatures (Battista et al., 2020).

Moreover, UHIs can influence social interactions and community engagement, particularly during periods of prolonged heatwaves. The discomfort and health risks associated with UHIs may deter outdoor activities and gatherings, limiting opportunities for social connection and recreation. This can lead to increased social isolation and decreased community engagement, impacting overall well-being and cohesion within urban neighborhoods (Pioppi et al., 2020).

*Table 3: Summary of UHI Effects on Urban Environments*

Category	Impacts	Implications	Potential Solutions
<b>Health</b>	Increased risk of heat-related illnesses (heatstroke, respiratory issues), especially for vulnerable populations.	Higher mortality rates during heat waves, increased hospital admissions, and reduced quality of life.	Implement cooling centers, improve urban shading, and increase green infrastructure.
<b>Environmental</b>	Altered ecosystems, reduced biodiversity, increased pollution (air and water).	Damage to urban ecosystems, rise in ground-level ozone, and loss of flora and fauna.	Expand green infrastructure, improve water management systems, and reduce emissions.
<b>Economic</b>	Increased energy consumption for cooling, higher healthcare costs, reduced property values in UHI-affected areas.	Strain on energy grids, economic losses for businesses, and a rise in operational costs for cities.	Enhance building energy efficiency, use of cool roofing, and tax incentives for green designs.
<b>Social and Community</b>	Exacerbates inequalities, decreases outdoor social interaction, and leads to greater isolation during heat events.	Marginalized communities face higher heat risks due to lack of resources (e.g., air conditioning).	Improve community outreach, invest in cooling resources for vulnerable populations.

#### 2.1.4 Advancements in UHIs detection methods

The evolution of UHIs detection techniques has seen significant advancements in recent years

1. **Infrared Thermography:** Measures surface temperatures using infrared cameras, which can detect heat emissions from urban surfaces. Software packages such as FLIR Tools and Testo IRSoft are used for infrared image analysis (Martin et al., 2022). Infrared thermography has been widely used in UHIs studies, with Chui et al. (2018) demonstrating its effectiveness in measuring near-surface temperatures. Meola et al. (2016) further highlights its diverse applications, including in thermo-fluid-dynamics, materials inspection, cultural heritage, and preventative maintenance. The technology has also been applied in astronomy and space exploration, as seen in Okada et al. (2020) work on thermal infrared cameras. Nardi further enhances UHIs detection by discussing the use of infrared thermography for evaluating energy leakages through building envelopes, which is crucial for UHIs mitigation measures (Nardi et al., 2018).
2. **Time-Series Analysis:** Examines temporal trends in air temperature data collected over multiple time intervals to identify changes in UHIs characteristics. Software like MATLAB, R, and Python with libraries such as Pandas and NumPy are commonly used for time-series analysis (Zhang et al., 2018). Time-Series Analysis and Change Detection involve the systematic examination of temporal trends and patterns in temperature data to discern changes in UHIs characteristics over time. This is done by analyzing sequential thermal imagery captured at different time intervals, through which researchers can track UHIs dynamics, assess seasonal variations, and identify long-term trends in UHIs intensity as well as spatial extent (Zhou et al., 2018). A range of studies have explored the use of time-series analysis and change detection in tracking UHIs dynamics. Wong found that

UHIs intensity varies throughout the day and is influenced by factors such as solar radiation and greenery density (Paulina et al., 2015) Ghaderpour provided a comprehensive review of time-series analysis and change detection techniques, highlighting their application in various fields (Ghaderpour et al., 2021). Chatfield discussed practical developments in time-series analysis, including the treatment of trend and seasonality, which are relevant to the study of UHIs characteristics over time (Chatfield, 1977).

3. **3D Mapping:** Visualizes the morphology and spatial distribution of UHIs in three-dimensional space, providing insights into their vertical structure. Software packages such as ArcGIS 3D Analyst and Blender are commonly used for 3D mapping of UHIs. Emerging Trends in UHIs Monitoring include innovative approaches like 3D mapping and hyperspectral imagery, offering improved spatial and spectral resolution for UHIs characterization. Three-dimensional mapping techniques visualize UHIs morphology and spatial distribution in 3D space, providing insights into the vertical structure of UHIs. Hyperspectral imagery detects subtle spectral signatures associated with UHIs, allowing more precise discrimination between urban and non-urban land cover types (Sidiqui et al., 2022). The use of 3D mapping and hyperspectral imagery in UHIs monitoring is a rapidly evolving field. Falco et al. (2015) and Marinoni et al. (2019) both highlight the potential of these technologies in accurately classifying land cover and monitoring human settlements and infrastructure. Roessner et al. (2011) further emphasizes the need for automated methods to extract information from hyperspectral imagery, particularly in the context of urban areas with diverse materials and structures. Weber et al. (2018) underscores the importance of defining the type of information that can be obtained from different sensors, and the potential of high-resolution hyperspectral imagery in characterizing urban land

surface properties. These studies collectively demonstrate the significant advancements in UHIs monitoring using 3D mapping and hyperspectral imagery.

4. **Machine Learning and Artificial Intelligence:** Machine Learning and Artificial Intelligence for UHIs Identification represent a significant change in detecting UHI, utilizing computational algorithms and data-driven models to automate the identification process. Machine learning techniques allow for extracting complex patterns from large-scale thermal datasets, leading to more precise UHIs mapping and analysis (Bahi et al., 2020). Software frameworks such as TensorFlow, PyTorch, and scikit-learn are commonly used for implementing machine learning algorithms (Weng et al., 2004). For instance, Medaiyese et al. (2022) applied wavelet transform analytics and machine learning algorithms for RF-based UAV detection and identification demonstrate the potential of machine learning and artificial intelligence for identification tasks, with applications in security, cybersecurity, and human behavior recognition. Machine learning and artificial intelligence algorithms for UHIs identification utilize thermal imagery, land cover data, geospatial information, meteorological data, and historical records. By analyzing these diverse datasets, algorithms automate UHI detection, providing precise mapping and analysis crucial for urban planning and climate resilience efforts (Bahi et al., 2020).
5. **Remote Sensing:** Utilizes satellite or aerial imagery to capture thermal data and detect temperature variations associated with UHIs (which will be explained in more detail in next section). While all techniques are valuable, remote sensing is particularly advantageous due to its ability to provide comprehensive and large-scale coverage of urban areas. It offers a wide range of spectral and spatial resolutions, allowing for detailed analysis of UHIs dynamics over large geographic regions. Additionally, remote sensing

data can be readily integrated with geographic information systems (GIS) for spatial analysis and visualization (Weng, 2009). In Table 4 the summery of detection methods, quantities detected and whether surface of air temperature can be detected are provided.

*Table 4: Summery table of findings in area of advancement in UHI detection methods*

<b>Detection Method</b>	<b>Quantities Detected</b>	<b>Type of UHI Detected</b>
<b>Infrared Thermography</b>	Surface temperatures, heat loss, thermal anomalies	Surface UHI
<b>Time-Series Analysis</b>	Temporal trends in air temperature	Both surface and air UHI
<b>3D Mapping</b>	Morphology and spatial distribution of UHIs Vertical structure of UHIs	Both surface and air UHI
<b>Remote Sensing</b>	Thermal data, temperature variations Spectral and spatial resolutions	Both surface temperature variations (surface UHI) and other types of temperature-related data, which may include air temperature (air UHI)

In conclusion, Given the diverse array of techniques discussed for UHIs detection, the utilization of remote sensing emerges as a potent tool for assessing the impact of climate change and devising mitigation strategies in urban environments. In the context of this research project on UHIs mitigation, we aim to leverage remote sensing technologies to analyze temperature patterns, land cover dynamics, and spatial variations, thereby contributing to effective urban planning and sustainable development efforts.

## 2.2 Remote sensing for UHI detection

### 2.2.1 Remote sensing and its applications

Remote Sensing for UHIs Detection and Monitoring involves utilizing various principles and techniques to accurately assess temperature variations and land cover characteristics in urban areas.

Remote sensing encompasses the gathering and analysis of data from a distance, typically employing sensors aboard satellites or aircraft, without direct physical contact. This process hinges on detecting and measuring electromagnetic radiation emitted or reflected by the Earth's surface to gather information about objects or phenomena (Z.-L. Li et al., 2020).

These remote sensing instruments capture electromagnetic radiation across different wavelengths, spanning from visible light to thermal infrared. Each wavelength offers unique insights into the target area, enabling the identification of specific features or characteristics (Yaoyu Lin et al., 2009a).

As electromagnetic energy interacts with the Earth's surface, it undergoes various processes such as absorption, reflection, and emission. Different surface materials exhibit distinct spectral signatures, allowing remote sensors to distinguish between various land cover types (Voogt & Oke, 2003).

This technology has numerous applications across various fields, Mertikas et al. (2021) highlights its role in environmental monitoring, including weather forecasting and pollution detection. Q. Zhou (2023) further discusses its use in monitoring vegetation, soil, water resources, and geology. EBERT (1984) and Saibi et al. (2018) both emphasize its significance in archaeology and

geoscience, respectively, for mapping, exploration, and hazard analysis. Li introduces a new method for quantifying UHIs intensity using the relationship between MODIS land surface temperature and impervious surface areas, improving the reliability of UHIs detection which also is based on remote sensing (H. Li et al., 2018). Moreover, Weng (2009) has introduced methods for characterizing and modeling UHIs using remotely sensed land surface temperature data, including a kernel convolution modeling method and object-based image analysis.

Satellite-based thermal imagery, particularly from sensors like MODIS and Landsat, has been instrumental in monitoring UHIs (Kaya et al., 2012; Keramitsoglou et al., 2011; Pongrácz et al., 2010). These sensors have been used to extract and analyze thermal patterns, identify UHIs boundaries, and assess the relationship between urban growth and UHIs (Kaya et al., 2012; Keramitsoglou et al., 2011). The data from these sensors has also been used to understand the physical content of different satellite-based parameters and analyze the impact of land development on UHIs (Pongrácz et al., 2010).

The application of satellite imagery in temperature measurements, particularly in identifying and analyzing UHIs, is a focal point of this research. Through the interpretation and analysis of thermal data obtained from satellite images, areas experiencing elevated temperatures characteristic of UHIs are pinpointed. This analysis involves identifying thermal anomalies and comparing temperature variations across different land cover types and urban settings.

Therefore, remote sensing enables precise UHI detection by analyzing temperature and land cover, which is vital for urban climate studies and planning.

### 2.2.2 Key principles guiding remote sensing applications

Remote sensing applications are guided by principles such as spectral signature analysis, spatial resolution, and radiometric and geometric corrections. These principles ensure the accuracy and reliability of remote sensing data for subsequent analysis (Yaoyu Lin et al., 2009).

**Passive vs. Active Remote Sensing:** Passive remote sensing relies on naturally occurring electromagnetic radiation, such as sunlight, while active remote sensing involves emitting and receiving signals to measure properties of the target area, such as radar imaging (Weng, 2009).

**Spectral and Spatial Resolution:** Spectral resolution refers to the ability of remote sensors to distinguish between different wavelengths of electromagnetic radiation. Spatial resolution, on the other hand, refers to the level of detail or spatial clarity in the imagery captured by remote sensors (Z.-L. Li et al., 2020).

**Radiometric and Geometric Corrections:** Radiometric corrections adjust remote sensing data for factors such as sensor calibration and atmospheric interference, ensuring consistency and accuracy. Geometric corrections rectify distortions in remote sensing imagery caused by factors such as terrain variations and sensor positioning (Zhou et al., 2018).

**Temporal Resolution:** Temporal resolution refers to the frequency at which data is captured over a specific area. It is crucial for monitoring changes over time, such as seasonal variations, vegetation growth, and land use dynamics. Higher temporal resolution allows for more frequent updates and better tracking of dynamic processes (Wang et al., 2023).

**Sensor Fusion:** Sensor fusion involves integrating data from multiple sensors with different characteristics to improve the overall quality and information content of remote sensing data. By combining data from sensors with different spectral, spatial, and temporal resolutions, researchers



can obtain a more comprehensive understanding of the target area and enhance the accuracy of analysis (Xiao et al., 2023).

**Calibration and Validation:** Calibration involves adjusting remote sensing instruments to ensure accurate and consistent measurements. Validation, on the other hand, involves comparing remote sensing data with ground truth information to assess the accuracy of the measurements. Both calibration and validation are essential for ensuring the reliability of remote sensing data and the credibility of subsequent analysis (Russell et al., 2023).

**Data Fusion and Integration:** Data fusion and integration involve combining remote sensing data with other sources of information, such as geographic information systems (GIS), field surveys, and socioeconomic data. This integration allows for a more comprehensive analysis of complex environmental and societal phenomena, facilitating better decision-making and resource management (Gao et al., 2023).

To sum up, the principles guiding remote sensing applications, including spectral and spatial resolution, radiometric corrections, and sensor fusion, are paramount for ensuring accurate and reliable data analysis in diverse environmental contexts, a comparison of these methods are gathered in Table 5.

*Table 5: Pros and cons of remote sensing methods*

Remote Sensing Method	Pros	Cons
Passive Remote Sensing	Energy-efficient, works well for large-scale monitoring.	Limited by weather and sunlight availability.
Active Remote Sensing	Can operate anytime, provides high accuracy.	Expensive, energy intensive.
Spectral and Spatial Resolution	High detail and differentiation of surfaces.	Requires large storage and high processing power for high resolution.
Radiometric and Geometric Corrections	Improves data accuracy and consistency.	Computationally intensive, may still have errors in complex terrains.

<b>Temporal Resolution</b>	Allows frequent updates and tracking of changes over time.	Large datasets that require more storage and management.
<b>Sensor Fusion</b>	Combines multiple datasets for comprehensive analysis.	Complex integration and processing.
<b>Calibration and Validation</b>	Ensures accuracy and reliability of data.	Requires time-consuming and costly ground validation.
<b>Data Fusion and Integration</b>	Enables deep analysis by combining diverse data sources.	Technically challenging, prone to alignment issues between different datasets.

## 2.3 UHI and climate change

### 2.3.1 Importance of climate change

Climate change refers to the long-term alteration of weather patterns and average temperatures on Earth. It is caused by human activities, such as the burning of fossil fuels and deforestation, which release greenhouse gases into the atmosphere. These greenhouse gases, including carbon dioxide and methane, trap heat and contribute to the warming of the planet (Feliciano et al., 2020).

This warming leads to a range of impacts, including rising sea levels, more frequent and severe weather events, changing ecosystems, and disruptions to agriculture and food production (Bandara & Cai, 2014). Also, the consequences of climate change, spanning ecosystems, biodiversity, human health, and socio-economic systems, are well-documented (Louis & Phalkey, 2016; Patz et al., 2014; Pongrácz et al., 2010). These disproportionately affect vulnerable populations, exacerbating inequalities and challenging global health and security. Addressing this necessitates mitigation, adaptation, and resilience-building measures, emphasizing human rights, social justice, and reducing greenhouse gas emissions (Pongrácz et al., 2010)

For example, a real case study that highlights the impact of climate change on human health is the increase in mosquito-borne diseases like malaria in regions such as Africa, Asia, and South America. furthermore, as temperatures increase and rainfall patterns shift, the habitats of disease-

carrying mosquitoes expand, leading to a higher risk of transmission to human populations (Campbell-Lendrum et al., 2015). Another example could be the increase in heat-related mortality, particularly among marginalized communities living in densely urbanized areas. These marginalized communities may lack access to air conditioning or other means of cooling, making them more vulnerable to extreme heat events (Haines et al., 2006).

Understanding and acting on climate change is pivotal for future generations' well-being. By comprehending its mechanisms and effects, we lay the groundwork for sustainable development. Cities can bolster resilience by addressing urban heat and climate change together. Collaborative efforts at all levels are vital for a prosperous and equitable future.

### 2.3.2 UHI and climate change dynamics

Climate change and UHIs have complex interactions, with UHIs exacerbating the effects of heat waves and contributing to higher temperatures in urban areas (Bornstein et al., 2012; Zhao et al., 2018). While UHIs contribute to temperature increases, true climatic warming remains primary. The synergistic effects of UHIs and heat waves vary based on local climate and future warming scenarios, impacting human thermal comfort significantly (Masson et al., 2020).

The UHIs effect, compounded by urbanization and climate change, significantly impacts health and contributes to global warming (Feinberg, 2022; Heaviside et al., 2017). Understanding this interplay is critical, particularly regarding heat stress during heat waves (Howden et al., 2007). Specific case studies, like Athens, Greece, reveal a potential positive feedback loop between UHIs and heat waves, intensifying thermal risk (Founda & Santamouris, 2017). Proposed mitigation measures include increasing albedo, vegetation fraction, and irrigation (Kong et al., 2021).

Estimates suggest UHIs may contribute 3-36% of global warming (Feinberg, 2022). Mitigation strategies, such as enhancing surface reflectivity and vegetation density, are essential to address amplified UHI effects in a warming world (Lee et al., 2014).

### 2.3.3 Studies on UHIs effect in Italian cities

A series of studies have investigated the UHIs effect in various cities in Italy Garzena et al. (2019b) analyzed long-term climate data for Turin, identifying the UHI and its evolution Noro & Lazzarin (2015b) and Straffelini & Tarolli (2023) both studied the UHI in Padua, with Noro reporting an increase in the UHI effect and Battistella exploring mitigation strategies. Straffelini & Tarolli (2023) used remote sensing and GIS methods to study the UHI in the Trieste area, finding a correlation between higher temperatures and building density. Susca et al. (2023) find that green façades are more effective than green roofs for cooling high-rise buildings, green walls work best in canyons parallel to wind direction, and scale matters for UHI mitigation strategies. Pauly et al. (2024) discovered that wind can mitigate the UHIs effect in Turin up to a certain velocity (4-4.5 m/s) and beyond which it has no positive impact on UHI.

Furthermore, Milelli et al. (2023) study identifies and characterizes the UHIs effect in Turin. Additionally, it observes the presence of an Urban Dry Island (UDI) effect during the daytime and investigates UHI effects at various levels using ground-level and vertical temperature profiles.

These studies collectively highlight the presence of the UHI effect in Italian cities and the need for effective mitigation strategies.

## 2.4 Mitigation strategies for UHIs

A range of synergistic solutions for mitigating UHIs and addressing climate change have been proposed. B. He (2019) emphasizes the co-benefits approach, which integrates UHI mitigation into existing urban development projects, such as sponge city construction in China. This approach can enhance public participation and rebalance institutional weights. Parsaee et al. (2019) highlights the need for a collaborative platform that links urban climate maps and UHI studies with urban development policies and action plans. Makvandi et al. (2023) suggests using GIS-CFD modeling to optimize building morphology and urban block configuration, particularly in rapidly urbanizing areas, to mitigate UHIs and improve air quality. Degirmenci et al. (2021) underscores the importance of integrating policy and technology responses, such as green building envelopes and cool surfaces, to effectively address UHIs. Weber et al. (2018) and Leal Filho et al. (2018) both emphasize the need for effective UHIs mitigation strategies, with Weber et al. (2018) specifically highlighting the resilience and effectiveness of strategies such as trees, shrubs, and high albedo materials. However, Yang et al. (2015) cautions that the use of reflective materials for UHIs mitigation may have unintended environmental impacts, suggesting that a city-specific approach is necessary. Weber et al. (2018) further underscores the importance of building form, orientation, and layout in UHIs mitigation. These studies collectively underscore the need for a nuanced, context-specific approach to UHIs research and mitigation, which can be facilitated by advancements in remote sensing technology. Let delve deeper into some solutions.

### 2.4.1 Urban planning

Urban planning plays a crucial role in mitigating UHIs by considering factors such as urban characteristics, local meteorological features, and the type of urban materials (Jusuf, 2018). Green

infrastructures, including urban green areas, are also key in this effort, as they can help cities adapt to climate change and enhance their sustainability and resilience (Sturiale & Scuderi, 2019). Furthermore, the presence of plants in urban spaces can significantly contribute to UHI mitigation by improving the urban climate (Önder, 2015). Implementation of UHI mitigation strategies, such as increased vegetative cover and higher-albedo surface materials, can reduce the impacts of biophysical hazards in cities (Solecki et al., 2005).

**Building orientation and shading:** Urban design interventions for reducing UHIs aim to mitigate heat accumulation in urban areas. Building orientation and strategic placement of shading elements, such as trees and awnings, help minimize solar heat gain and lower the overall temperature within cities. Optimizing building orientation can effectively mitigate UHI effects, enhancing thermal comfort and energy efficiency for residents (Bahi et al., 2020; Feng et al., 2019).

A range of studies have highlighted the potential of building orientation and shading as effective urban design interventions for reducing UHIs. Elshiwihy (2019) and Valladares-Rendón (2017) both emphasize the importance of optimized shading techniques in reducing energy consumption and enhancing daylighting. Abu Bakar et al. (2015) further supports this, demonstrating the potential of smart shading structures in mitigating UHIs in hot arid urban environments. Jentsch et al. (2013) adds to this by emphasizing the role of street canyon orientation in solar shading and urban microclimate. These studies collectively underscore the significance of building orientation and shading as key strategies in UHI reduction.

**Natural ventilation and airflow optimization:** Natural ventilation and airflow optimization can significantly contribute to reducing the UHIs effect by facilitating the movement of cooler air and dissipating excess heat within urban areas. Research has shown that well-designed urban layouts and building configurations can enhance airflow, allowing for the exchange of indoor and outdoor

air. This process helps to cool urban surfaces and lower ambient temperatures, thereby mitigating the heat island effect (Abshaev et al., 2023; Aram et al., 2019; Zhang et al., 2018)

For instance, B.-J. He et al. (2020) found that precinct ventilation can effectively mitigate UHI and improve outdoor thermal comfort. Short et al. (2004) demonstrated the potential of passive stack ventilation and passive draught cooling in maintaining thermal comfort in non-domestic buildings within UHIs. J. Li & Donn (2017) highlighted the influence of building height variability on natural ventilation and UHI, emphasizing the need for accurate modeling in dense urban environments. Rossi et al. (2015) explored the use of retroreflective façades for UHI mitigation, indicating the potential of cool materials in reducing surface overheating. These studies collectively underscore the importance of natural ventilation and airflow optimization in UHI reduction.

#### 2.4.2 Transforming buildings

Energy efficiency plays a crucial role in UHI mitigation efforts, as excessive energy consumption contributes to heat generation and exacerbates UHIs effects. By incorporating energy-efficient technologies and building practices, such as improved insulation, efficient HVAC systems, and optimized building orientation, cities can minimize energy demand and reduce heat emissions from buildings, thereby mitigating UHIs (B. He, 2019).

Research has identified several building modifications to combat UHIs. Kandya & Mohan (2018) suggests using natural materials with high thermal resistivity, such as bamboo and rammed earth, to reduce the cooling load of buildings. Stolz (2012) introduces new concepts for building protection, including high performance concretes, which could potentially be applied to UHI mitigation. Loh & Bhiwapurkar (2022) and Nifatova (2022) both emphasize the importance of

design-based approaches, with Loh proposing a new generation of climate-responsive building forms and facades, and Nifatova focusing on the modernization of internal and external envelopes. Gregório & Seixas (2017) suggests a spatial-based methodology for energy renovation in historic centers, while David Thorpe (2024) reviews the potential for reducing energy consumption and carbon emissions in high-rise buildings. These studies collectively highlight the need for innovative design strategies and holistic approaches to address UHIs and improve energy efficiency in urban structures.

A range of strategies have been proposed to mitigate the UHIs effect, including the use of cool roofing membranes and coatings, reflective building materials, and automated shading systems (Ziaemehr et al., 2023). Green roofs and walls, permeable paving, and passive cooling strategies such as natural ventilation and daylighting have also been suggested (Lee et al., 2014). Cool pavements, which can reflect solar radiation and negate evaporative cooling, are another potential solution (Qin, 2015). Additionally, the use of double skin façades and shading strategies, as well as the optimization of building insulation, have been identified as effective UHI mitigation technologies (Andoni & Wonorahardjo, 2018).

To summarize, the list of building modifications that can effectively combat UHIs includes:

**Energy Efficiency:** Utilization of energy-efficient technologies and practices, including improved insulation, efficient HVAC systems, and optimized building orientation.

**Material Selection:** Incorporation of natural materials with high thermal resistivity, such as bamboo and rammed earth, alongside high-performance concretes, and innovative building protection concepts.



**Design Approaches:** Adoption of design-based approaches focusing on climate-responsive building forms and facades, as well as spatial-based methodologies for energy renovation in historic centers.

**Cooling Strategies:** Exploration of strategies for reducing energy consumption and carbon emissions in high-rise buildings, including cool roofing membranes, reflective building materials, and automated shading systems.

**Green Infrastructure:** Integration of green roofs, walls, and permeable paving to enhance natural cooling, alongside passive cooling strategies such as natural ventilation, daylighting, and cool pavements.

**Building Envelope Optimization:** Utilization of double skin façades, shading strategies, and optimized building insulation for effective UHI mitigation.

### 2.4.3 Vegetation and green infrastructure

Harnessing the cooling power of vegetation is a crucial strategy in mitigating the UHIs effect. By strategically planting trees and other greenery, cities can significantly reduce ambient temperatures. Trees provide shade, which helps lower surface temperatures and decrease the heat absorbed by buildings and pavement. Additionally, vegetation releases moisture through a process called transpiration, which further cools the air through evaporation (B.-J. He, 2019).

Research consistently shows that the strategic use of vegetation can significantly reduce the UHIs effect (Gunawardena et al., 2017; B.-J. He, 2019; Price et al., 2015; Wong et al., 2021). Vegetation, including trees, green roofs, and green walls, provides shade, lowers surface temperatures, and releases moisture through transpiration, all of which contribute to cooling the urban environment. However, the cooling potential of vegetation varies depending on factors such as scale, extent, and

design (Wong et al., 2021). While greenery on the ground can reduce peak surface temperatures by 2-9°C, green roofs and walls can reduce surface temperatures by approximately 17°C (Wong et al., 2021). It is important to note that the cooling effect of water bodies may not be as significant as that of vegetation (Theeuwes et al., 2012)

Promoting biodiversity in urban environments is another key aspect of effective urban greening efforts. Diverse plant species support a healthier ecosystem and provide a wider range of benefits, including improved air quality, enhanced habitat for wildlife, and increased resilience to pests and diseases. Introducing native plant species can be particularly beneficial as they are well-adapted to local climate conditions and require less maintenance (Bayulken et al., 2021).

However, there are challenges to implementing successful urban greening initiatives. One common obstacle is limited space in densely populated urban areas. Finding suitable locations for planting trees and creating green spaces can be difficult, especially in areas with high levels of development. Additionally, there may be competing interests for land use, such as for housing or infrastructure projects, which can hinder efforts to prioritize green spaces (Liu et al., 2021).

To address these challenges, cities can adopt innovative solutions such as green roofs and vertical gardens, which utilize underutilized spaces like rooftops and walls for vegetation. These approaches not only help combat the UHIs effect but also provide additional benefits such as improved stormwater management and energy efficiency (Al-Kayiem et al., 2020).

Furthermore, community engagement and collaboration are essential for the success of urban greening efforts. Involving local residents in the planning and implementation process can help build support for green initiatives and ensure that green spaces meet the needs and preferences of the community. Partnering with businesses, non-profit organizations, and government agencies

can also provide valuable resources and expertise to overcome challenges and achieve shared goals (Liu et al., 2021).

#### 2.4.4 Case studies: Cities battling UHIs and climate change

Examining case studies of cities around the world provides valuable insights into the diverse approaches and innovative strategies employed to address the challenges posed by UHIs and climate change. By analyzing successful initiatives and lessons learned, cities can identify best practices and tailor solutions to their unique contexts.

1. **Masdar City, United Arab Emirates:** Masdar City, located in Abu Dhabi, UAE, is a sustainable urban development known for its innovative approach to building orientation and shading. The city utilizes compact urban design principles and carefully planned building orientations to maximize shade and minimize solar exposure. Additionally, Masdar City incorporates passive shading strategies, such as overhangs, louvers, and greenery, to reduce heat gain and create comfortable outdoor spaces even in hot desert climates.



*Figure 2: Masdar City plan design and perspective*

*Source: <https://meconstructionnews.com/10400/masdar-city-in-abu-dhabi-outlines-5-year-expansion>*

2. **The Pearl-Qatar, Qatar:** The Pearl-Qatar is an artificial island development in Doha, Qatar, that prioritizes building orientation and shading to mitigate heat island effects. The island's master plan incorporates waterfront promenades, narrow streets, and strategically placed buildings to optimize shading and airflow. Furthermore, buildings on The Pearl-Qatar are designed with adjustable shading devices and reflective surfaces to minimize solar heat gain and enhance thermal comfort for residents and visitors.



*Figure 3: Pearl-Qatar island*

*Source: <https://www.callisonrtkl.com/projects/the-pearl-qatar-united-development-company/>*

3. **Vauban, Germany:** The Vauban district in Freiburg, Germany, is renowned for its sustainable urban planning initiatives, including natural ventilation and airflow optimization. The neighborhood features pedestrian-friendly streets, green spaces, and passive solar design principles that maximize airflow and promote natural ventilation. Additionally, Vauban incorporates energy-efficient building designs with cross-ventilation systems and adjustable shading devices to enhance indoor air quality and reduce reliance on mechanical cooling (David Thorpe, 2024).



*Figure 4: Vauban, plan and bird view perspective*

Source: <https://www.greencitytimes.com/europe-s-most-sustainable-city/>

4. **Singapore: Greening the City-State:** Singapore has emerged as a global leader in urban greening, implementing initiatives such as the "City in a Garden" vision and extensive green infrastructure projects. The city-state has strategically integrated green spaces, parks, and vertical gardens into its urban fabric, mitigating the heat island effect, enhancing biodiversity, and improving residents' quality of life.



*Figure 5 Singapore: Greening the City-State ([Green Acres by Singapore's Skyscrapers - The New York Times](https://www.nytimes.com/2016/01/25/world/asia/singapore-gardens-by-the-bay.html) (nytimes.com))*

By learning from the experiences of these cities and others, urban policymakers, planners, and stakeholders can gain valuable insights into effective strategies for combating UHIs and climate

change. By sharing knowledge, fostering collaboration, and scaling up successful initiatives, cities can build resilience, enhance sustainability, and create healthier, more livable urban environments for all residents.

## 2.5 Conclusion

This chapter provides a comprehensive review of existing literature on UHIs, with a focus on their formation, contributing factors, and potential mitigation strategies. The review underscores the detrimental impacts of UHIs on human health, thermal comfort, and energy consumption in urban environments.

Key findings from the reviewed literature and case studies reveal several important points, particularly regarding the implementation phase, as outlined in Table 6:

*Table 6. Summary of Mitigation Strategies for UHIs based on literature*

Category	Strategy	Implementation Phase
<b>Urban Planning</b>	Green infrastructure (e.g., parks, green spaces)	Before
	Building orientation and layout	Before
	Strategic shading (trees, awnings)	Before and After
	Natural ventilation and airflow optimization	Before
	Urban climate maps integration	Before
<b>Building Design</b>	Energy-efficient technologies and practices (insulation, HVAC systems)	Before and After
	Use of natural materials with high thermal resistivity	Before
	Innovative building protection concepts (high-performance concretes)	Before
	Climate-responsive building forms and facades	Before
	Cool roofing membranes and coatings	After
	Reflective building materials	After
	Automated shading systems	After
	Green roofs and walls	After
	Permeable paving	After
	Double skin façades	Before and After
	Planting trees and other greenery	Before and After

<b>Vegetation and Green Infrastructure</b>	Promoting biodiversity through diverse plant species	Before and After
	Green roofs and vertical gardens	After
<b>Cooling Strategies</b>	Passive cooling strategies (natural ventilation, daylighting)	Before and After
	Cool pavements	After
	Shading strategies	Before and After
	Optimized building insulation	After

The highlighted strategies, which can be implemented after construction, serve as key mitigation measures identified in this research.



# 3 Methodology

Within this chapter, the research framework and different steps of the methodology are revealed, encompassing all methods, software, and tools that are introduced. Additionally, the data needed for each step will be discussed, and limitations and challenges regarding this proposed approach will be addressed at the end.

## 3.1 Research design and framework

The methodology is designed to leverage advanced remote sensing techniques, detailed analysis using the Dragonfly plugin, climate change projections, and innovative solutions to address the challenge of UHIs. The research framework is represented in Figure 6.

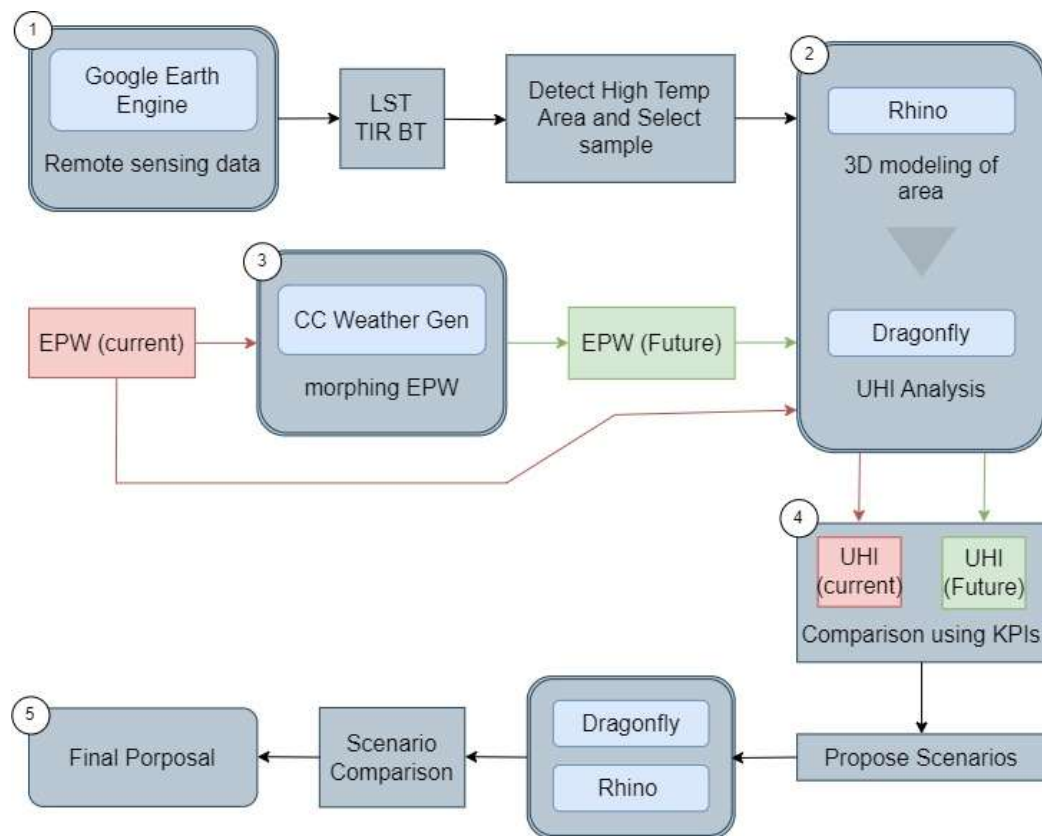


Figure 6: The research Framework and methodology steps



Each section of the graph and its corresponding number are explained in detail below.

### Step 1: Data Collection by Remote Sensing Techniques

The first step involves the collection of data using remote sensing technology. Google Earth Engine is employed to detect and map areas with potential for UHI formation. This is achieved by analyzing temperature variations and land cover characteristics to identify regions prone to high temperatures.

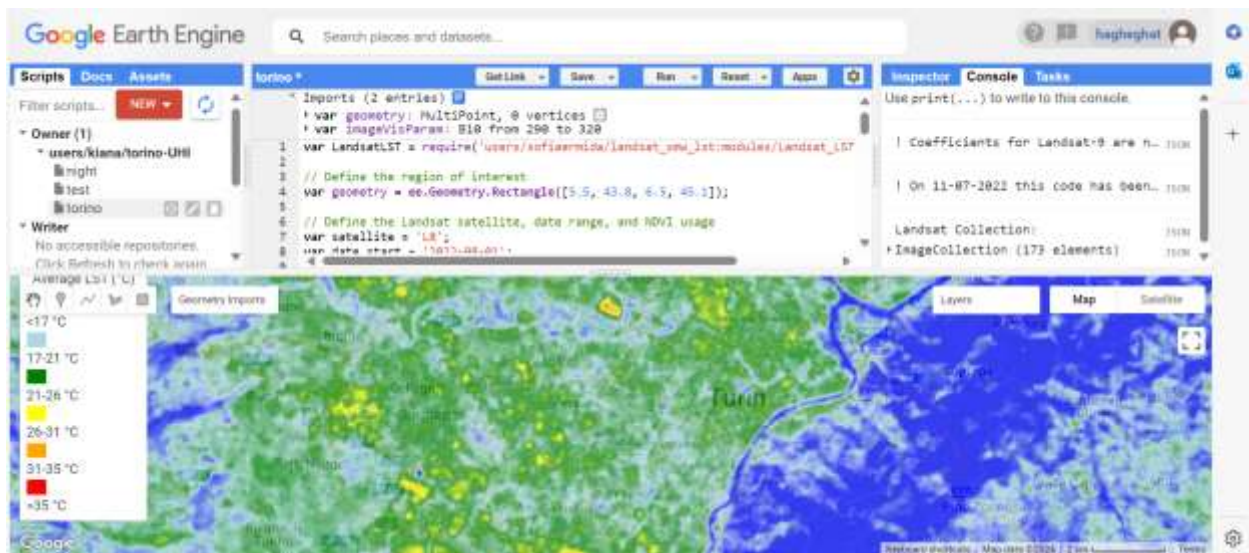


Figure 7: The environment of Google Earth Engine

### Step 2: Detailed Analysis Using Dragonfly

Subsequently, the Dragonfly plugin within Rhino software is utilized for a comprehensive analysis of the identified UHI-prone regions. This involves 3D modeling of the area and in-depth simulation of various parameters that contribute to the UHI effect.

### Step 3: Climate Change Projection

The impact of climate change on UHI-prone areas is projected, and the effects of UHIs are analyzed for current and future. This step is crucial for understanding the long-term implications

of UHIs. For this step CCWorldWeatherGen tool is used to convert current weather data to future scenarios.

#### **Step 4: Comparison of Scenarios**

A range of qualitative and quantitative solutions are proposed to mitigate the effects of UHIs in. These solutions, generated using Dragonfly software, include urban planning strategies, building modifications, and the creation of green spaces. Different scenarios for UHI mitigation are compared to assess their effectiveness and feasibility. This comparison enables the selection of the most suitable and sustainable solutions under various scenarios, including worst-case projections. This comparison is based on some KPIs<sup>2</sup> which is UTCI, UHI Intensity, HDD and CDD. Look at section 3.3. Here the Design explorer tool also will be used to detect best scenario.

#### **Step 5: Promise for Urban Planners and Policymakers**

The research holds immense promise for providing insights to assist urban planners and policymakers. The findings can inform future decision-making processes and enhance the resilience of Turin against the effects of UHIs.

## **3.2 Data acquisition and software selection**

### **3.2.1 Remote sensing data**

For this methodology, remote sensing data are first required. There are several websites where free remote sensing maps can be downloaded in various formats, along with metadata.

---

<sup>2</sup> Key Performance Indicators

1. **USGS EarthExplorer:** This platform offers a wide array of satellite imagery and remote sensing data from different missions, such as Landsat and Sentinel. It provides various format options and comprehensive metadata. Website: [USGS EarthExplorer](#)
2. **NASA Earthdata Search:** This resource, part of NASA's Earth Observing System Data and Information System (EOSDIS), provides abundant remote sensing data from satellites like MODIS and VIIRS. Users can search data by location, time, and dataset type, and download both imagery and metadata. Website: [NASA Earthdata Search](#)
3. **European Space Agency (ESA) Earth Observation Data:** ESA offers access to remote sensing data through its Copernicus program, including Sentinel satellites. Data can be obtained via portals like the Copernicus Open Access Hub, which provides free access to Sentinel data along with metadata. Website: [ESA Earth Observation Data](#)
4. **NOAA National Centers for Environmental Information (NCEI):** NCEI provides various environmental data, including remote sensing imagery from satellites like NOAA's GOES. Data can be downloaded in different formats, accompanied by metadata. Website: [NOAA NCEI](#)
5. **Google Earth Engine (GEE):** Though not a conventional data download site, Google Earth Engine grants access to an extensive archive of remote sensing data from multiple sources, including Landsat and MODIS. Users can directly analyze and visualize data on the platform or export it for further analysis, often with metadata included. Website: [Google Earth Engine](#)

### **Selected platform**

This research utilizes Google Earth Engine as the platform for remote sensing data analysis. The choice of Google Earth Engine is justified by its unique features and capabilities. Its ability to

enable coding directly within the platform sets it apart from other sources, simplifying data interpretation and visualization (After downloading data from the first four sources, external software is needed to interpret the data). Additionally, Google Earth Engine offers access to a wide range of datasets, including those crucial for analyzing Earth's surface temperature and other geospatial data. Its powerful analysis capabilities empower researchers, scientists, and developers to detect changes, map trends, and quantify differences effectively. Overall, Google Earth Engine provides a comprehensive and efficient solution for conducting remote sensing data analysis, making it the preferred choice for this research. More detail of this platform will be given in section 5.1.

### 3.2.2 Weather data

After that we need to analysis part of Turin in Dragonfly which we need a 3D model File of Turin case study part and weather files for current and future scenarios.

There are several types of weather data files, which in this research EPW<sup>3</sup> will use be used. This file is a type of weather data file specifically designed to support building simulations. It stands for a Typical Meteorological Year (TMY) data set<sup>4</sup>, which is a collation of selected weather data for a specific location, listing hourly values of meteorological elements for a one-year period. The values are generated from a data bank much longer than a year in duration, at least 12 years. EPW file typically contains, **Hourly** weather data for a full year With Meteorological parameters such as temperature, humidity, solar radiation, wind speed, and direction (OneBuilding, 2023).

---

<sup>3</sup> EnergyPlus Weather Format

<sup>4</sup> It is a collation of selected weather data for a specific location, listing hourly values of meteorological elements for a one-year period. The values are generated from a data bank much longer than a year in duration, at least 12 years.

The current weather data for Turin can be easily downloaded from each of following website:

1. **EnergyPlus EPW:** EnergyPlus is a widely used building energy simulation program, and it offers EPW weather files for different locations. Website: <https://energyplus.net/weather>
2. **EPW map:** Ladybug Tools provides access to weather data in EPW (EnergyPlus Weather) format. weather files for various locations around the world can be find on their website: <https://www.ladybug.tools/epwmap/>

It is important to note that the EPW file used in this research, obtained from the EPW map, is in TMY format. For future weather files as well, recent research and methods exist to modify current EPW files for various future scenarios.

### **Selected tool**

The research utilizes the "CCWorldWeatherGen" tool for generating future EPW files.

CCWorldWeatherGen is a tool designed to generate climate change weather files for global locations, tailored for use in building performance simulation programs. The tool converts present-day EPW weather files into climate change EPW or TMY2<sup>5</sup> file. This Microsoft Excel-based tool is a valuable resource for professionals in the field of architecture, urban planning, and environmental science, offering a streamlined approach to assess climate change impacts on building performance and urban area. Details on the underlying methodology used in CCWorldWeatherGen can be found in Jentsch et al. (2013) publication. It utilized data from the

---

<sup>5</sup> Typical Meteorological Year, version 2: provides historical hourly solar radiation and meteorological data from the 1961-1990 NSRDB for simulating energy system performance.

IPCC<sup>6</sup> **Third Assessment Report (TAR)** model summary, specifically from the **HadCM3 A2 experiment ensemble**.

The **Third Assessment Report (TAR)** model summary data from the **HadCM3 A2 experiment ensemble** refers to climate simulations conducted using the HadCM3 model for the IPCC's Third Assessment Report. These simulations are based on the A2 emissions scenario, which provides data for climate projections under this particular scenario (Nakicenovic et al., 2000). Figure 8 shows an example of global surface warming based on different scenarios, including A2, facilitating an easier comparison of A2 senario with others.

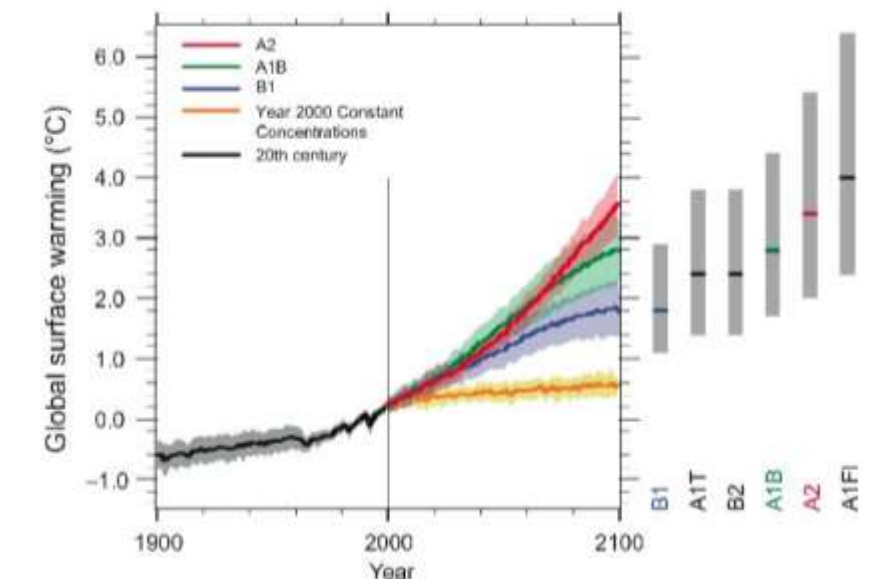


*Figure 8 Multi-model Averages and Assessed Range for Surface Warming*

<https://www.narccap.ucar.edu/about/emissions.html>

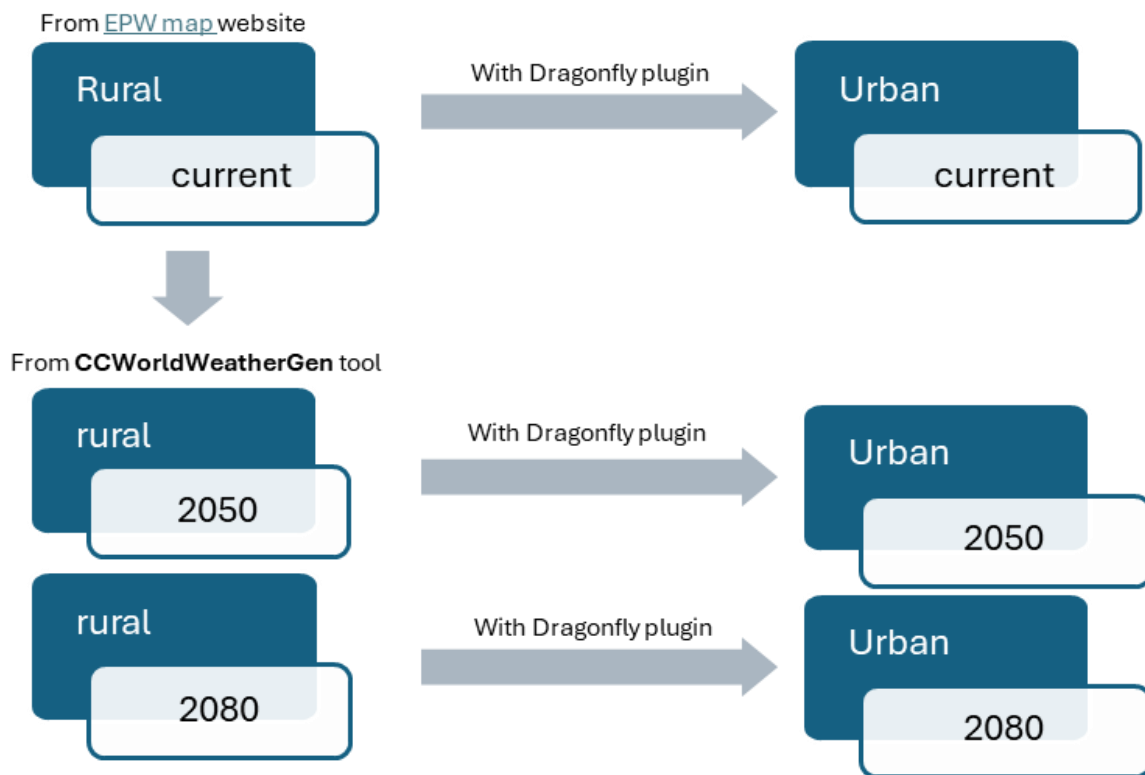
## Summary of weather files used in this research

---

<sup>6</sup> Intergovernmental Panel on Climate Change

To provide a clear overview of the weather files employed in this study, Figure 9 presents a thematic diagram illustrating the six EPW files and their respective sources.

- **Current Rural<sup>7</sup>**: Sourced from the *EPW map* website, this is the baseline weather file.
  - **2050 Rural & 2080 Rural**: Generated using the *CCWorldWeatherGen* tool, which models future climate scenarios based on the baseline current rural EPW file.
  - **Urban Files**: Using the Dragonfly plugin, these rural EPW files are converted to urban weather files, simulating the UHI effect for each time period (current, 2050, and 2080).
- More information of Dragonfly will be explained in section 3.2.3 and 5.2.



---

<sup>7</sup> From now on, to simplify understanding, the EPW file and its results that includes the effects of the UHI will be referred to as "urban," while the original EPW file, which generally does not account for UHI effects, will be referred to as "rural."

*Figure 9: The six EPW file used in this research and their references*

### 3.2.3 UHIs analysis data

Various computational software programs and models have been developed to simulate and assess the impact of climate on urban environments, emphasizing accuracy and efficiency (Ibrahim et al., 2020). For instance, user-friendly software tools like ENVI-met, RayMan, and CitySim Pro are acknowledged for their capability to evaluate outdoor thermal comfort and their integration with CAD or GIS software. These tools have undergone evaluation against observations and are regarded as reliable for specific purposes (Jänicke et al., 2021; Tsoka et al., 2018). Moreover, Ladybug Tools, particularly Dragonfly, has been noted for its parametric capabilities and time efficiency in simulating and optimizing building and urban geometry configurations (Ibrahim et al., 2020). This study employs Dragonfly for UHI detection.

#### **Introduction to Dragonfly plugin in Rhino software**

Dragonfly, a part of the Ladybug Tools suite, is a robust tool for environmental analysis within Rhino/Grasshopper (SADEGHIPOUR ROUDSARI et al., 2013). It enables the import of EnergyPlus Weather (EPW) files and provides interactive graphics, aiding decision-making during the design process. This open-source tool simplifies analysis, automates calculations, and integrates parametric tools for real-time feedback on design changes (Ladybug Tools | Dragonfly, n.d). **Dragonfly uses the Urban Weather Generator (UWG)** to convert rural EPW files into urban ones, adjusting parameters like building geometry and anthropogenic heat to simulate urban climate conditions, particularly the Urban Heat Island (UHI) effect. The [UWG Model Schema](#) on Ladybug Tools provides detailed input data and preset values essential for these simulations. Some of these data are shown in Table 7.



Table 7: Urban Weather Generator (UWG) Model Data Schema

Category	Attribute	Details	Range/Default	Units
Site Characteristics	Modeling Method	Method used for urban data input.	Method 1: 3D files	N/A
			Method 2: 2D files	
Building Geometry	Building Type	Specifies building categories such as Full-Service Restaurant, Hospital, Large Hotel, etc.	Various types	N/A
	Building Age	Indicates the construction era.	Before 1980, 1980-present, Newly Constructed	N/A
	Average Building Height	The mean height of city buildings.	Variable	Stories
	Building Wall-to-Site Ratio	The proportion of building walls compared to the total site area.	Variable	Percentage (%)
Surface Properties	Road Surface Type	Type of road surface used in urban areas.	Asphalt	N/A
	Asphalt Albedo Coefficient	Reflectivity ratio of asphalt.	0.1 to 0.3	Dimensionless
	Asphalt Thickness	Thickness of asphalt used in roads.	50 to 100	Millimeters (mm)
	Thermal Conductivity of Asphalt	Heat flow capacity of pavement.	1	W/m-K
	Volumetric Heat Capacity of Asphalt	Energy required to raise the temperature of asphalt.	1,600,000	J/m <sup>3</sup> -K
Vegetation	Vegetation Type	Type of vegetation covering the area.	Trees, Grass	N/A
	Albedo Coefficient	Reflectivity ratio of vegetated surfaces.	Default: 0.25	Dimensionless
	Growing Season	Start and end month of active energy contribution of vegetation.	Estimated based on climate data	Month
	Latent Heat of Vegetation	Fraction of solar energy absorbed and released as latent heat through evapotranspiration.	Trees: 0.7 Grass: 0.5	Dimensionless
	Vegetation Coverage	Percentage of the area covered by vegetation, differentiated by type (grass or trees).	Variable	Percentage (%)
Traffic	Sensible Heat Generation	Non-building heat generation from sources like vehicles, lighting, and human metabolism.	Residential: 4 Downtown: 20	W/m <sup>2</sup>

---

<b>Traffic Data Schedule</b>	24-hour profile defining the hourly distribution of human-generated heat.	Typical commercial area pattern (default)	Hourly Profile
------------------------------	---	---	----------------

---

### 3.3 UHI assessment indicators

When simulating UHIs, the resulting weather file (EPW) can be compared to a baseline rural EPW file. This comparison provides insight into the magnitude and characteristics of the UHI effect. The KPIs used for analysis will be derived either directly from the newly generated EPW file or through a comparison with the rural baseline. A detailed explanation of how these KPIs is extracted from the simulation data will be provided in Section 5.2. In this section, here we will focus on introducing the following KPIs used to evaluate UHI performance:

#### 3.3.1 Universal Thermal Climate Index (UTCI)

The **Universal Thermal Climate Index (UTCI)** is a widely recognized measure of human thermal comfort, designed to assess the combined effects of air temperature, humidity, wind speed, and mean radiant temperature in outdoor environments. Unlike conventional indices that focus on a single variable, UTCI offers a more comprehensive approach, considering the interaction of multiple climatic parameters to evaluate how hot or cold it feels for humans. Due to its robustness and sensitivity to various environmental conditions, UTCI has become a preferred index for outdoor thermal comfort analysis.

UTCI is selected over other thermal indices because it is highly responsive to a variety of climate variables, providing a holistic measure of thermal stress and comfort under different weather

conditions. Its utility spans various applications, including urban climate studies, building design, and public health.

The formula for UTCI, developed from foundational studies such as Blazejczyk et al. (2012), is well-regarded for its accuracy in representing thermal stress under diverse conditions. In the software implementation, the open-source code by [Chris Mackey \(GitHub\)](#) will be utilized for calculating the UTCI values across different time periods using Equation (1).

$$UTCI = f(T_a, RH, v, T_{mrt}) \quad (1)$$

Where:

- $T_a$  = Air temperature (°C)
- RH = Relative humidity (%)
- $v$  = Wind speed (m/s)
- $T_{mrt}$  = Mean radiant temperature (°C)

These variables collectively determine the UTCI, which reflects the thermal conditions experienced by humans.

### **Time Periods for UTCI Calculation**

To assess thermal comfort across different seasons and times of day, the UTCI will be calculated for the following time periods:

- **Mean summer daytime**
- **Mean summer nighttime**
- **Mean winter daytime**

- **Mean winter nighttime**

These periods are chosen to account for the variability in thermal stress due to seasonal and diurnal changes in climate variables, providing a more granular understanding of outdoor comfort levels.

### 3.3.2 Urban Heat Island Intensity (UHI Intensity)

This metric measures the average difference in air temperature between an urban area and a reference rural area, providing a single value to assess the overall UHI effect under different scenarios. In this study, the reference temperature used to calculate UHI intensity is the Universal Thermal Climate Index (UTCI), which represents a more accurately adjusted temperature for this analysis. This will calculate for the same time period as UTCI.

This KPI was chosen because it directly quantifies the severity of UHI effects, helping to identify areas where mitigation efforts should be prioritized. It's a standard measure in UHI research and provides clear insights into how built environments contribute to localized warming.

So here Equation (2) is used for calculating UHI intensity.

$$UHI\ Intensity = UTCI_{urban} - UTCI_{rural} \quad (2)$$

Where:

- $UTCI_{urban}$  = Universal Thermal Climate Index for the urban area (°C)
- $UTCI_{rural}$  = Universal Thermal Climate Index for the rural reference area (°C)

### 3.3.3 Heating Degree Days (HDD) and Cooling Degree Days (CDD)

By definition, HDD index is a weather-based technical index designed to describe the need for the heating energy requirements of buildings. CDD index is on the other hands designed to describe the need for the cooling (air-conditioning) requirements of buildings.

HDD and CDD, expressed by Equations (3) and (4), are crucial indicators of energy requirements for buildings, reflecting climate change impact (Corrales-Suastegui et al., 2021). In EnergyPlus, the default set points for calculating HDD and CDD are typically 18°C (65°F) for heating and 24°C (75°F) for cooling. Which is considered in this study.

These KPIs provide practical insights into how UHI effects impact energy consumption, making them valuable for urban planners and policymakers interested in reducing energy usage and optimizing urban infrastructure. Energy consumption models could have been employed, but HDD and CDD are simpler, well-established indicators that directly relate to the energy impacts of temperature changes caused by UHI effects.

$$HDD = \sum_{i=1}^n \max(T_{base} - T_{avg,i}, 0) \quad (3)$$

$$CDD = \sum_{i=1}^n \max(T_{avg,i} - T_{base}, 0) \quad (4)$$

Where:

- $T_{base}$  = Base temperature (18°C for heating and 24°C for cooling)
- $T_{avg,i}$  = Average outdoor temperature on day i (°C)
- $n$  = Number of days in the period

### 3.4 Challenges and limitations

Navigating through the complexities of UHIs analysis involves confronting several inherent limitations and challenges that impact the reliability and accuracy of the findings.

- **Data Availability:** Despite advancements in remote sensing, obtaining comprehensive urban datasets remains challenging. While platforms like Google Earth Engine offer extensive archives of remote sensing data, limitations such as low resolution and potential missing metadata hinder the acquisition of precise datasets necessary for detailed UHI analysis in Turin.
- **Model Assumptions:** Acknowledging the complexities of urban environments, it's important to recognize that simplifications in UHI models may limit accuracy. Despite efforts to utilize up-to-date data, the inherent simplifications in modeling may not fully capture the intricacies of real-world conditions, necessitating cautious interpretation of results.
- **Uncertainties in Climate Projections:** The reliability of UHI analysis can be affected by uncertainties in climate projections. Future climate scenarios, along with the accuracy of climate models, introduce uncertainties that must be considered when interpreting results, ensuring a nuanced understanding of potential impacts on UHI dynamics.
- **Spatial and Temporal Variability:** High-resolution data and models are crucial for capturing microscale and temporal variations in urban environments. However, limitations in data availability and model capabilities may hinder accurate assessment. Specifically, model simplifications may not accurately represent the shapes of buildings and trees, impacting the analysis of UHIs.

### 3.5 Conclusion

Methodology introduces the framework, software, and data essential for the upcoming research on UHIs in Turin. The methodology outlines the approach, including remote sensing techniques, the Dragonfly plugin for analysis, and climate change projections. Various sources for remote sensing data are discussed, with Google Earth Engine selected. Future weather data will be generated using the CCWorldWeatherGen tool. Additionally, Dragonfly within Rhino software will be used for detailed UHI analysis, with outlined data requirements. Anticipated challenges such as data availability and uncertainties in climate projections are acknowledged.

## 4 Case study (Turin, Italy)

This chapter will introduce the specific case study (Turin city) characteristics, including details about geography of city, Climate data and its future trends.

### 4.1 Geographic location and characteristics

Turin, known in Italian as Torino, is a city rich in history and culture, located in the Piedmont region of northern Italy. The city's geographic coordinates are approximately 45°04'N latitude and 7°40'E longitude. It was the first capital of Italy from 1861 to 1865 and is now the capital of the Metropolitan City of Turin. The city's population is approximately 843,514 as of October 2023 (Bonetto et al., n.d.; *Superficie Di Comuni Province e Regioni Italiane al 9 Ottobre 2011*, n.d.), which is the 4<sup>th</sup> most populated city in Italy.



Figure 10: Piemonte, Italy, location





Figure 11: Turin city map and a photo with its famous building, the Mole, and the Alps on the horizon

## 4.2 Climate data and future trends

Located in northwestern Italy at the foot of the Alps, Turin features a mid-latitude, four season and Humid subtropical climate (Cfa) based on Köppen climate classification (Beck et al., 2018; Belda et al., 2014).

Winters are moderately cold and dry; summers are mild in the hills and quite hot in the plains. Rain falls mostly during spring and autumn; during the hottest months, otherwise, rains are less frequent but heavier (thunderstorms are frequent). During the winter and autumn months banks of fog, which are sometimes very thick, form in the plains, but rarely on the city because of its location at the end of the Susa Valley. Snowfalls are not uncommon during the winter months, although substantial accumulation is quite uncommon (*Torino Turistica - Servizio Telematico Pubblico - Città Di Torino*, n.d.).

The following are pictures depicting current and future weather data of Turin, gathered from the Ladybug plugin in Rhino software. The future data is based on the A2 emissions scenario as described in 3.2.2.

The weather data used here does not yet reflect the UHIs effect. These data are derived from current rural conditions and the projected rural conditions in 2050 and 2080, generated using the CCWorldWeatherGen tool as shown in Figure 12.

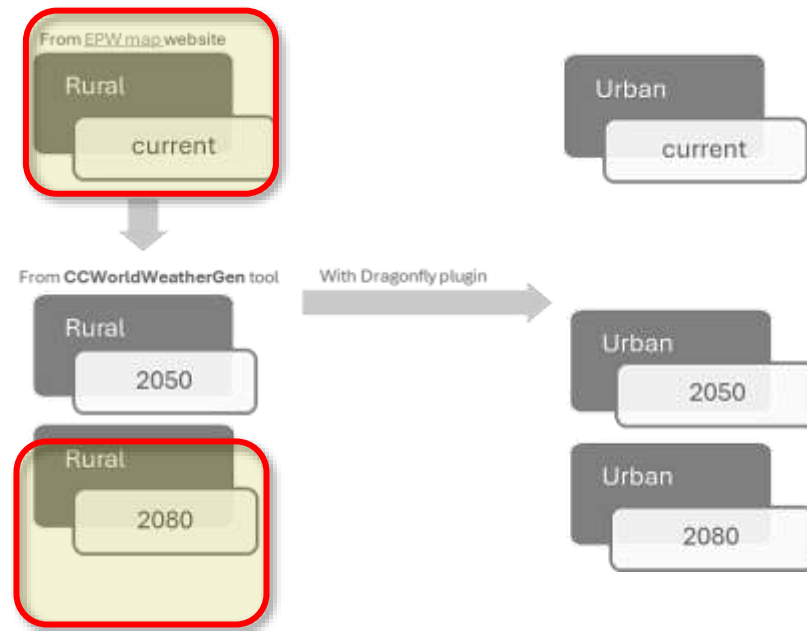


Figure 12: Weather file selected for comparison of current and future weather of Turin

The purpose of this analysis is to compare the **current rural weather conditions** with projected conditions for **2080** to assess how climate change will impact Urban Heat Island (UHI) dynamics in Turin. The comparison focuses on rural areas as they provide a **baseline reference** for understanding temperature increases without the influence of urban infrastructure. By isolating rural data, we can clearly observe the natural progression of temperature changes due to global climate factors rather than local urban modifications.

Only these two datasets are used because:

1. **Current Rural Weather** offers a **baseline** that reflects natural climatic conditions without the amplification effects of urban development. This baseline is essential for quantifying the UHI effect when compared to urban temperatures.
2. **2080 Rural Weather** is included to project future temperature increases in natural conditions. Comparing the current and future rural data allows us to assess how much temperatures are expected to rise under **climate change scenarios**, without the confounding influence of urban heat effects.

By focusing on **current and future rural data**, the analysis provides a clear understanding of how natural climate trends will evolve. This will help differentiate the impacts of climate change from the intensified effects caused by urban infrastructure in later sections of the study.

### Temperature

The graph shows that the temperature in Turin is predicted to increase significantly by 2080. The average current temperature is 12.18 °C, and the average future temperature is predicted to be 16.59 °C.

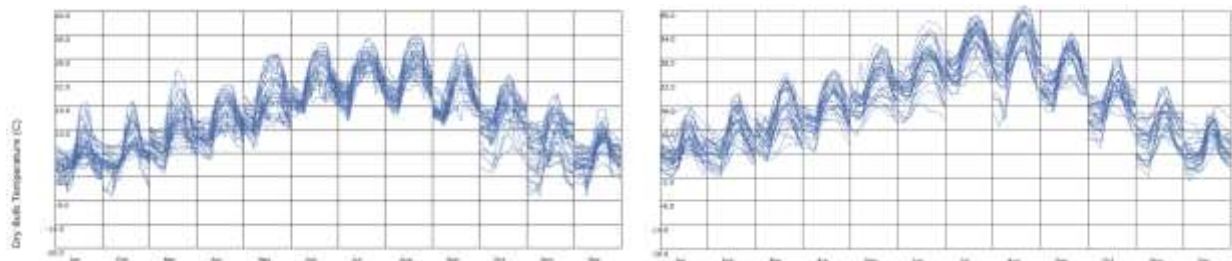


*Figure 13: Hourly temperature data for current (Left) and Future, 2080 (Right) of Turin*

### Relative humidity

The relative humidity in Turin is currently high, averaging at 68.7%, and is projected to increase to 75% in the future, exacerbating comfort conditions. Although it can be observed that during cold months, as well as at night or in the morning, humidity levels are higher.

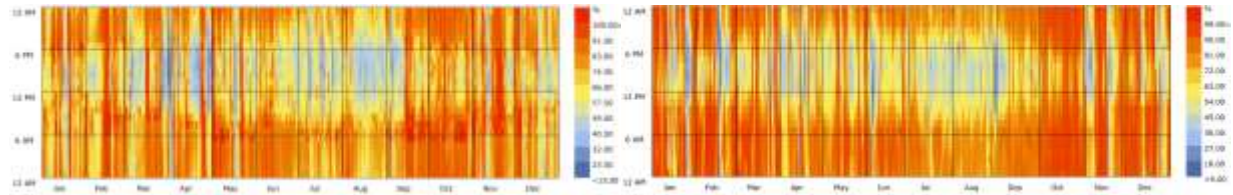


Figure 14: Hourly relative humidity in Turin current (Left) and future (Right)

## Wind

During the summer months, from May 22nd to August 22nd, the prevailing wind direction in Turin is mostly from the west-north and east-north. This trend is expected to shift further towards the north in the future. As for the temperature of the winds, it typically ranges from 20 to 31 degrees Celsius, but in the future, it is projected to increase to a range of 20 to 39 degrees Celsius. In the future, approximately 42% of the time is projected to have no wind, whereas currently, around 11% of the time is calm.

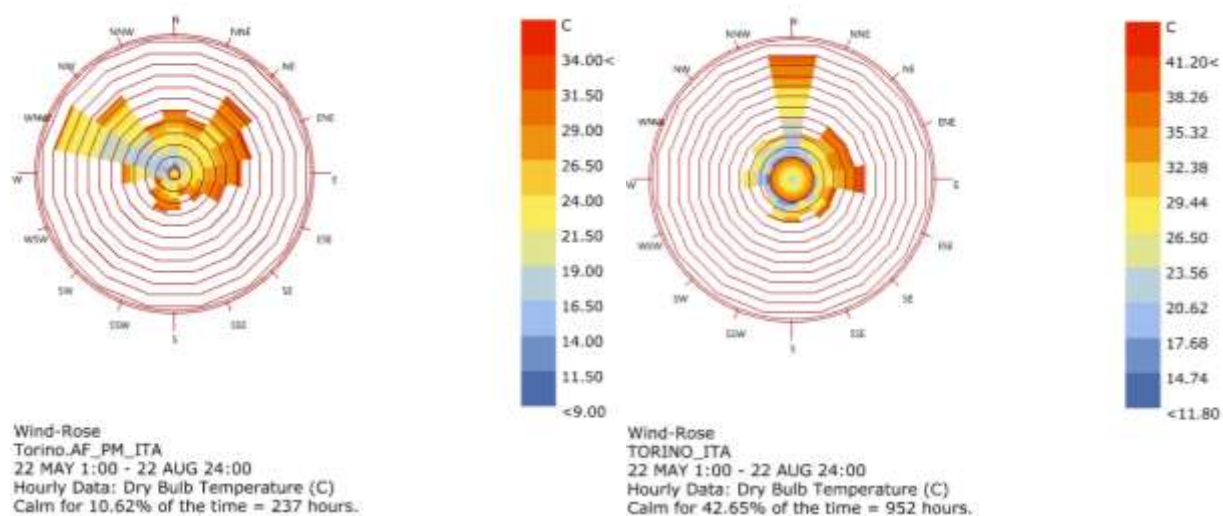


Figure 15: Wind rose in Turin current (Left) and future (Right)

Based on the weather data, the average wind speed in the current situation is 0.97 m/s, while in the future, it is projected to be slightly higher at 1.01 m/s.

### **Cloud cover**

Currently, cloud cover is generally high (45% covered in average), especially during nighttime. However, in the future, there will be some days with total intense cloud cover and other days that are clear (41.6%).

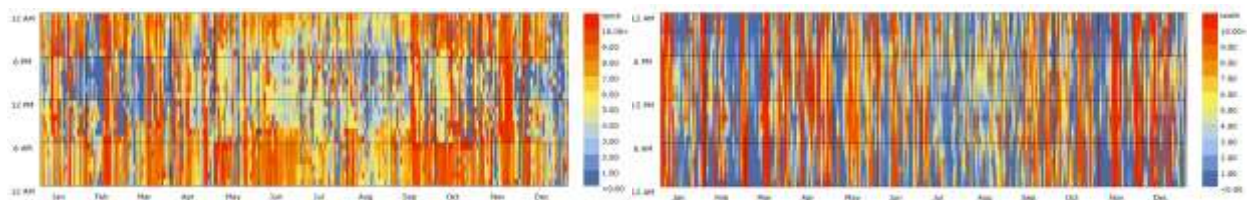


Figure 16: Hourly cloud cover in Turin current (Left) and future (Right)

### **Radiation**

In the future, the average direct normal radiation is projected to increase from 118 to 146 Wh/m<sup>2</sup>, global horizontal radiation from 147 to 161 Wh/m<sup>2</sup>, and total solar radiation from 1475 to 1601.57 kWh/m<sup>2</sup>.

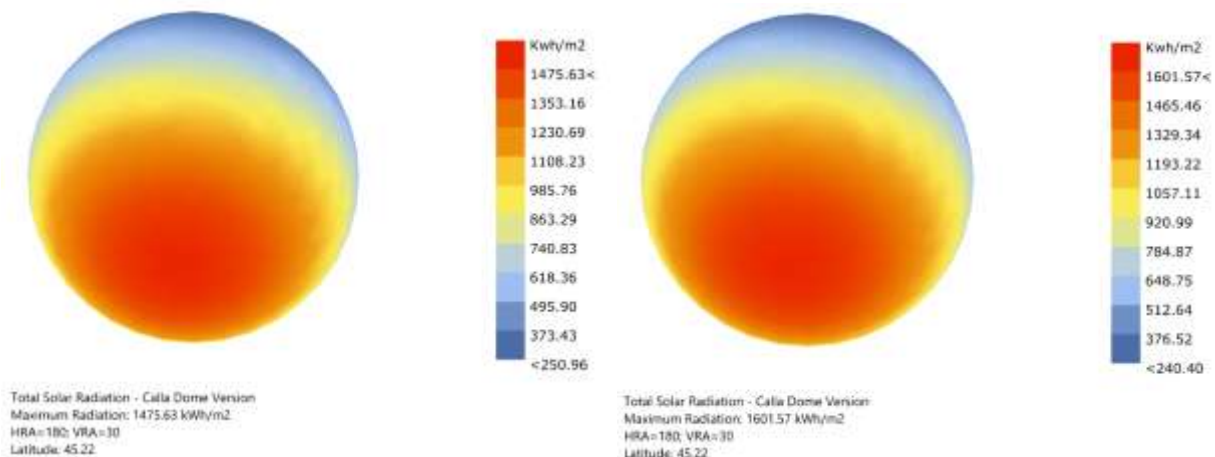


Figure 17: Total solar Radiation in Turin in current (Left) and future (Right)

### **Thermal comfort (Psychrometric Chart)**

The provided Psychrometric Chart not only displays properties such as temperature, humidity ratio, enthalpy, and dew point but also incorporates thermal comfort which its code was written in grasshopper software. It accounts for passive design strategies Passive strategies optimize thermal comfort and energy savings by using natural elements like sunlight and ventilation, minimizing reliance on mechanical heating or cooling systems.

In Turin, it's observed that currently, 8.18% of the time falls within the comfort range, which increases to 46.24% when passive strategies are considered. However, these figures are expected to decrease in the future to 5.5% and 41.7%, respectively.

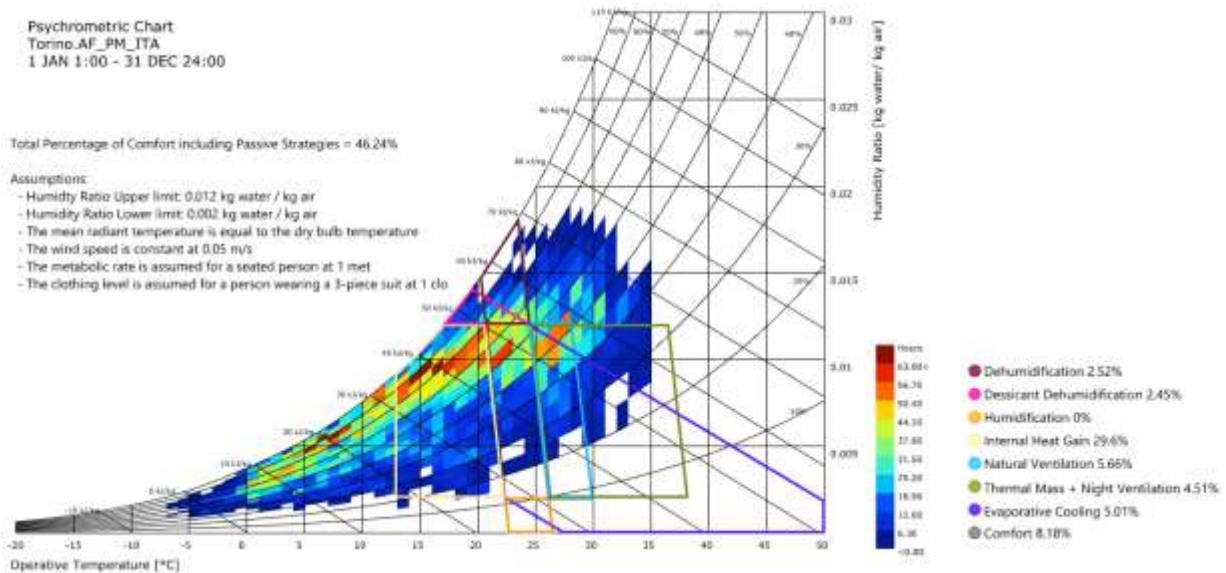


Figure 18: Current Psychrometric Chart of Turin with comfort passive strategies

It is evident that the curved lines representing humidity are increasing, indicating higher humidity levels. Additionally, the temperature range on the horizontal axis is rising, with the maximum temperature increasing from 35 to 44 degrees Celsius.



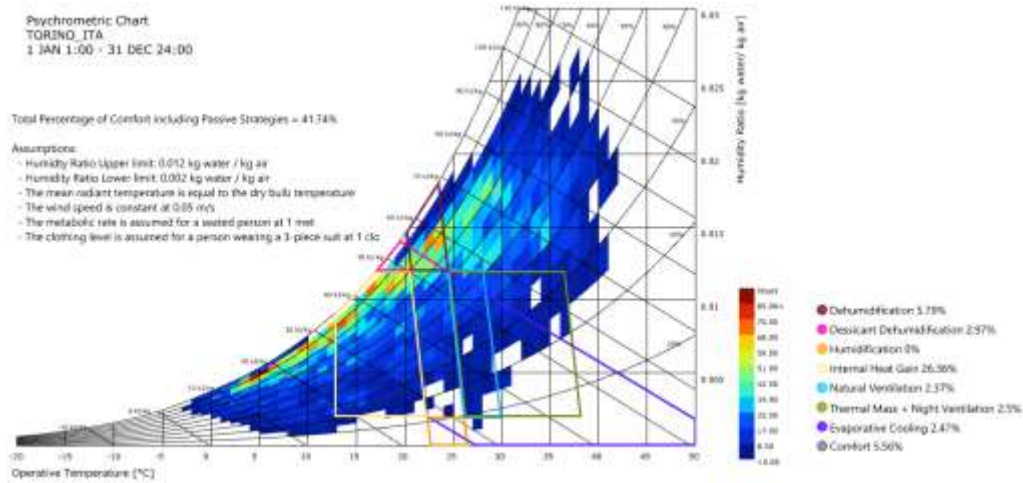


Figure 19: Future Psychrometric Chart of Turin with comfort passive strategies

### Universal Thermal Comfort Index

Following are graphs of the Hourly Universal Thermal Comfort Index (UTCI) for Turin, Italy. As mentioned in section 3.3 The UTCI is a temperature scale that considers humidity, wind speed and radiation as well as air temperature (Park et al., 2014). A UTCI of 9°C is considered to be the lower limit of the comfort zone, and a UTCI of 26°C is considered to be the upper limit for representing in Figure 20.

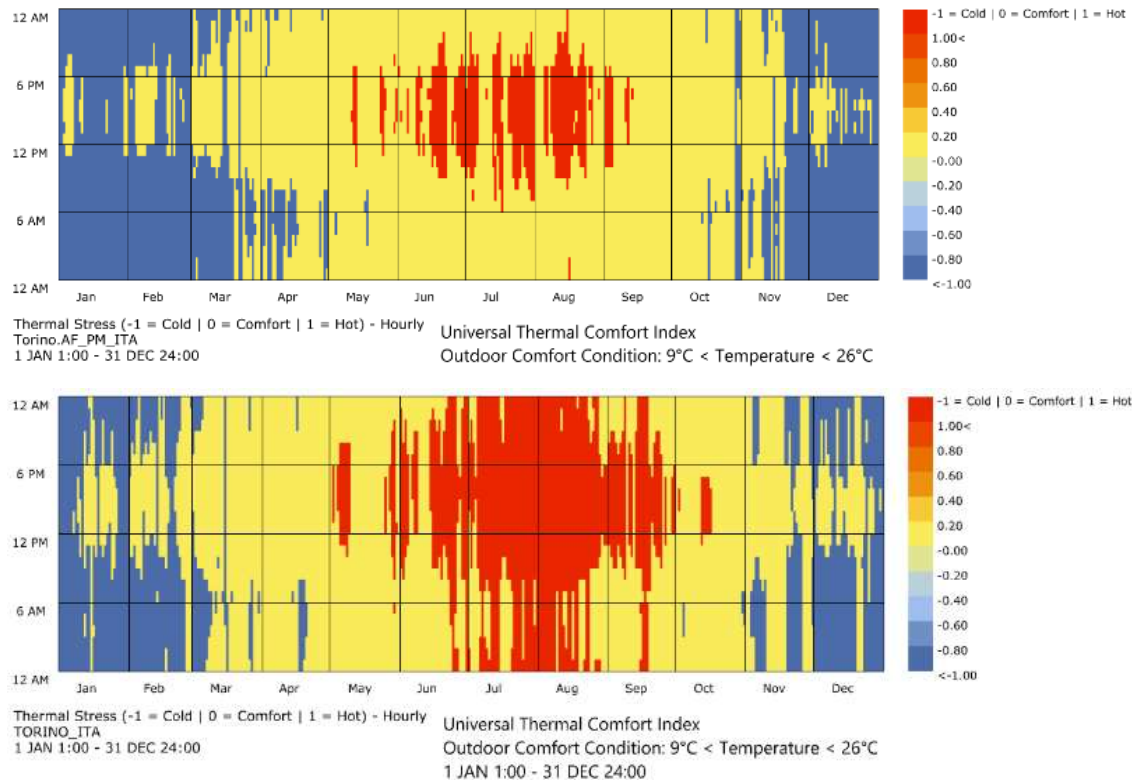


Figure 20: Hourly Universal Thermal Comfort Index in Turin in current (Up) and future (Down)

Despite the current indication that summer nights fall within the comfort zone, typically ranging between 9 to 26 degrees Celsius, many people experience difficulty sleeping without air conditioning due to the heat (based on personal experience). Looking into the future, within less than 50 years, there are projected to be around 10 days of extreme heat conditions where temperatures will not drop below 26 degrees Celsius, both during the day and night. These prolonged periods of intense heat, known as heat waves, can lead to health problems and even fatalities.

Given these projections, it's evident why air conditioning and redesigning buildings should be considered essential for European cities like Turin to prepare for future extreme events resulting from climate change.



### 4.3 Turin UHI dynamics

Turin, Italy, serves as a compelling case study for investigating UHI phenomena due to a unique combination of geographical and urban development factors. Situated amidst the Alpine Mountain chain and the Superga hills, the city experiences limited circulation of foehn winds, fostering a microclimate marked by dry summers and mild wet winters (Ellena et al., 2023). However, this geographical configuration, combined with extensive urbanization and industrialization, has exacerbated UHI effects, amplifying the intensity and frequency of extreme weather events.

The socio-economic transition in the 1950s and 60s led to significant waves of migration, resulting in the abandonment of industrial spaces, which now cover approximately 10 million square meters of the urban landscape (Piemonte, 2020). These abandoned areas exhibit significantly higher temperatures, up to 3°C above the city's average during extreme events, further exacerbating UHI effects. Moreover, Turin's land use dynamics have contributed to the consumption of 64.69% of the city's total surface area, intensifying heat retention and UHI effects (Munafò, 2019).

Climate change exacerbates these challenges, with Turin experiencing a progressive warming trend since the 1990s, leading to heightened health risks (Morabito et al., 2015). Studies indicate a significant UHI effect in Turin, with temperature differentials between urban and rural areas reaching up to 2.4°C in winter and 4.4°C in summer, further intensifying during heatwaves (Mutani et al., 2018). Notably, Turin exhibits one of the highest land surface temperature (LST) differentials between urban and rural areas in Italy during summer, highlighting the city's susceptibility to UHI effects (Biasin et al., 2023; Munafò, 2019).

The significance of Turin as a case study lies in its manifestation of complex UHI dynamics within a densely populated urban area. The city's experience underscores the urgent need for tailored

mitigation and adaptation strategies to alleviate the adverse effects of UHI and climate change on public health and urban resilience.

## 4.4 Conclusion

Chapter 4 delves into a comprehensive case study focusing on Turin, Italy, exploring its geographic characteristics and climate data along with future trends. Turin's rich history, cultural significance, and unique urban landscape are highlighted, showcasing its diverse land use patterns and functional diversity. Moreover, the chapter provides a detailed analysis of Turin's climate, revealing a shift towards warmer temperatures, increased humidity, and altered wind patterns in the future. These climatic changes pose challenges to the city's thermal comfort and underscore the importance of proactive measures, such as sustainable urban planning and adaptation strategies, to mitigate the impacts of climate change.

At the end, Turin, Italy, exemplifies the challenges of UHIs due to limited air circulation, extensive dark surfaces from abandoned industrial areas, and high land consumption. These factors combine with climate change to create a significant UHI effect, making Turin an ideal case study for exploring mitigation strategies.

# 5 Unveiling Urban Heat Islands in Turin

Chapter 5 focuses on the comprehensive analysis of UHI effects in Turin. It begins by identifying UHI-prone areas using remote sensing data and Land Surface Temperature (LST) analysis. The chapter then details the development of a 3D model using the Dragonfly plugin in Rhino to simulate microclimatic conditions and understand the factors contributing to UHI formation. Additionally, it involves generating future weather data to evaluate potential changes in UHI intensity under different climate scenarios. Through these methods, the chapter aims to provide a thorough understanding of UHI dynamics and the factors influencing heat accumulation in urban environments.

## 5.1 Spatially identifying UHI prone areas

The first stage of this research involves using remote sensing technology to identify areas in Turin that are prone to UHIs formation. Land Surface Temperature (LST) data from Google Earth Engine (GEE) is crucial for this analysis. As mentioned in section 3.2.1 GEE provides a platform for accessing, processing, and analyzing geospatial data (Mokhtari et al., 2019). Specifically, Thermal InfraRed (TIR) bands within the LST data will be employed to detect temperature variations across Turin. These variations can indicate zones likely to experience higher temperatures compared to surrounding areas.

For this purpose, a code (write by author) based on the research by Ermida et al. (2020) is provided to represent the LST of Turin and its surroundings. In this study, the surface temperature of Turin was detected using Landsat-8 satellite imagery processed with custom scripts. The imagery has a resolution of 10 meters per pixel, providing detailed spatial information. The analysis uses an

average of data from 2022 to 2024 to capture typical temperature variations. In GEE the surface temperature mapping with the Split-Window (SMW<sup>8</sup>) Algorithm was employed to compute LST from Landsat data. This algorithm, developed by CM-SAF (EUMETSAT's Satellite Application Facility on Climate Monitoring), uses empirical relationships and linear regression techniques. It relies on a linearized radiative transfer equation, which depends on surface emissivity, to relate Top of Atmosphere (TOA) brightness temperatures in the TIR channel to LST. The algorithm's coefficients, including  $A_i$ ,  $B_i$ , and  $C_i$ , are determined through linear regression analysis and are stratified by Total Column Water Vapor (TCWV) levels. Unlike other algorithms, these coefficients are not stratified by satellite view angle due to the narrower near nadir Field of View (FOV) of Landsat sensors. This method enables accurate LST estimation, providing valuable insights into surface temperature dynamics for applications like UHI monitoring, environmental assessments, and climate studies.

The equation for Land Surface Temperature (LST) estimation using the Split-Window (SW) Algorithm is given by **Error! Reference source not found.**

$$LST = A_i \frac{Tb}{\varepsilon} + B_i \frac{1}{\varepsilon} + C_i \text{ [K]} \quad (5)$$

Where:

- LST = Land Surface Temperature (Kelvin, K)
- Tb = Brightness temperature at the Top of Atmosphere (TOA) in the thermal infrared (TIR) channel (Kelvin, K)

---

<sup>8</sup> Split-Window Method

- $\varepsilon$  = Surface emissivity (dimensionless)
- $A_i, B_i, C_i$  = Empirically derived coefficients:
  - I.  $A_i$  (dimensionless)
  - II.  $B_i$  (Kelvin, K)
  - III.  $C_i$  (Kelvin, K)

$A_i$ ,  $B_i$ , and  $C_i$  are empirically derived coefficients that adjust the relationship between the brightness temperature and LST. These coefficients are specific to each Landsat sensor and are stratified by Total Column Water Vapor (TCWV) levels to account for atmospheric conditions (Ermida et al., 2020).

The term  $\frac{T_b}{\varepsilon}$  represents the brightness temperature corrected for surface emissivity, while  $\frac{1}{\varepsilon}$  adjusts for the emissivity's influence on the surface's radiative properties. The coefficients  $A_i$ ,  $B_i$ , and  $C_i$  are obtained through a linear regression analysis that incorporates various atmospheric conditions, as characterized by TCWV levels. This approach helps mitigate the effects of atmospheric water vapor on the radiative transfer process, enhancing the accuracy of LST estimates.

The mentioned code is provided in appendix 1 and the result in GEE are presented in Figure 21. The temperatures in this figure are averaged from 173 available images from most recent (last two years including 2022, 2023, 2024) dataset of landsat8.

The Land Surface Temperature (LST) map of Turin and its surrounding regions reveals significant spatial variations in temperature, highlighting a clear gradient from cooler to hotter zones. Cooler areas, represented in blue on the map, are primarily located on the outskirts and in natural environments, where temperatures are recorded below 17°C. In contrast, the urban core and industrial zones, depicted in yellow and red, show considerably higher temperatures, ranging from

31°C to above 35°C. This pattern underscores the UHIs effect, where built-up areas—characterized by extensive concrete and asphalt surfaces—tend to retain more heat than vegetated or rural landscapes. Notable hotspots are particularly evident in industrial districts like Mirafiori Nord and Lingotto, as well as in densely populated urban centers, suggesting that intensive human activities and infrastructure development significantly contribute to higher LSTs in these locations.

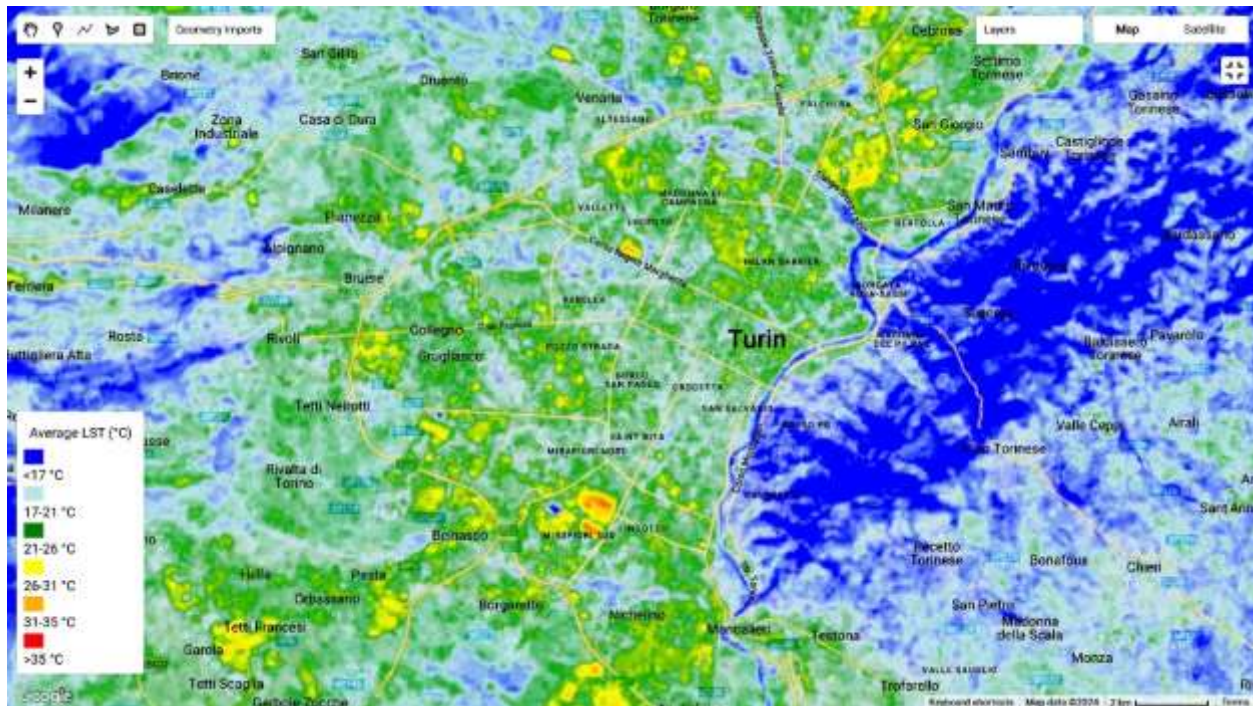


*Figure 21: Turin and its surrounding areas: LST Results*

The study focuses on a single selected zone in Turin due to practical constraints, including limited PC power and time. The comprehensive analysis of the entire city was not feasible because the detailed 3D modeling process required significant computational resources, making it impractical to model all urban areas comprehensively. This decision ensures a focused, manageable analysis within the available resources.

Within Turin, this study examines various regions to identify a specific zone for detailed analysis, guided by predetermined criteria. A key factor in selecting the case study area is the potential for significant future transformations. The study focuses on areas where interventions to enhance future resilience or mitigate climate change impacts are considered feasible. Feasibility is assessed based on factors like ease of implementation, with a preference for zones where modifications are more practical, such as government-owned properties, industrial areas, or commercial complexes, rather than residential neighborhoods where altering existing structures may be more challenging.

The selected area is about 1,300,000 square meter and 5000 m perimeter in Mirafiori Sud area in southesth part of Turin as shown in Figure 22. The area chosen for analyzing the UHIs effect is the Mirafiori complex in Turin, Italy. The company named **Torino Nuova Economia S.p.A. (TNE)** was established by local authorities to redevelop this disused industrial area, originally a Fiat factory inaugurated in 1939. Following the Memorandum of Understanding with Fiat in 2005, TNE has facilitated the reindustrialization of the area, attracted private companies and launched initiatives like the 2015 international competition of ideas for urban redevelopment. The Mirafiori complex, now part of Stellantis, spans 2,000,000 m<sup>2</sup> and employs around 18,000 people, producing vehicles such as the Fiat 500e and Maserati models.

Beyond manufacturing, the complex includes various facilities: the Motor Village showroom, the Heritage Hub Museum, the FCA<sup>9</sup> Bank headquarters, and the Citadel of Design and Sustainable Mobility, a center for research in sustainable transportation. These developments have turned Mirafiori into a hub for innovation and sustainable development, making it an ideal case study for

---

<sup>9</sup> Fiat Chrysler Automobiles



examining the UHIs effect in a post-industrial context. The revitalization efforts and diverse functions of the area provide a rich context for this analysis.



*Figure 22: The selected area in Mirafiori Sud, Turin.*

Figure 23 shows the Land Surface Temperature (LST) distribution in the Mirafiori Sud area of Turin, highlighting temperature variations from cooler blue zones (below  $17^{\circ}\text{C}$ ) to hotter red zones (above  $35^{\circ}\text{C}$ ). This map, derived using the Split-Window Algorithm and satellite data, indicates significant UHI effects in areas with dense infrastructure and minimal vegetation. The selection of Mirafiori Sud for detailed study is based on these marked temperature differences and the area's suitability for potential urban interventions to mitigate UHI impacts.





*Figure 23: The Mirafiori sud area selected with temperature more than 25 and in some spot more than 35.*

## 5.2 In-depth analysis with Dragonfly

After identifying potential UHIs zones using remote sensing data from Google Earth Engine, a more detailed analysis will be conducted using the Dragonfly plugin within the Rhino software.

Geometric data for the selected areas in Turin will be imported into Dragonfly to construct a three-dimensional (3D) model of the city. The geometric data was manually gathered by the author using measurements from Google Earth and from site. This 3D model will serve as the foundation for integrating various parameters that affect UHI formation, including:

- **Building heights** (Sourced from Google Earth measurements and verified through site observations.)
- **Land cover characteristics** (e.g., vegetation, surface albedo)
- **Anthropogenic heat sources** (e.g., traffic, industrial activity also from)

Land cover characteristics and anthropogenic heat sources were chosen based on site observations and guided ranges provided by Dragonfly.

More detailed data on the amounts and characteristics of these parameters are provided in Section 3.2.3, "UHIs Analysis Data."

By incorporating these parameters into the 3D model, Dragonfly will simulate microclimatic conditions across Turin and generate a modified EPW file. This modified EPW file includes detailed weather data such as temperature, humidity, solar radiation, wind speed, and other relevant climate variables shown in Figure 24. The generated EPW file reflects the unique microclimatic characteristics of the urban area, which can then be compared to the original EPW file typically sourced from outside the city or at higher altitudes. This comparison allows for a comprehensive assessment of how urban features, such as building density and surface materials, influence local weather conditions, contributing to UHI formation.

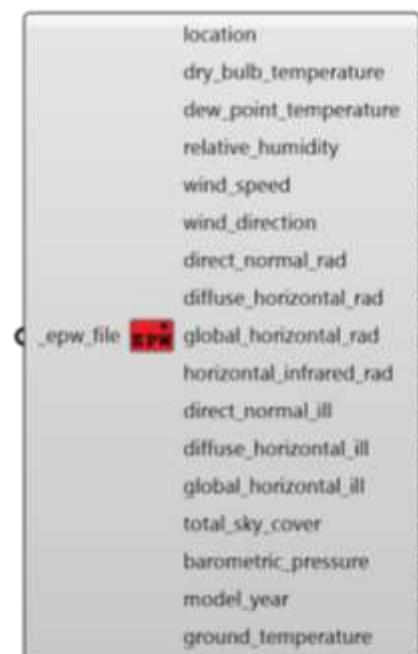
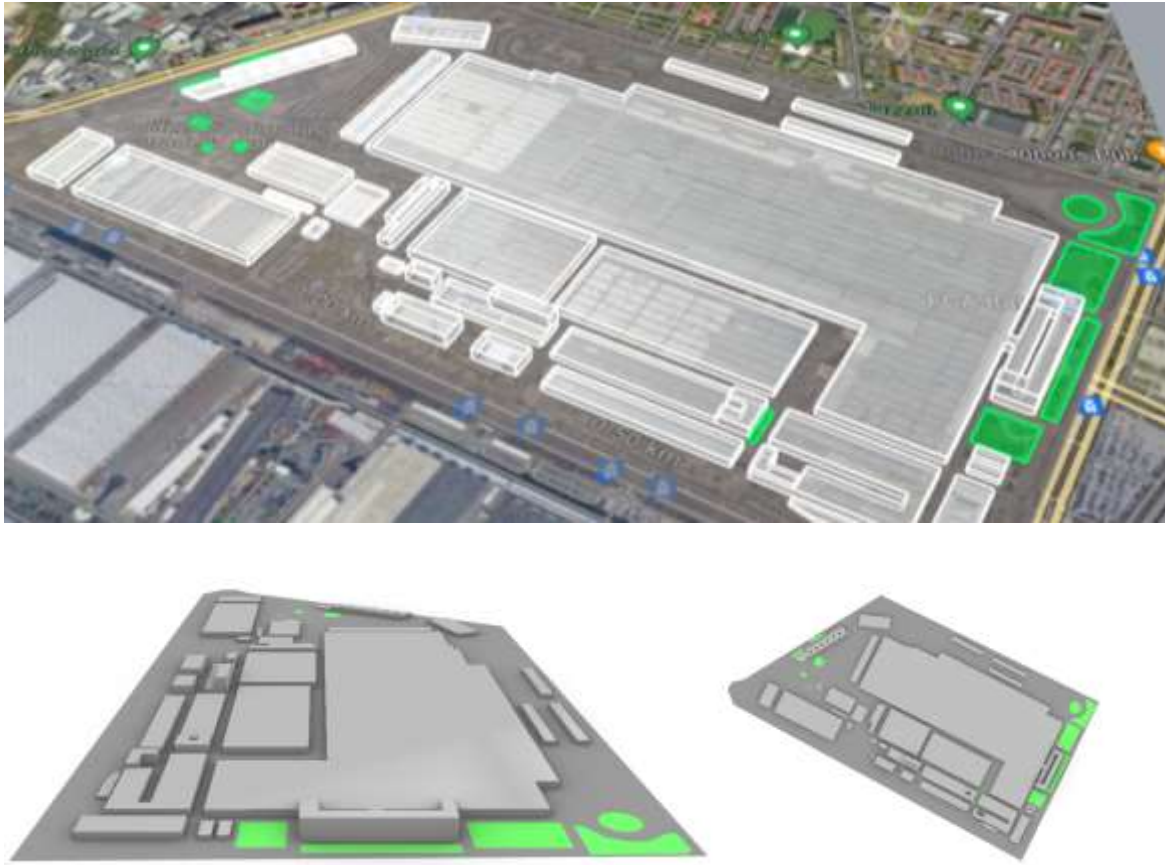


Figure 24: EPW file extracted parameters

### 5.2.1 Modelling and parameterization of selected region

The first step involved creating a simplified 3D model of the area using Rhino software. Shown in Figure 25.



*Figure 25: Rhino modeling of selected area in Turin*

Then, in the Grasshopper environment, a parametric algorithm was written with using component of the Dragonfly and build-in Grasshopper component to simulate the UHIs effect. The grasshopper environment is shown in Figure 26, each part of algorithm will be discussed afterward.

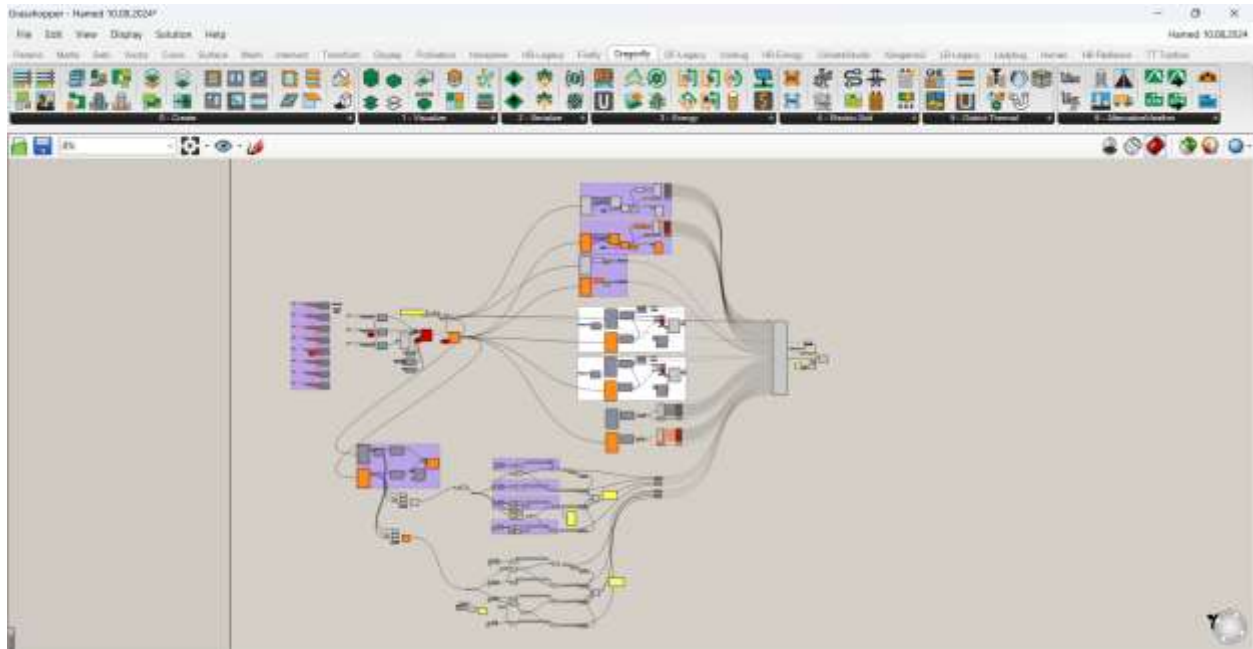


*Figure 26: Grasshopper algorithm setup for UHI analysis in Rhino environment.*

In Figure 27, several key parameters used in the analysis are displayed. These include traffic parameters such as sensible heat (Sailor, 2011b) and weekly schedules, vegetation parameters like albedo and latent heat for trees and grass (Taha, 1997), and pavement parameters including albedo, thickness, conductivity, and volumetric heat capacity (Sreedhar & Biligiri, 2016). These parameters are essential for modeling the UHIs effect in the Grasshopper environment.

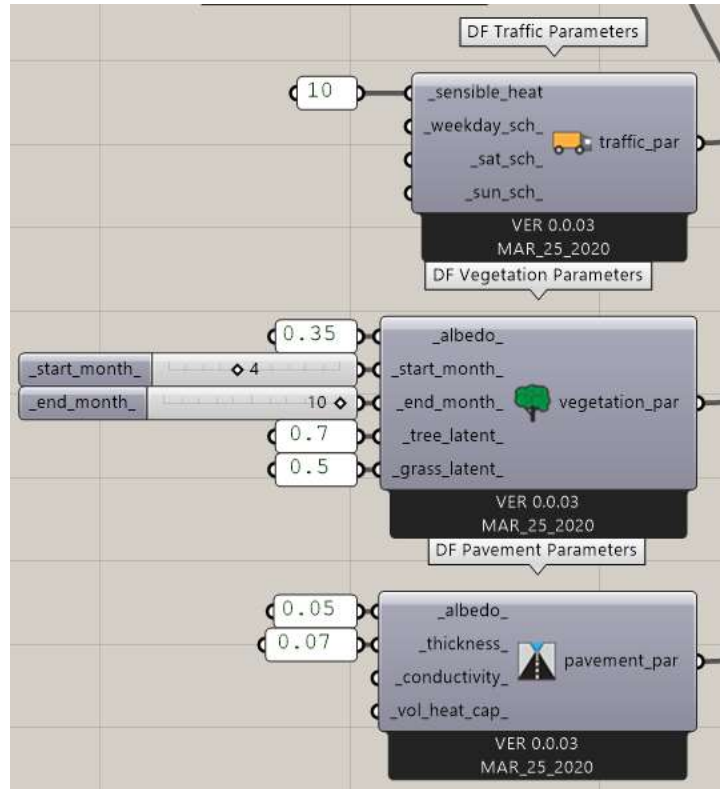


Figure 27: traffic Vegetation and pavement parameter

Figure 28 illustrates a parametric workflow for simulating urban environmental conditions using the Dragonfly and Ladybug plugins. The purple group sliders adjust parameters like roof albedo and the percentage of roof vegetation coverage for each building typology on the site, feeding into the **DF City** component. Trees, grasses, and terrain are provided as surface inputs, while traffic, vegetation, and pavement parameters Figure 27 are also connected. Once all parameters are inputted into the **DF City** component, it generates the urban model, which is fed into the **DF Run Urban Weather Generator**. The Rural weather data is then used to create a modified urban EPW file, incorporating UHI effects. This urban EPW file is essential for calculating and comparing KPIs against the baseline rural data.

This workflow is executed three times for each climate period (current, 2050, and 2080) generating a total of six EPW files. These files allow for a detailed comparison of the scenarios and their parameters.

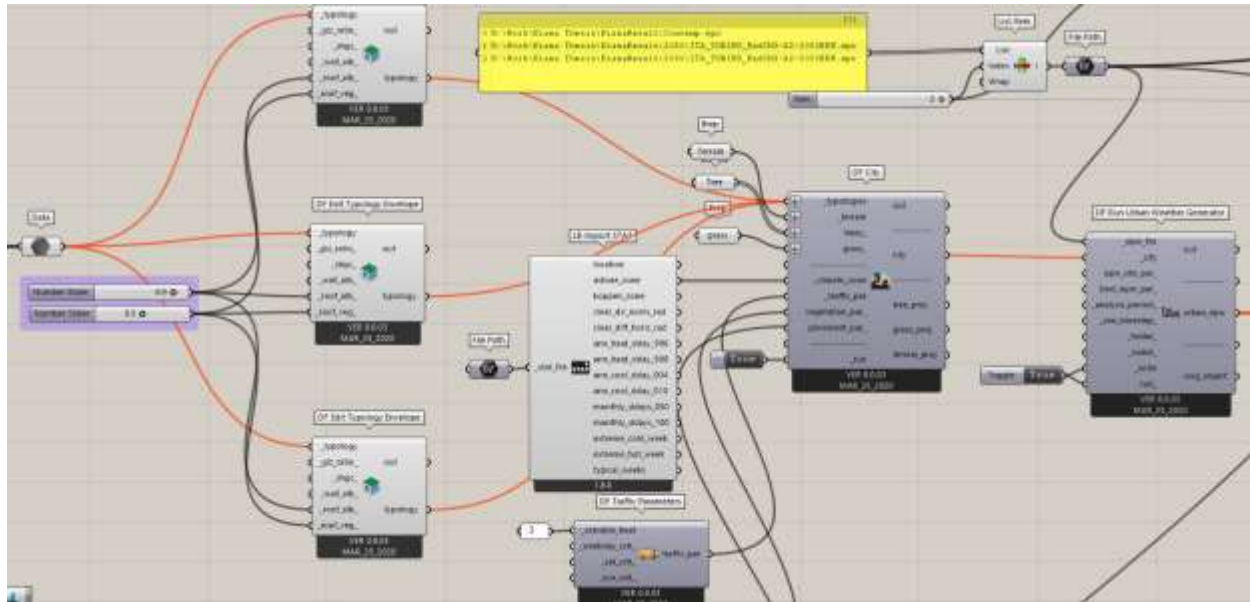


Figure 28: main parameter of dragonfly

Figure 29 illustrates the process of extracting and averaging monthly temperature data for both urban and rural environments, using Ladybug tools. In the upper section, the EPW file (which contains rural climate data without UHI) is imported into Ladybug. The data includes parameters such as temperature, humidity, wind speed, and radiation. The "Ladybug\_Average Data" component processes this data by averaging it over the selected analysis period (monthly). The exploded tree structure separates the monthly temperature values for each month, and the arithmetic mean is calculated to derive the annual average temperature without UHI effects. In the lower section, the same process is repeated for urban data (with UHI effects).



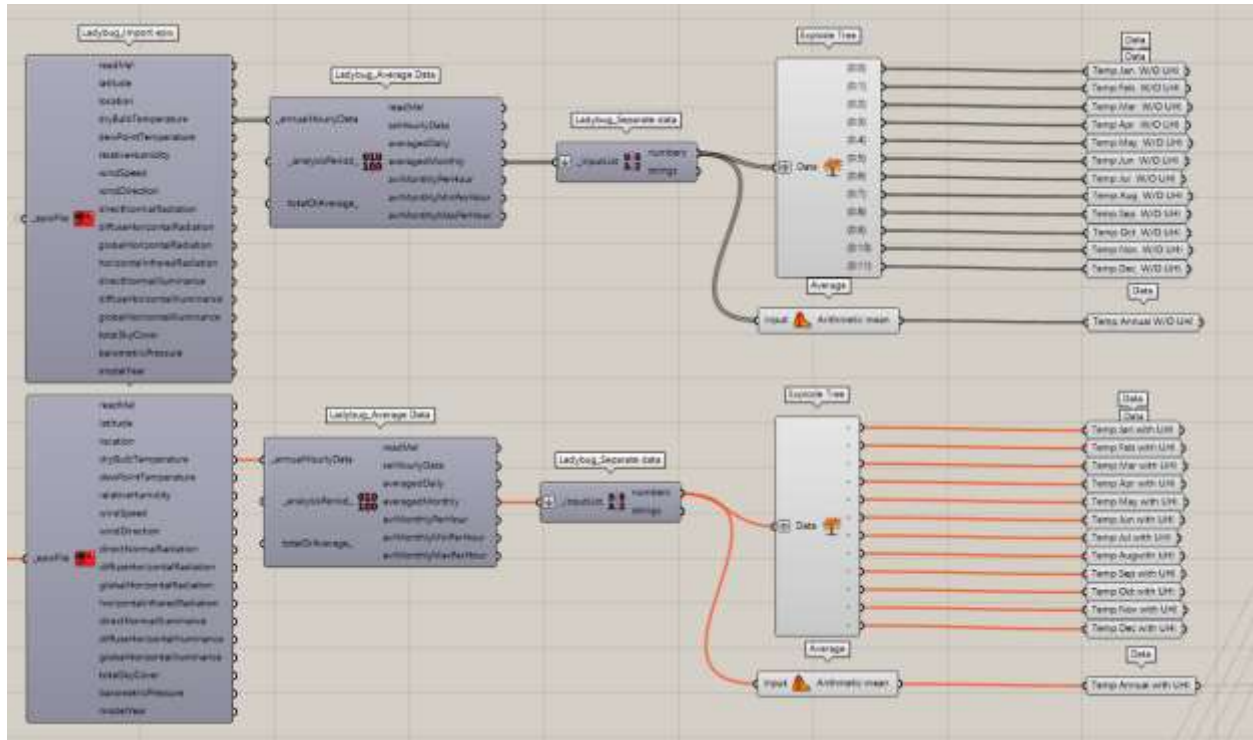


Figure 29: averaged monthly temperature data extraction for Urban and Rural

In Figure 30, the workflow creates a graph comparing December temperatures with and without UHI effects using EPW files for rural and urban conditions. Data is processed in Ladybug and visualized in a bar chart to highlight UHI impact. This process is also repeated for July. In this thesis, the results for July are presented, while the Grasshopper file with both month analyses is provided in Appendix 2.

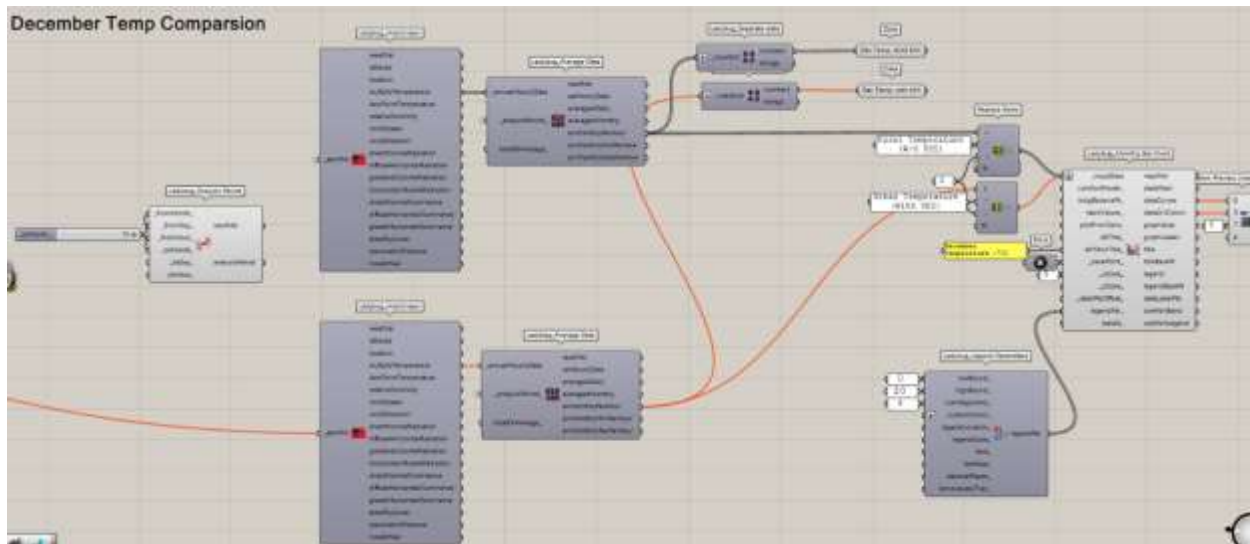


Figure 30: providing graph for UHI effect In December

Workflow in Figure 31 calculates HDD and CDD with and without UHI effects by comparing EPW files for rural and urban conditions. Ladybug components process dry bulb temperature data to compute hourly heat and cool loads, providing insights into how UHI impacts energy demand for heating and cooling.

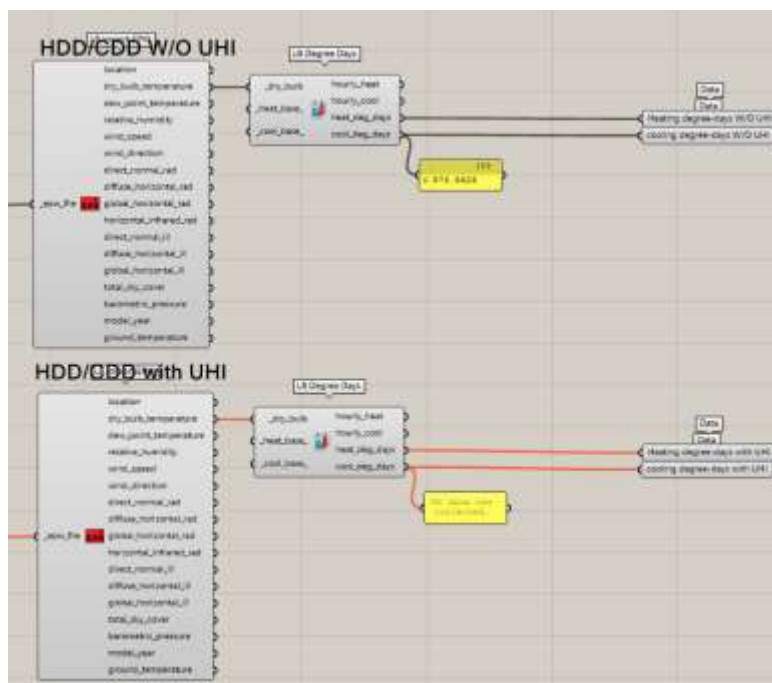


Figure 31: HDD and CDD extraction from EPW file for Urban EPW (down) and Rural EPW (up)



In Figure 32, the workflow creates UTCI data using an EPW file. Ladybug components import environmental data, including temperature, wind, and radiation, and compute solar radiation and Mean Radiant Temperature (MRT). This processed data is then used to calculate UTCI values, offering insights into outdoor comfort levels across different time intervals. The output includes monthly UTCI values for both rural and urban scenarios, which can be averaged and compared for further analysis.

Figure 32: creating UTCI data based on EPW file

In Figure 33, the workflow illustrates the calculation of UHI intensity based on UTCI values for four specific defined periods: summer day, summer night, winter day, and winter night. It subtracts the rural (R) UTCI values from the urban (U) UTCI values for each period, producing UHI intensity results for each time frame. These values help quantify the difference in thermal comfort between rural and urban areas, indicating how UHI impacts different times of the day and seasons.

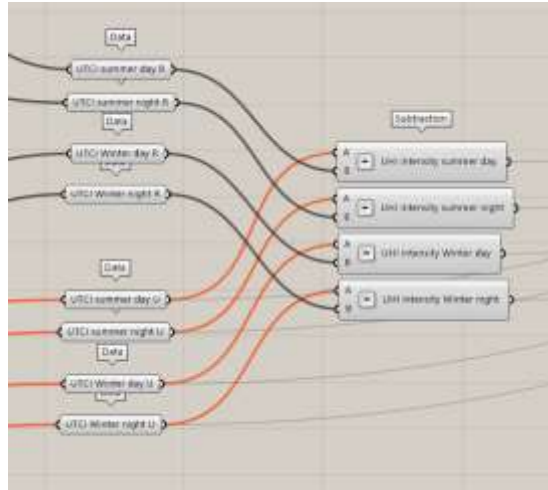


Figure 33: calculation UHI intensity for defined 4 time period based on UTCI value

Figure 34 shows a Grasshopper algorithm designed to extract data for specific time periods from hourly data inputs. It defines four distinct periods. Using conditional filters, the algorithm processes hourly data based on the defined time frames and calculates the average values for each period. These values are then used to determine metrics like UTCI and temperature.

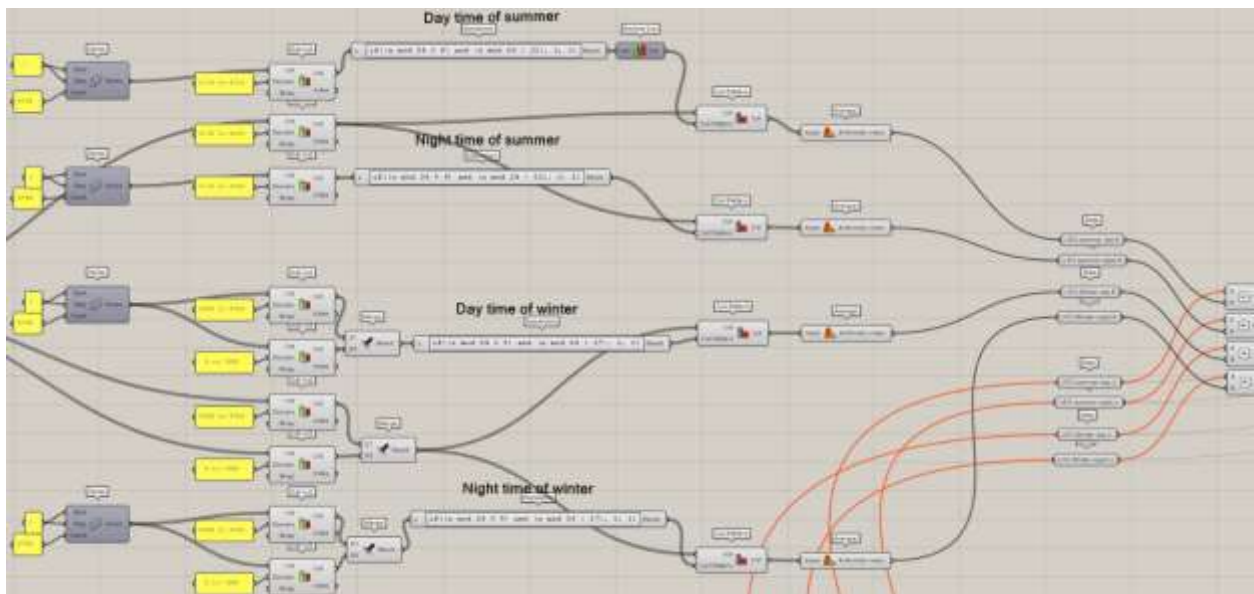


Figure 34: grasshopper algorithm for creating data for defined time period from hourly data

### 5.2.2 Future weather data generation

To analyze the potential future impacts of climate change on UHIs intensity in Turin, future weather data is required. In this research, the future weather data is generated using [CCWorldWeatherGen](#) tools, which are open-source Excel files available to the public for the world. These tools generate future climate scenarios based on a baseline file of current weather data (Jentsch et al., 2013).

The weather data is formatted in the EPW (EnergyPlus Weather) format, as this is the required format for the Dragonfly plugin, which is used for UHI detection. Climate change projections are incorporated into the methodology to create representative climate scenarios for Turin for different future periods, specifically the years 2050 and 2080, based on the HadCM3 A2 experiment ensemble.

The generated future climate data will be incorporated into Dragonfly simulations to evaluate how UHIs might develop under different climate conditions. The subsequent sections will present the results of this future UHI analysis in comparison to the current scenario, with a specific emphasis on the month of July, which is typically the hottest month. This focus aims to identify potential heatwave events and their implications under future climate scenarios.

## 5.3 UHIs analysis result

Based on the groundwork laid in sections 5.2.1 and 5.2.2, which covered the creation of the 3D model, integration with Grasshopper, and inclusion of current and future weather data, the setup is now ready, allowing the simulations to be performed.

It is worth mentioning that the temperatures discussed are averaged values derived from the 3D model simulations using the EPW file. These values are based on hourly simulations, and the results are summarized as daily and monthly averages of these hourly data points. Following are the results of simulations.

### 5.3.1 Current UHIs analysis result

The annual UHIs effect is clearly illustrated in Figure 35. This figure shows the average daily temperatures for rural and urban areas throughout the year. The data reveals noticeable differences between rural and urban temperatures, with urban areas consistently displaying higher average temperatures, particularly during warmer months. This highlights the presence of the UHI effect in the current climate scenario.

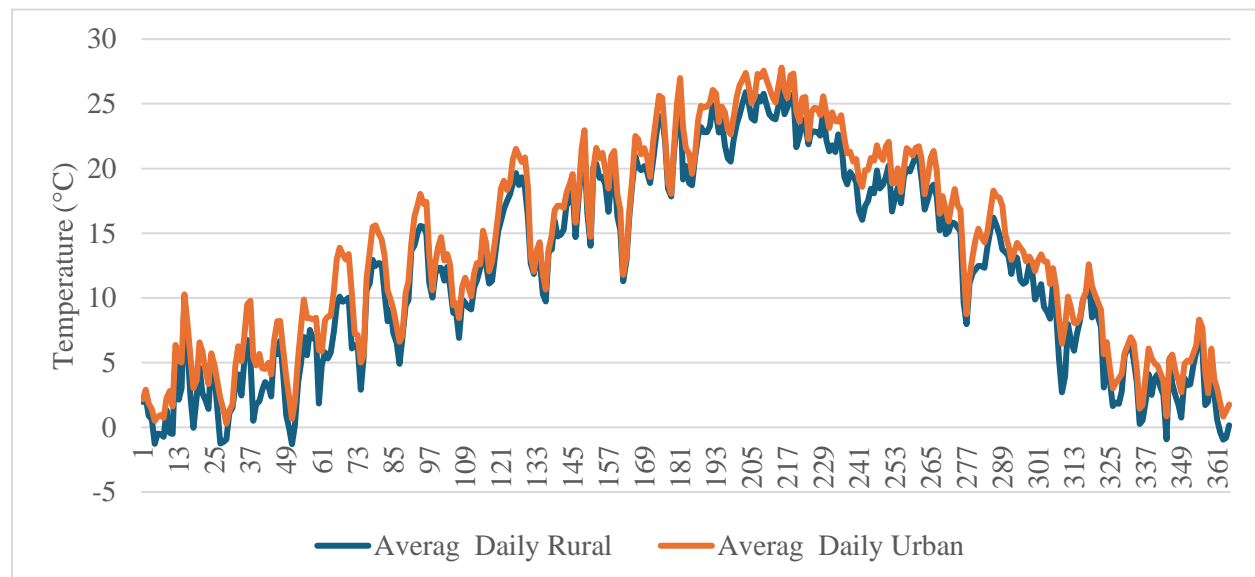


*Figure 35: Annual Average Daily Temperatures for Rural and Urban Areas*

In the current scenario, the temperature difference between urban and rural areas ranges from 1.1°C to 2.3°C, with an average difference of 1.7°C. This variation is evident in both Table 8 and Figure 36, which highlight the monthly average temperatures for urban and rural settings.

Table 8: Monthly Average Temperatures for Urban and Rural with Temperature Differences

Monthly Average tempreture		
Rural	Urban	Difference
1.8	3.4	1.6
3.9	6.1	2.3
8.1	10.4	2.2
11.9	13.3	1.4
16.0	17.3	1.3
19.5	20.6	1.1
23.0	24.8	1.7
22.0	23.8	1.8
18.2	19.8	1.7
12.4	14.2	1.9
6.3	7.8	1.5
2.6	4.1	1.5

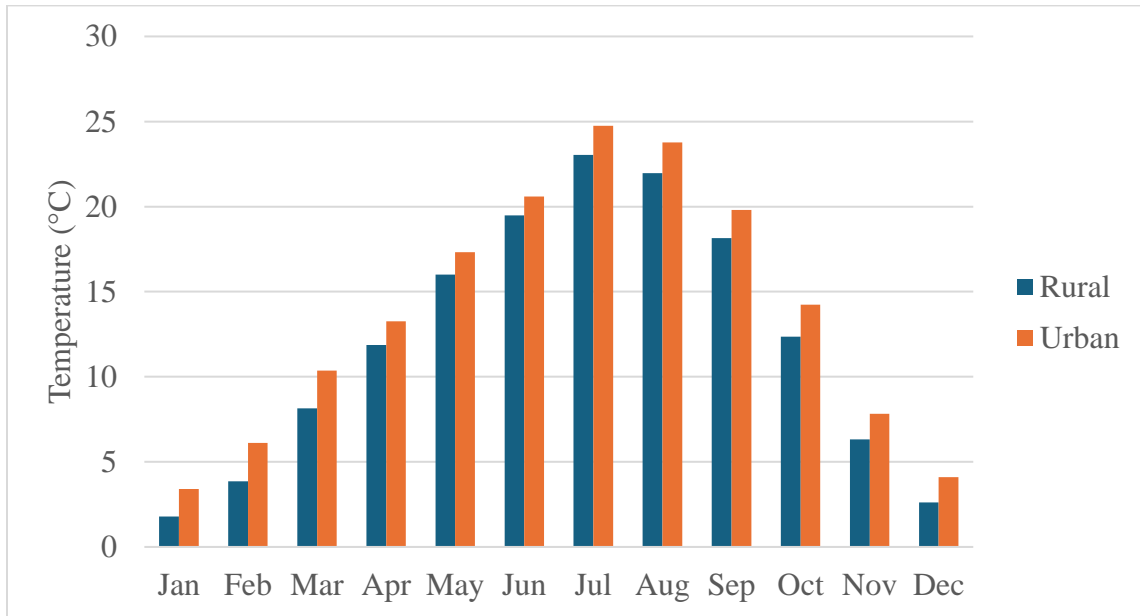
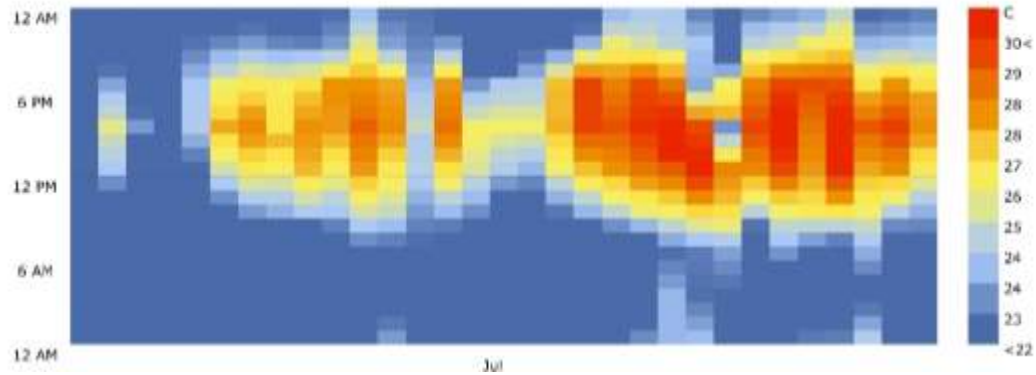


Figure 36: Monthly Average Temperatures for Urban and Rural

To provide a more precise analysis, July has been chosen as the critical month for detailed examination. In the rural weather file, before accounting for the UHI effect, the heat map displays July's rural dry bulb temperatures, which peak in the afternoon and evening. Temperatures range

from below 22°C to above 30°C, with significant fluctuations observed throughout the month (see Figure 37).



*Figure 37: July hourly rural dry bulb temperature*

The corresponding heat map after accounting for the UHI effect is shown in Figure 38. This figure demonstrates the impact of urbanization on temperature profiles.

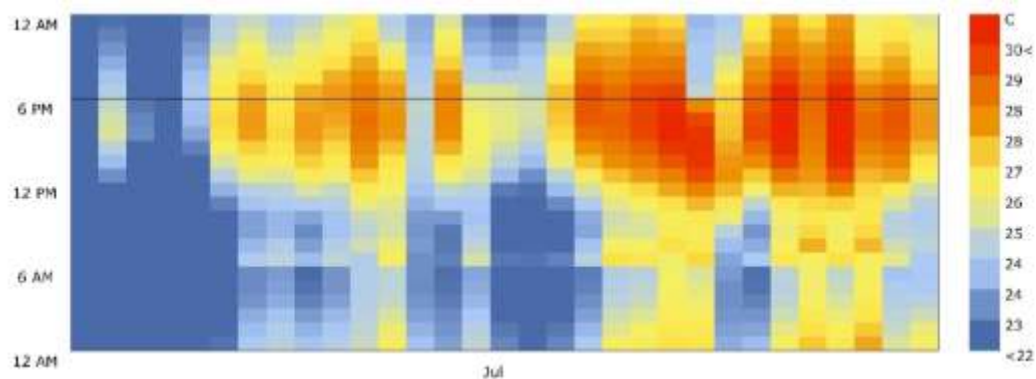


*Figure 38: July hourly rural dry bulb temperature*

For better comparison, the Figure 39 shows the difference between July temperatures before and after considering the UHI effect. Urban temperatures exhibit similar daily patterns but show higher overall temperatures and more pronounced evening peaks compared to rural areas, highlighting the UHIs effect. The urban temperature pattern also demonstrates less amplitude variation throughout the day, even though the maximum temperatures reached are nearly the same for both

urban and rural areas. This reduced temperature oscillation in urban environments is attributed to the higher heat capacity of urban materials, which store and slowly release heat, thereby moderating temperature fluctuations and sustaining higher temperatures during the evening.

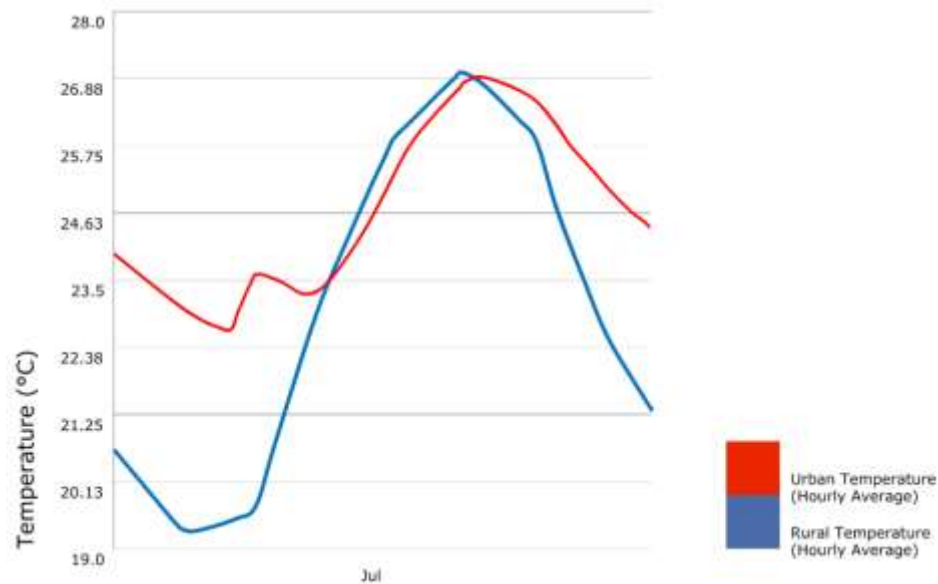


Figure 39: July temperatures showing UHI effect

### 5.3.2 2050 UHIs analysis result

To provide a comprehensive comparison with the current situation, the color legend used in the following figures remains consistent with previous sections.

Figure 40 illustrates the hourly rural dry bulb temperature for July in the year 2050. As observed, there is a notable increase in the average temperatures compared to the present day, with higher peaks during the afternoon and a more extended duration of elevated temperatures throughout the day and night.

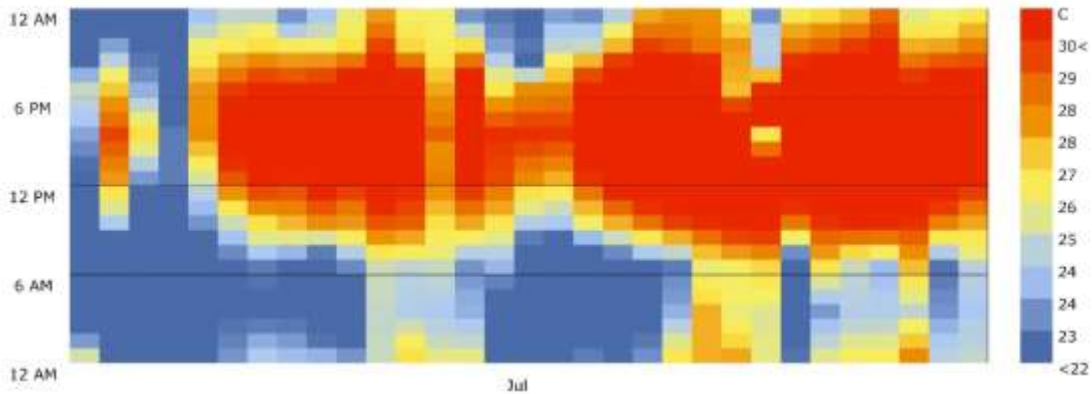


Figure 40: July hourly **rural** dry bulb temperature for 2050

Figure 41 displays the hourly urban dry bulb temperature for July in 2080. The urban temperatures are significantly higher than rural temperatures, particularly during the evening and nighttime hours, further emphasizing the intensification of the UHIs effect in urban areas. The data suggests a stronger and more prolonged heat retention in urban environments due to climate change impacts.

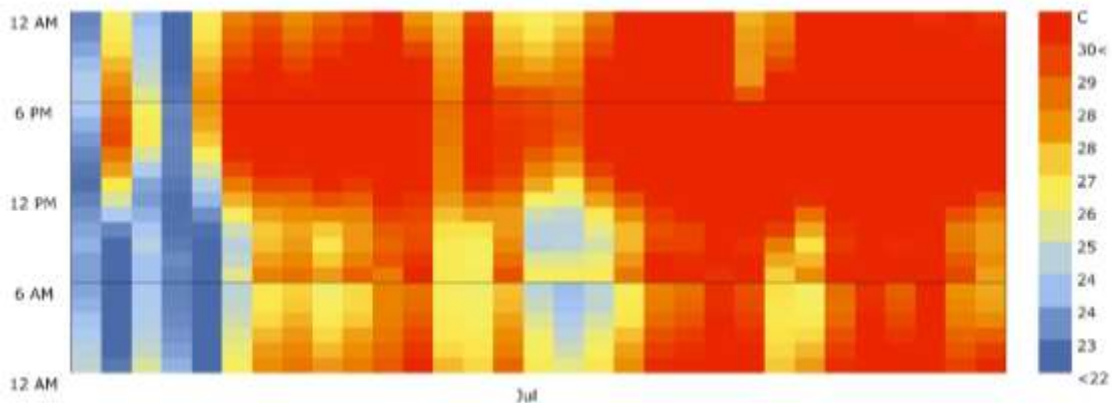
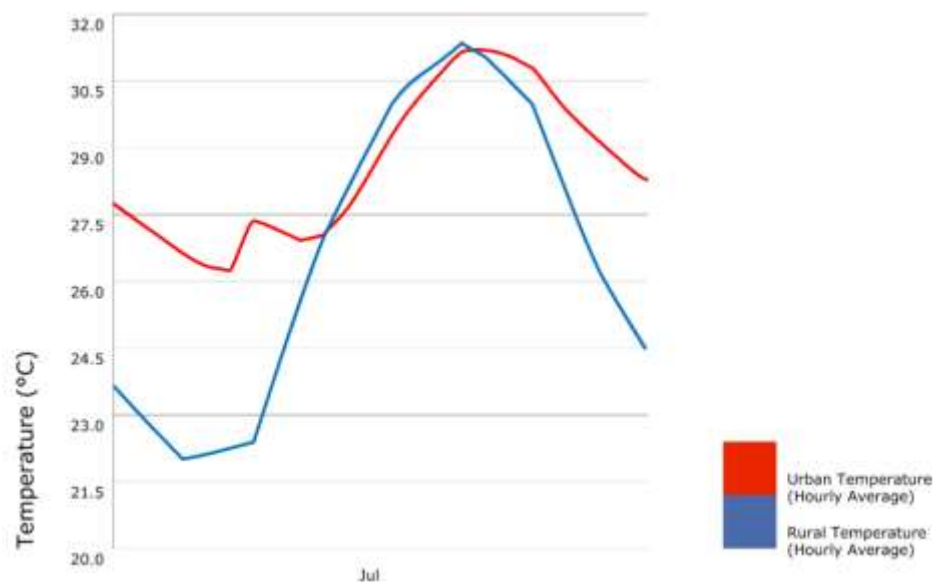


Figure 41: July hourly **urban** dry bulb temperature for 2050

Figure 42 presents the UHI effect for July in 2050. The graph clearly demonstrates that urban temperatures (represented by the red line) are consistently higher than rural temperatures (represented by the blue line) throughout the day, with the most pronounced differences occurring during peak afternoon and evening hours. This indicates an amplified UHI effect in the future



climate scenario for 2050, highlighting the growing challenge of managing urban heat in a warming climate.



*Figure 42: July 2050 UHI effect*

These figures underline the potential escalation of urban heat challenges in the future and the necessity for adaptive urban planning and climate mitigation strategies to address the heightened UHI effects projected for 2050.

### 5.3.3 2080 UHIs analysis result

The 2080 analysis reveals a further intensification of the UHIs effect compared to both the current and 2050 scenarios. Maintaining the same color legend for consistency, the results show a noticeable rise in average temperatures throughout July, especially during peak daytime hours.

In rural areas, there is a marked increase in average temperatures, with a more extended duration of higher temperatures into the late afternoon. Urban areas, however, show even more significant

temperature elevations, with prolonged periods of heat extending into the evening. This reflects a worsening UHI effect, where urban environments retain heat much longer (See Figure 43 till Figure 45).

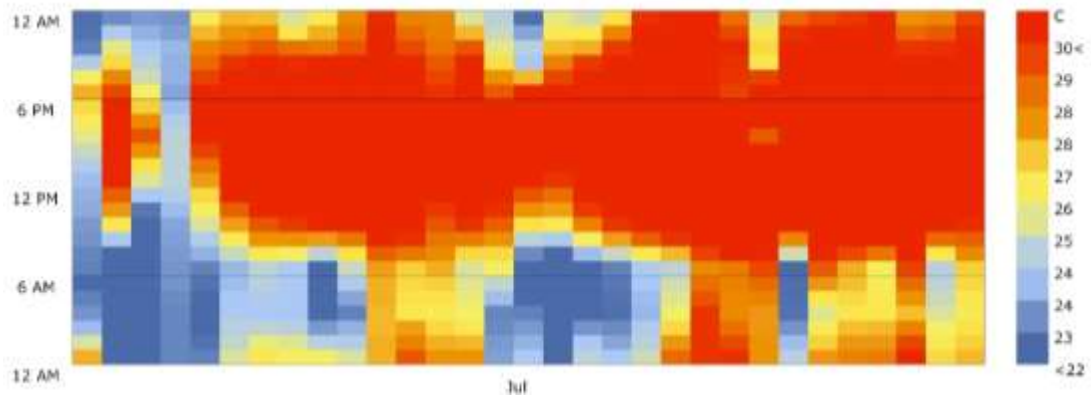


Figure 43: July hourly **rural** dry bulb temperature for 2080

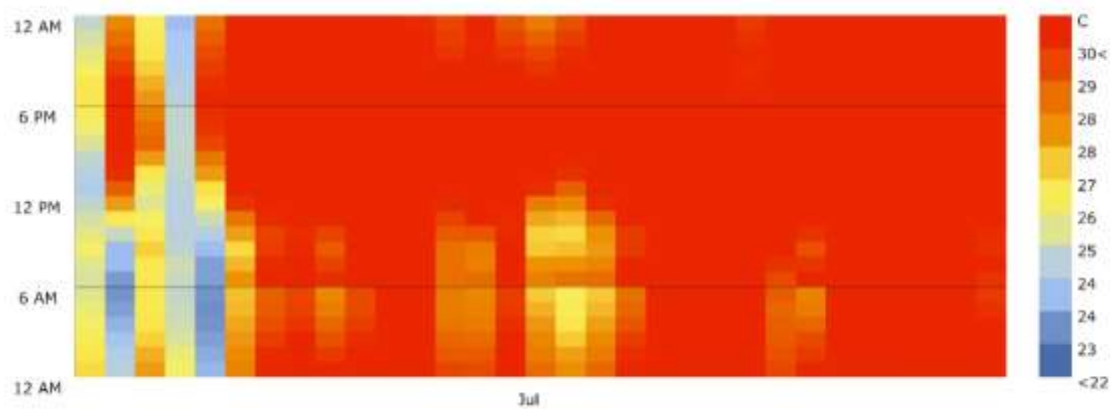
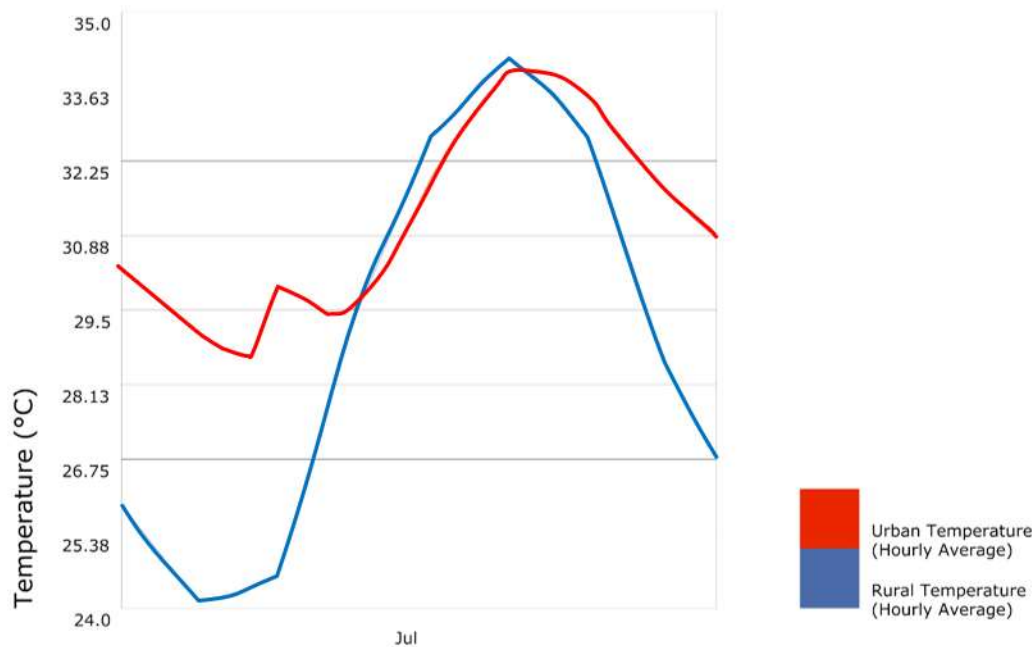


Figure 44: July hourly **urban** dry bulb temperature for 2080



*Figure 45: July 2080 UHI effect*

Furthermore, there are several instances where maximum temperatures surpass 30°C for three consecutive days, meeting the Italian Alert System's definition of a heatwave (Lo Scalzo et al., 2009). This increase in heatwave days presents a substantial health risk, particularly for vulnerable populations without access to adequate cooling solutions.

#### 5.3.4 Comparison of current and future UHI effects in defined KPIs

Figure 46 presents a comparative analysis of July urban temperatures for the current period, 2050, and 2080 which presented before. The figure uses the same temperature scale and legend across all three graphs to illustrate the projected rise in temperatures over time. The comparison highlights a significant increase in temperature levels in future scenarios, with notable warming observed, especially during evening and nighttime hours.

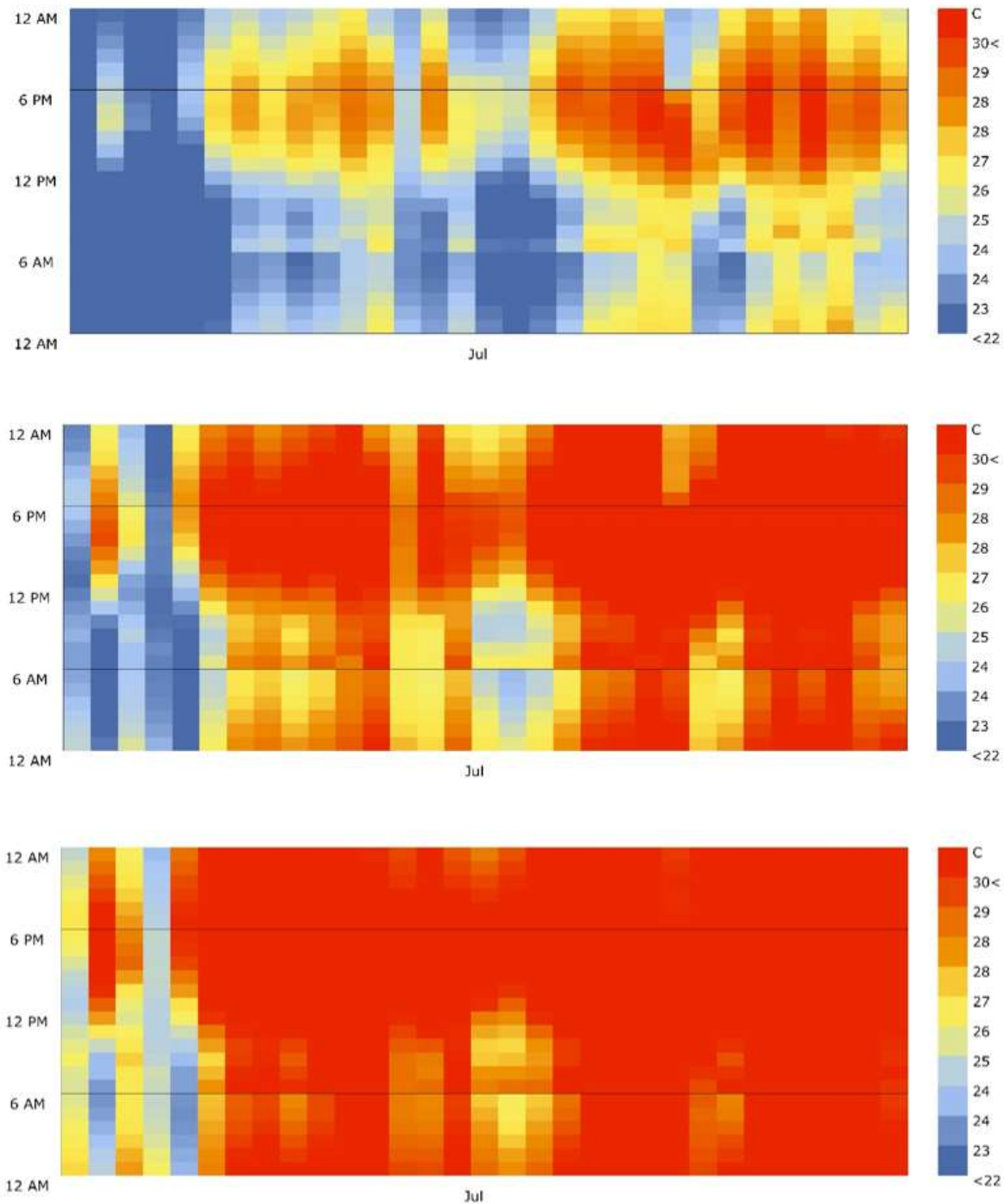


*Figure 46: July urban temperature graph for current, 2050 and 2080 arranged from top to bottom*

The analysis indicates that UHIs effects are expected to become more severe from the current period to 2050 and further into 2080. As shown in Figure 47, the UHI effect intensifies over time, increasing progressively from the current period to 2050, and even more so by 2080. This figure

highlights a clear trend of rising temperatures, especially during the summer months, reflecting the growing heat retention in urban areas (Values in the figure are hourly averaged throughout month).

These findings underscore the urgent need for effective strategies to manage the increasing heat stress in urban environments, as the data points to a future with more extreme UHI effects if no mitigation measures are implemented.

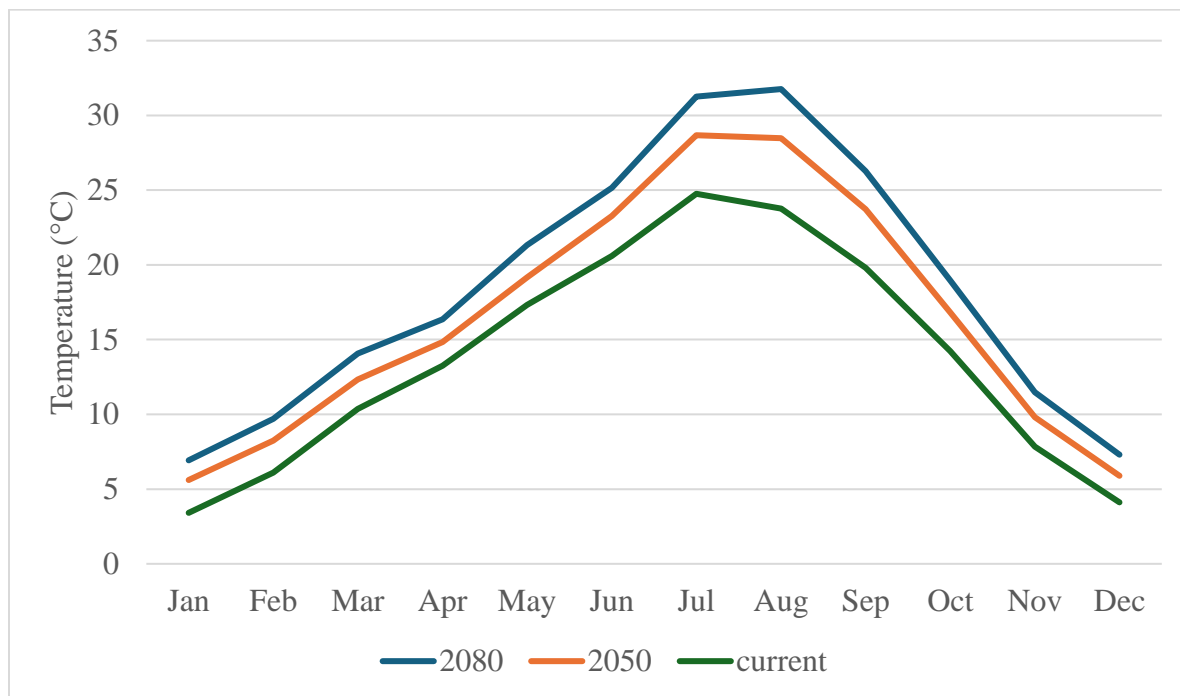


*Figure 47: Comparison of UHI effects (Urban) for current, 2050, and 2080 periods.*

Figure 48 provides a detailed comparison of average monthly temperatures for both rural and urban areas for current and 2080. It illustrates that while temperatures rise in both environments, urban areas experience a significantly more pronounced increase. The gap between rural and urban temperatures widens over time, emphasizing the intensifying impact of urbanization and climate change on heat exposure.

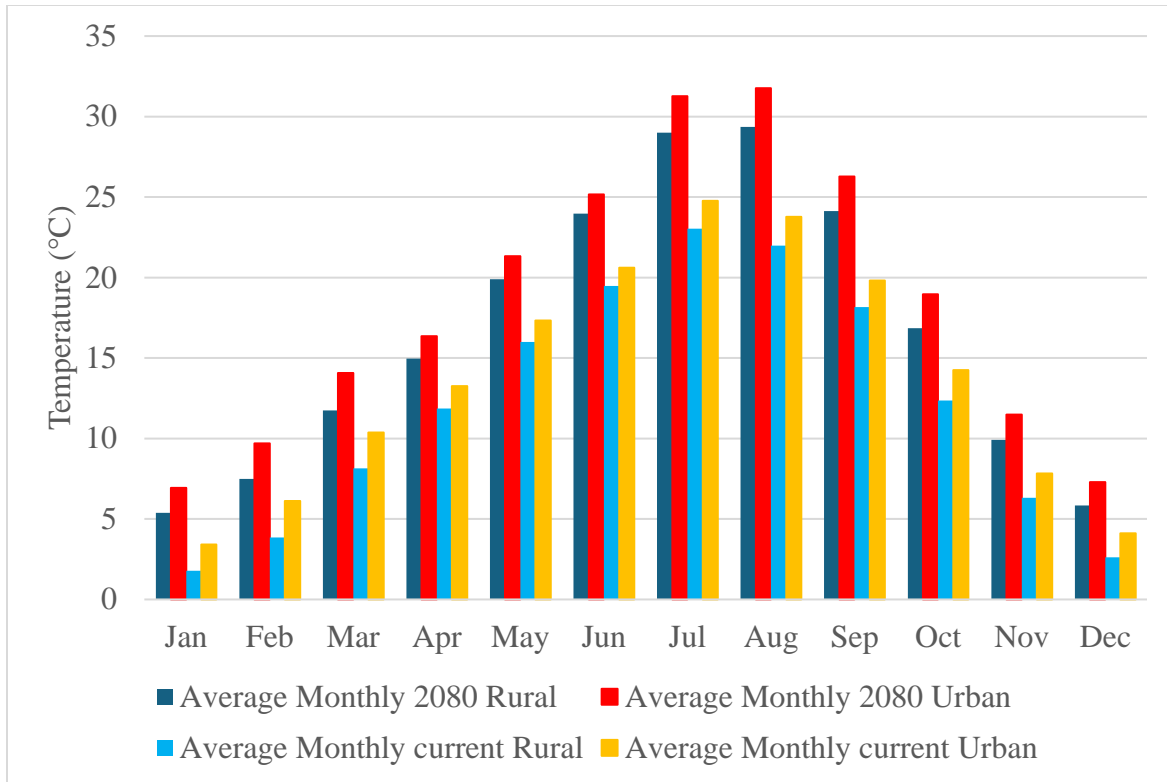


Figure 48: Average monthly temperatures for rural and urban areas in the current, 2050, and 2080 periods.

According to the results gathered in Table 9, the average annual temperature in Turin's rural areas is projected to reach 16.4°C by 2080, representing a 19.86% increase from the current average of 13.8°C. In urban areas, the average annual temperature is expected to rise to 18.38°C by 2080, which marks a 26.99% increase from the current average of 14.47°C.

Table 9: Projected Average Annual Temperatures in Turin (°C)

Area	Current	2050	2080
Urban	14.47°C	16.40°C (+13.35%)	18.38°C (+26.99%)
Rural	13.80°C	14.69°C (+6.45%)	16.54°C (+19.86%)

As mentioned in the KPIs section, parameters such as UTCI, UHI Intensity, HDD, and CDD will be analyzed and compared following the implementation of UHI reduction scenarios.

#### 5.3.4.1 *UTCI*

The UTCI is a comprehensive measure of perceived temperature, factoring in humidity, wind speed, and radiation, offering a more realistic "feels-like" temperature compared to standard air temperature readings.

To compare the annual UTCI with average temperatures, Figure 49 illustrates the changes over time for both rural and urban areas. The UTCI, which represents the 'real feel' of temperature, is consistently higher on average than the actual temperatures. This indicates that perceived heat will be more intense in both rural and urban areas, with both UTCI and temperatures projected to increase from the current period to 2050 and 2080. The table also reflects the percentage of growth compared to the current situation. This increase is noticeable for both UTCI and actual temperatures. In rural areas, average temperatures are expected to increase by 6.4% by 2050 and 8.5% by 2080. Urban temperatures are projected to grow by 13.3% by 2080, further emphasizing the impact of UHIs.

As mentioned, the UTCI is designed to capture the "real feel" temperature, which makes it inherently more responsive to changes in both meteorological conditions and human thermal comfort. For example, a rise in temperature combined with high humidity levels can significantly affect UTCI, even if the actual temperature change is modest.

In scenarios where heatwaves become more frequent or prolonged (as projected for 2050 and 2080), the UTCI will reflect these changes more dramatically than standard temperature metrics.

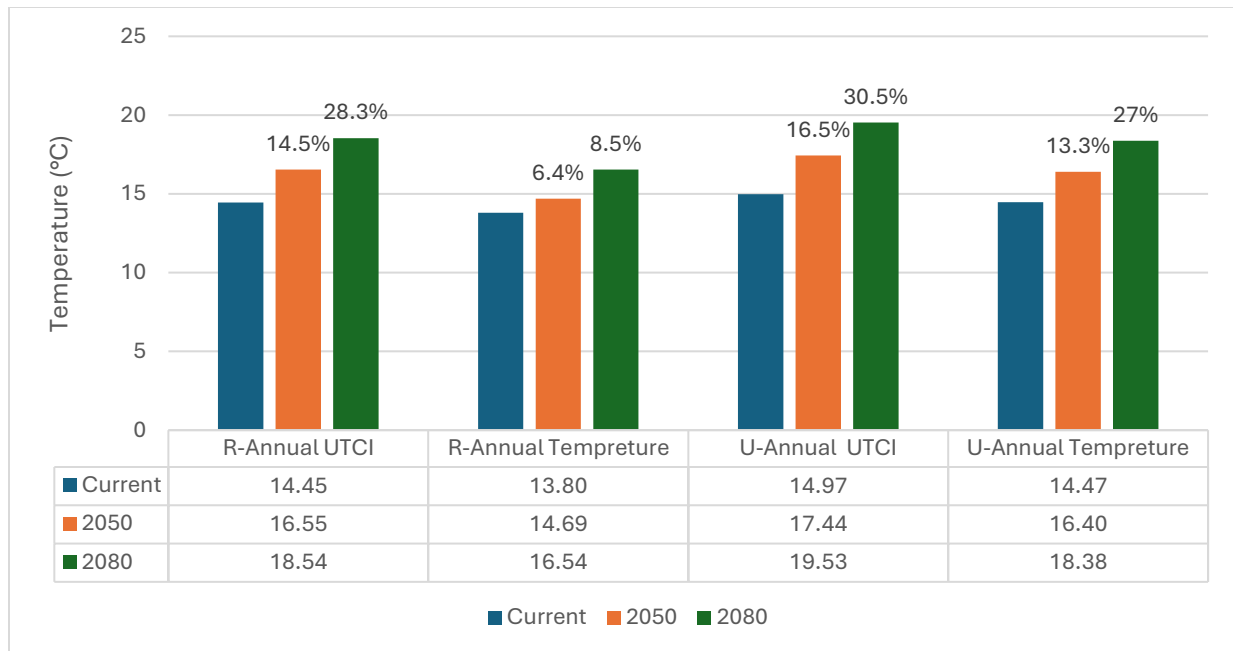


Figure 49: Projected Changes in Annual UTCI and Average Temperatures for **R**ural and **U**rban Areas in Turin (Current, 2050, 2080)

As discussed earlier, this study will compare UTCI across four periods:

- Mean summer daytime air temperature UHI
- Mean summer nighttime air temperature UHI
- Mean winter daytime air temperature UHI
- Mean winter nighttime air temperature UHI

This is because during summer daytime, the UHI effect amplifies heat stress due to high solar radiation, while nighttime analysis reveals the persistence of elevated temperatures in urban areas, impacting recovery from daytime heat. Winter daytime and nighttime comparisons are crucial for understanding how UHI modifies cold stress and overall energy demands in urban settings.

The results for the current situation of the site are provided in Figure 50 and Figure 51.



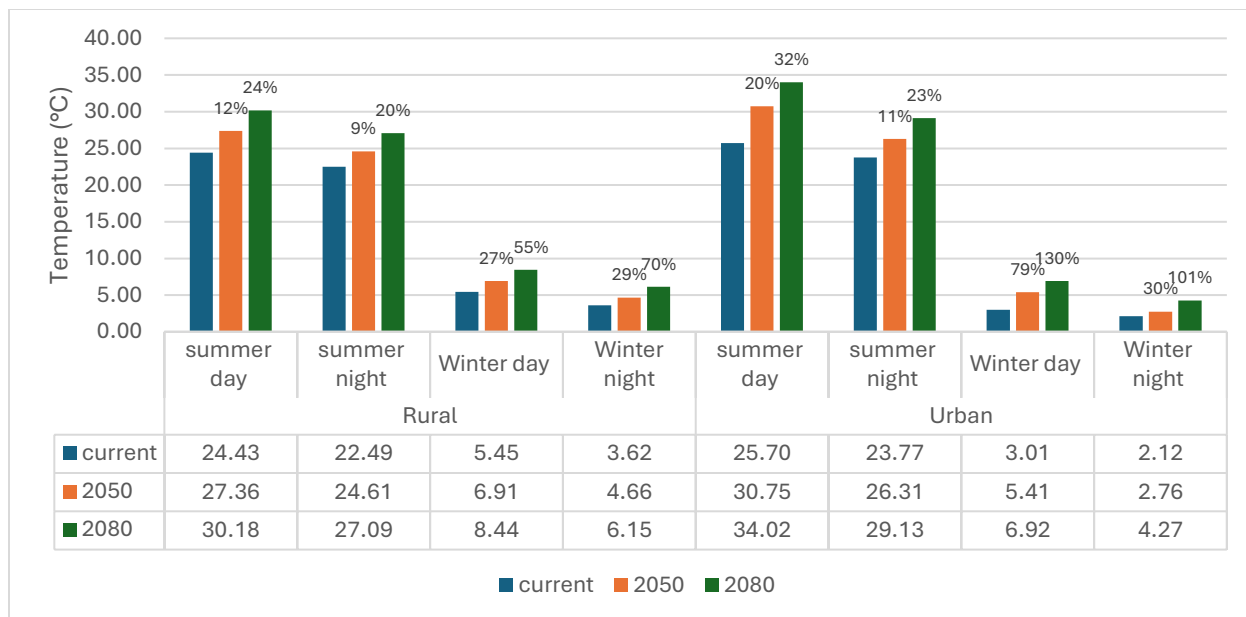


Figure 50: Seasonal Average UTCI Projections for Rural and Urban Areas in Turin: Contemporary, 2050, and 2080

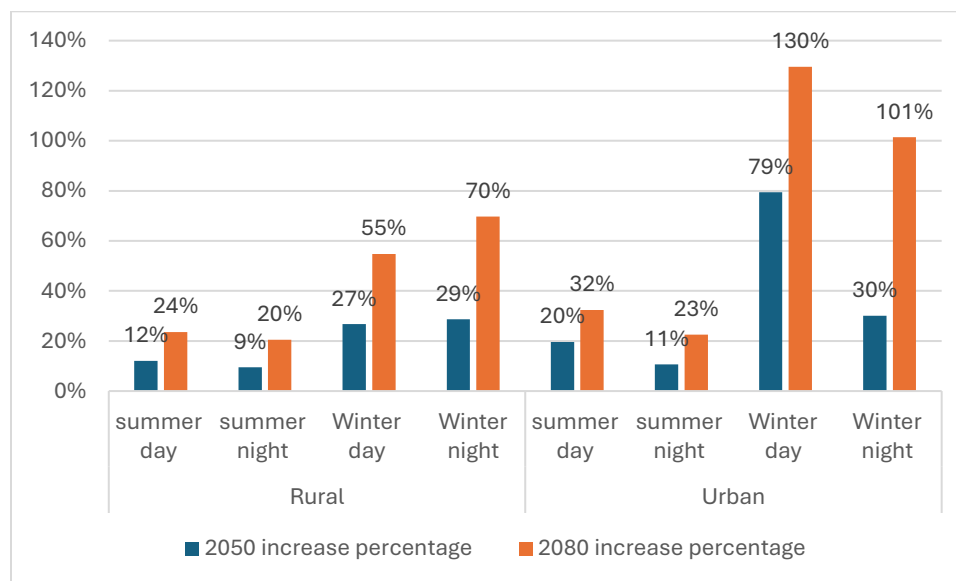


Figure 51: The percentage of increase in UTCI in different time of year for Urban and Rural for 2050 and 2080

**Summer Day and Night:** Both rural and urban areas show a clear increase in UTCI values from the present day to 2050 and 2080. The rise is more significant in urban areas due to the Urban Heat

Island (UHI) effect, with night-time temperatures showing notable growth. This indicates increasing thermal discomfort, particularly in cities, where the warming effect is amplified.

**Winter Day and Night:** Although winter UTCI values are lower than summer, the projected increases by 2050 and 2080 are still substantial. Urban areas, in particular, will experience dramatic increases in winter day and night UTCI, signaling that even the coldest periods will become warmer. This trend points to a clear warming effect throughout the year.

**Urban vs. Rural:** Urban areas show consistently higher UTCI values compared to rural areas across all seasons. For example, urban summer day UTCI is expected to increase by over 30% by 2080, while rural areas will see a rise of around 24%. Similarly, urban winter UTCI will experience much sharper growth, with up to 130% increases, compared to more moderate rises in rural areas. This indicates that urban environments will face heightened thermal stress, particularly in summer and winter, necessitating focused mitigation strategies.

#### *5.3.4.2 UHI Intensity*

In this section, the difference between the rural and urban UTCI values will be calculated for selected time periods. See Figure 52.

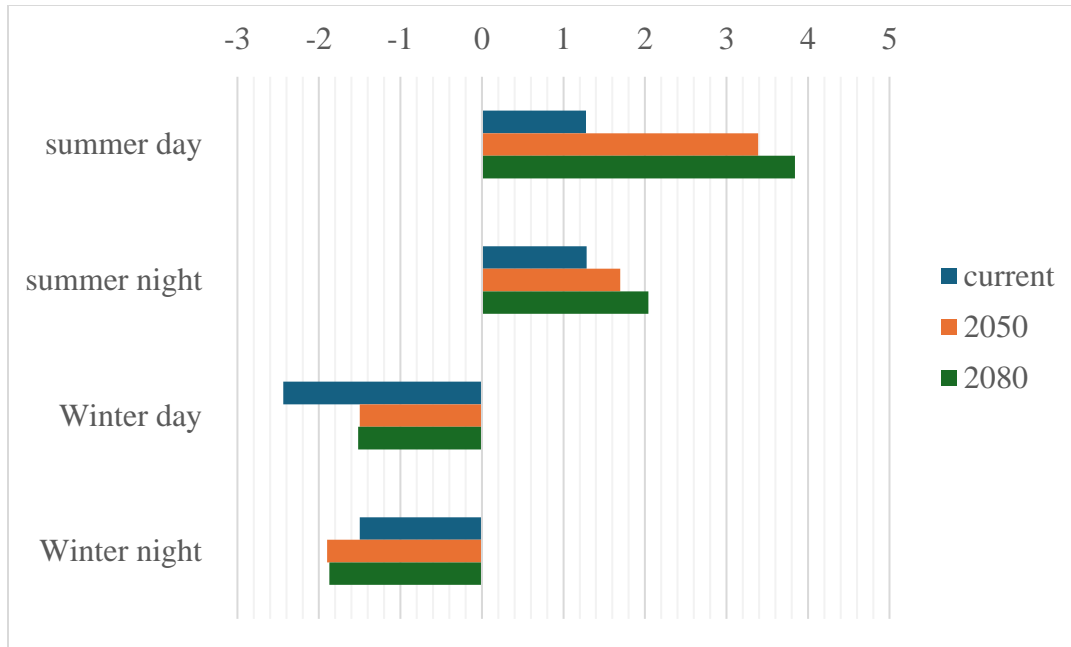


*Figure 52: Projected UHI Intensity Differences Between Rural and Urban Areas Across Seasons and Time of Day (Current, 2050, 2080)*

The data reveals that the UHI effect is most pronounced during the summer, particularly during the day, and this intensity is expected to increase significantly by 2080. Conversely, in winter, urban areas tend to be cooler than rural ones, with minimal changes projected over time. This occurs due to reduced solar radiation in winter, which lowers the heat retention effectiveness of urban materials like concrete and asphalt. In rural areas, snow or frost cover can reflect sunlight and maintain lower temperatures. Consequently, the temperature difference between urban and rural areas is less pronounced in winter, as the typical heat-retaining properties of urban environments are not as impactful under these conditions.

#### 5.3.4.3 HDD and CDD

The analysis for Turin indicates a general warming trend, resulting in a decrease in HDD and an increase in CDD from contemporary times to the years 2050 and 2080 (Figure 53). This trend is more pronounced in urban areas due to the UHIs effect, where urban areas consistently show lower

HDD and higher CDD compared to rural areas, suggesting warmer conditions year-round. Specifically, HDD with UHI is projected to decrease by approximately 14.4% from current levels to 2080, while CDD with UHI is expected to increase by around 352% over the same period. As a result, Turin will experience a shift in energy demand from heating to cooling, particularly in urban environments, impacting future building designs, HVAC<sup>10</sup> systems, and energy policies.

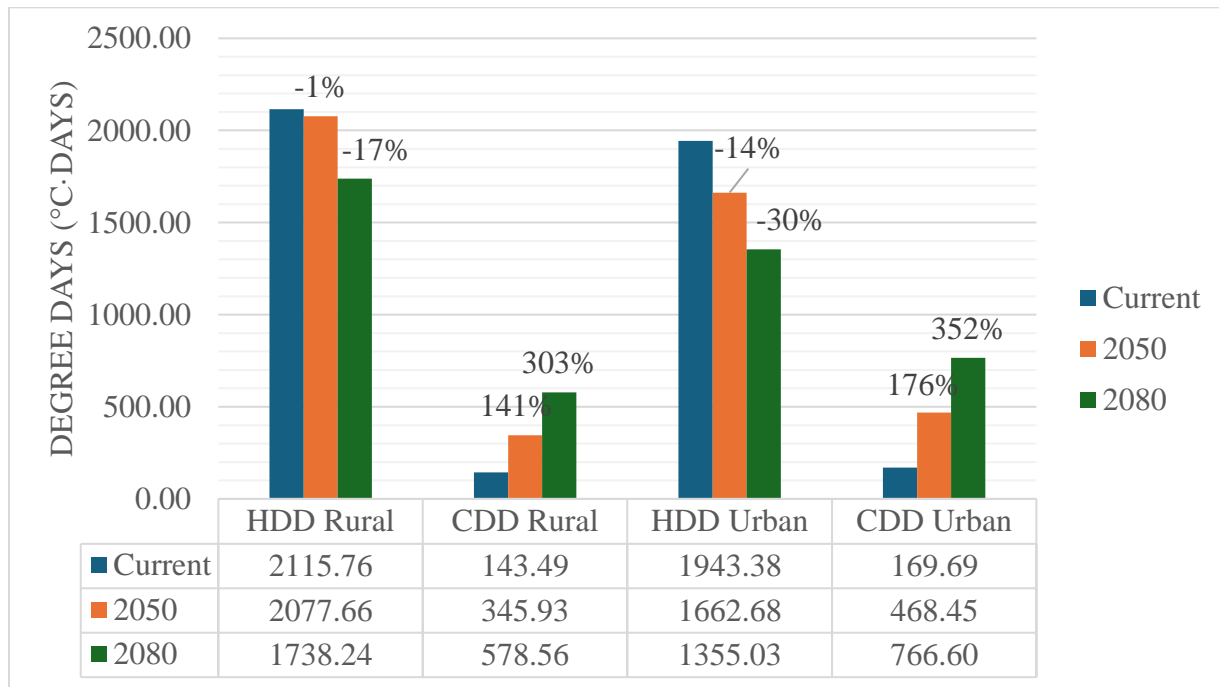


Figure 53: Projected Changes in Heating and Cooling Degree Days (HDD and CDD) for Rural and Urban Areas with UHI Effect (Current, 2050, 2080)

## 5.4 Conclusion

This chapter explores the phenomenon of UHIs in Turin, employing remote sensing and advanced 3D modeling techniques to pinpoint and analyze areas most susceptible to elevated temperatures.

<sup>10</sup> Heating, Ventilation, and Air Conditioning

Utilizing data from Google Earth Engine and Dragonfly within the Rhino environment, the study effectively maps land surface temperatures (LST) and simulates microclimatic conditions to gain insights into UHI dynamics. The findings reveal significant heat retention in urban cores and industrial zones, particularly in areas like the Mirafiori complex, underscoring the importance of targeted mitigation strategies.

Simulations project an increase in UHI intensity, with urban temperatures consistently surpassing rural ones. The study forecasts a rise in CDD and a decrease in HDD by 2050 and 2080, indicating a shift towards greater cooling needs in urban environments due to intensifying heat retention. These trends highlight the growing challenge of managing heat stress and energy demand in cities as climate change progresses.

The results emphasize the urgent need for sustainable urban planning and effective UHI mitigation measures, such as increasing vegetation, utilizing reflective materials, and optimizing urban design to enhance airflow, ultimately aiming to create more resilient and livable urban environments.

# 6 Assessing mitigation strategies

## 6.1 Development of mitigation scenarios

Building upon the findings from previous chapters, this section explores targeted strategies to mitigate UHI effects in Turin. The focus is on practical approaches that leverage both environmental and material modifications to enhance urban resilience.

While many more strategies can be implemented in real life, the strategies presented here are developed considering software limitations and capabilities. The proposed mitigation strategies focus on three main approaches:

- **Material and albedo modifications:** Implementing surfaces with high reflectivity to reduce heat absorption.
- **Green space development:** Increasing vegetation coverage to provide cooling effects through shade and evapotranspiration.
- **Combination strategies:** Integrating multiple approaches to maximize cooling potential and urban resilience.

These scenarios are evaluated using the previously defined KPIs (UTCI, UHI intensity, HDD, and CDD). Following the development of these potential mitigation strategies, Dragonfly will be used to simulate various UHI mitigation scenarios for Turin. These simulations will enable a comparison of the effectiveness of different strategies in mitigating UHIs and enhancing thermal comfort within the city. These scenarios are represented in Figure 54.

It should be noted that these parameters change by adjusting their value or percentage in Dragonfly, not by modifying the 3D model itself. For example, it can be specified that 50% of the roof is vegetation or 90%, as discussed in Section 5.2.1 and shown in Figure 28.

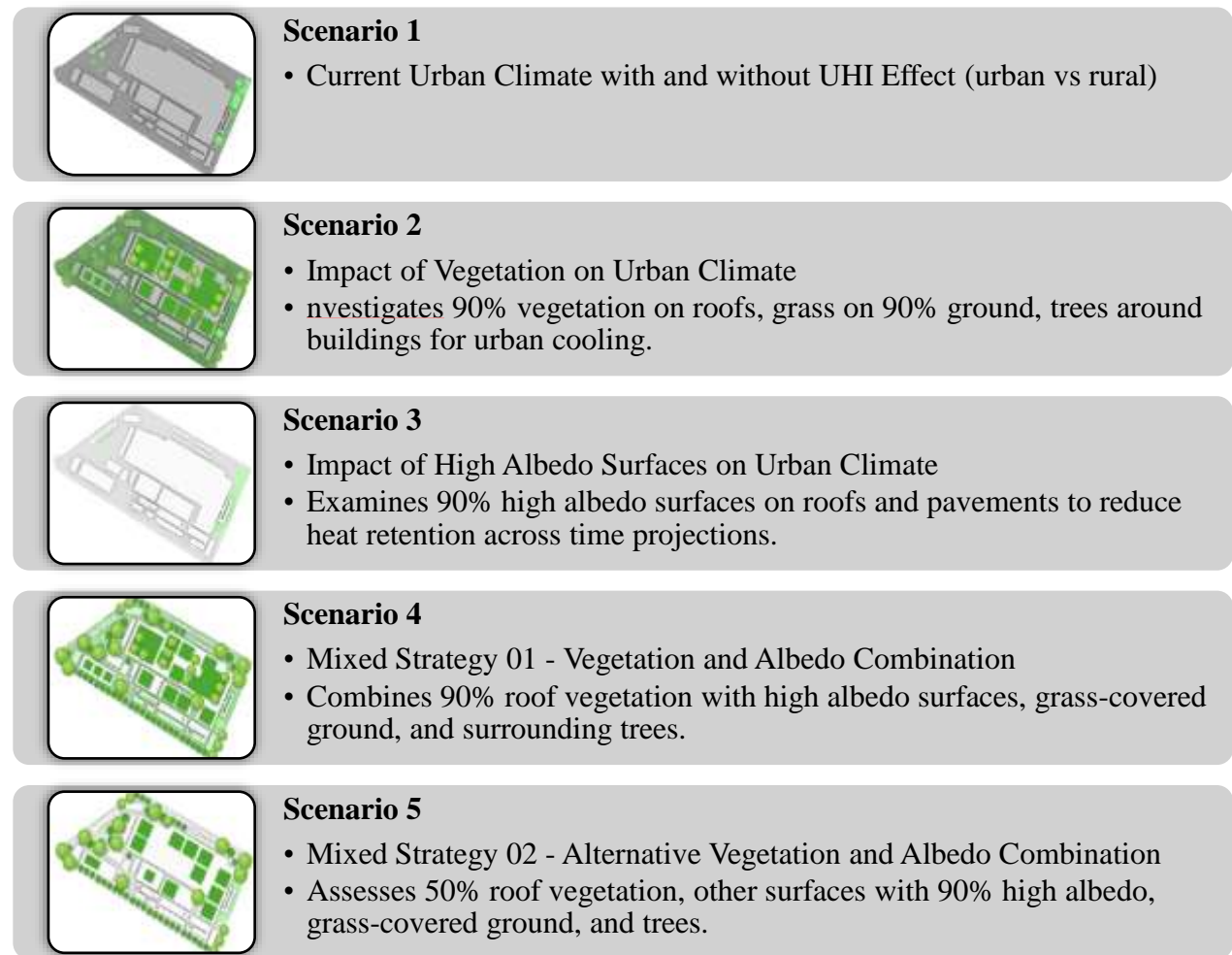


*Figure 54: defining 5 main scenarios for comparison*

## 6.2 Result of analysis

### 6.2.1 Scenario 1

This is a foundational scenario that was introduced in detail in Chapter Five. It serves as a basis for comparison with other scenarios presented in this chapter (Table 10 and Table 11).

As discussed before the results show that both UTCI and Temp increase from contemporary levels to 2050 and 2080 in rural and urban contexts, indicating rising temperatures. In urban settings, UTCI values are higher for Summer Day and Night compared to rural areas, reflecting the influence of UHI effects. HDD values decrease over time, while CDD values rise, pointing to a growing need for cooling in both environments. These trends emphasize the significance of addressing UHI effects in urban planning to improve thermal comfort and manage future cooling demands effectively.

*Table 10: scenario 1 Rural data*

<b>KPIs</b>	<b>Current</b>	<b>2050</b>	<b>2080</b>
<i>UTCI Annual [°C]</i>	14.46	16.56 (+14.52%)	18.54 (+28.22%)
<i>Temp Annual[°C]</i>	13.8	14.64 (+6.09%)	16.54 (+19.86%)
<i>UTCI Summer Day[°C]</i>	24.43	27.36 (+11.99%)	30.18 (+23.54%)
<i>UTCI Summer Night[°C]</i>	22.48	24.61 (+9.48%)	27.09 (+20.51%)
<i>UTCI Winter Day[°C]</i>	5.45	6.91 (+26.79%)	8.44 (+54.86%)
<i>UTCI Winter Night[°C]</i>	3.62	4.66 (+28.73%)	6.14 (+69.61%)
<i>Heating Degree-Days [°C-days]</i>	2115.75	2077.65 (+-1.80%)	1738.24 (+-17.84%)
<i>Cooling Degree-Days[°C-days]</i>	143.49	345.93 (+141.08%)	578.56 (+303.21%)

*Table 11: scenario 1 Urban data*

<b>KPIs</b>	<b>Current</b>	<b>2050</b>	<b>2080</b>
<i>UTCI Annual [°C]</i>	14.97	17.44 (+16.50%)	19.54 (+30.53%)
<i>Temp Annual[°C]</i>	14.47	16.41 (+13.41%)	18.38 (+27.02%)



<i>UTCI Summer Day[°C]</i>	25.7	30.75 (+19.65%)	34.01 (+32.33%)
<i>UTCI Summer Night[°C]</i>	23.77	26.3 (+10.64%)	29.13 (+22.55%)
<i>UTCI Winter Day[°C]</i>	3.01	5.41 (+79.73%)	6.92 (+129.90%)
<i>UTCI Winter Night[°C]</i>	2.12	2.76 (+30.19%)	4.27 (+101.42%)
<i>Heating Degree-Days [°C-days]</i>	1943.38	1662.68 (+-14.44%)	1355.03 (+-30.27%)
<i>Cooling Degree-Days[°C-days]</i>	169.69	468.45 (+176.06%)	766.6 (+351.76%)

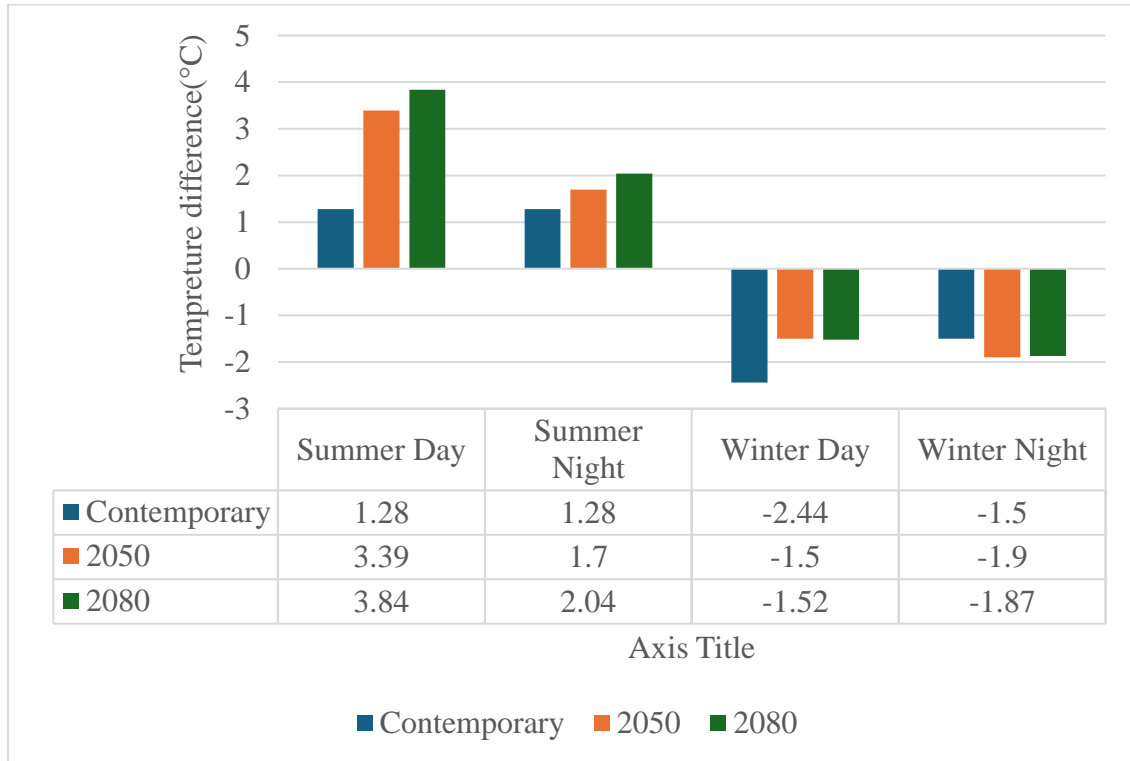


Figure 55: UHI Intensity for current situation of site

Figure 55 shows increasing urban-rural temperature differences in Turin, especially in summer, due to the UHIs effect, with a peak by 2080. In winter, the temperature differences decrease, indicating a reduced UHI effect during colder months.

### 6.2.2 Scenario 2

Scenario 2 introduces vegetation on 90% of roofs and surrounding factory areas to study its effect on urban climate and thermal comfort, while keeping albedo constant. Compared to Scenario 1,

Scenario 2 shows slightly lower UTCI Annual and Temp Annual values by 2080, suggesting a modest reduction in overall thermal stress due to increased vegetation. However, UTCI Summer Day and Night values in Scenario 2 are like Scenario 1, indicating comparable heat stress levels during the warmer months (Table 12). UHI Intensity is slightly lower in Scenario 2, reflecting reduced UHI effects from enhanced vegetation. Additionally, Scenario 2 presents slightly higher CDD and lower HDD, pointing to increased cooling needs and reduced heating requirements, emphasizing the effectiveness of vegetation in mitigating UHI effects and enhancing urban thermal comfort (Figure 56).

*Table 12: Simulation Results for Scenario 2*

<b>KPIs</b>	<b>Current</b>	<b>2050</b>	<b>2080</b>
<i>UTCI Annual [°C]</i>	14.94	17.41 (+16.53%)	19.5 (+30.52%)
<i>Temp Annual[°C]</i>	14.43	16.36 (+13.37%)	18.34 (+27.10%)
<i>UTCI Summer Day[°C]</i>	25.59	30.62 (+19.66%)	33.87 (+32.36%)
<i>UTCI Summer Night[°C]</i>	23.77	26.3 (+10.64%)	29.13 (+22.55%)
<i>UTCI Winter Day[°C]</i>	2.94	5.35 (+81.97%)	6.85 (+132.99%)
<i>UTCI Winter Night[°C]</i>	2.1	2.75 (+30.95%)	4.26 (+102.86%)
<i>Heating Degree-Days [°C-days]</i>	1950.48	1668.53 (+-14.46%)	1359.77 (+-30.29%)
<i>Cooling Degree-Days[°C-days]</i>	165.05	460.45 (+178.98%)	757.27 (+358.81%)

Figure 56 indicates a significant rise in summer temperatures by 2050 and 2080, with day temperatures increasing from 1.16°C to 3.69°C. Winter temperatures show a slight warming trend, reducing the cooling effect. Overall, future projections suggest more extreme summer heat compared to milder winter changes.

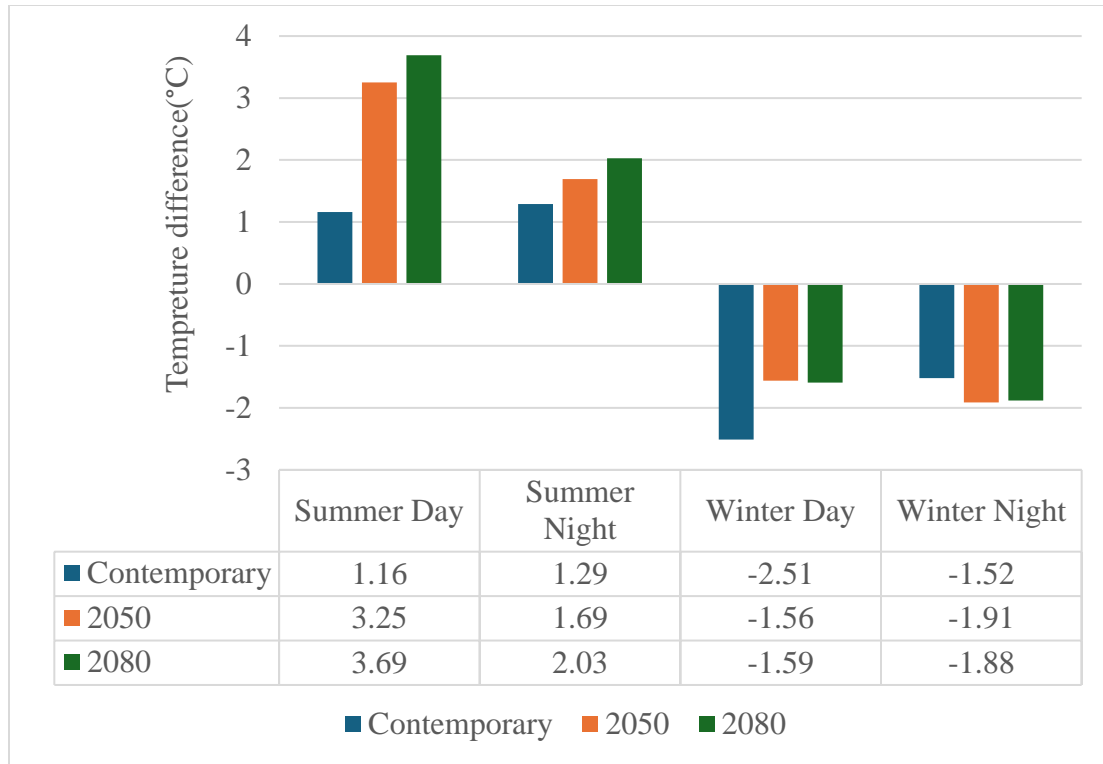


Figure 56: UHI intensity for scenario 2

### 6.2.3 Scenario 3

**Scenario 3** explores the effects of using high albedo (reflective) surfaces on 90% of roofs and 70% of pavements, without incorporating vegetation. It shows similar trends to **Scenario 1**, with slight reductions in UTCI and CDD, suggesting some mitigation of UHI effects. However, its impact is less pronounced compared to **Scenario 2**, which combines high albedo surfaces with extensive vegetation. While Scenario 3 achieves some improvement in reducing heat stress, it is less effective than Scenario 2 in enhancing urban thermal comfort due to the absence of vegetation's cooling benefits (Table 13 and Figure 57).

Table 13: Simulation Results for Scenario 3

KPIs	Current	2050	2080
UTCI Annual [°C]	14.95	17.42 (+16.52%)	19.52 (+30.57%)
Temp Annual[°C]	14.45	16.38 (+13.36%)	18.35 (+26.99%)

<i>UTCI Summer Day[°C]</i>	25.62	30.66 (+19.67%)	33.91 (+32.36%)
<i>UTCI Summer Night[°C]</i>	23.78	26.31 (+10.64%)	29.14 (+22.54%)
<i>UTCI Winter Day[°C]</i>	2.96	5.34 (+80.41%)	6.85 (+131.42%)
<i>UTCI Winter Night[°C]</i>	2.12	2.75 (+29.72%)	4.27 (+101.42%)
<i>Heating Degree-Days [°C-days]</i>	1947.49	1666.58 (+-14.42%)	1358.6 (+-30.24%)
<i>Cooling Degree-Days[°C-days]</i>	167.43	464.77 (+177.59%)	762.17 (+355.22%)

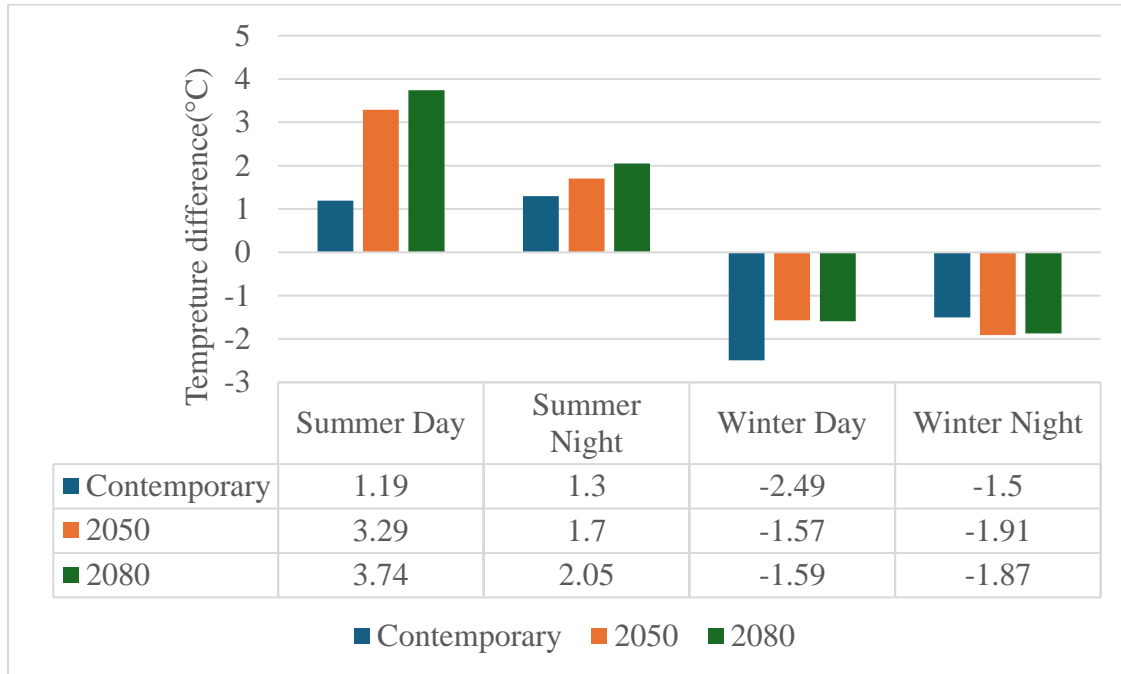


Figure 57: UHI intensity for scenario 3

#### 6.2.4 Scenario 4

Scenario 4 features a multi-faceted approach to mitigate UHIs effects. It includes 90% of roofs covered with vegetation for enhanced insulation and reduced heat gain, while the remaining roofs have a high-reflective coating with an albedo of 90%. Additionally, 90% of the ground is covered with grass, and trees are strategically planted around buildings for shade. High-albedo materials are also used for asphalt (albedo 0.7) and roofs (albedo 0.9), effectively reflecting sunlight and minimizing heat absorption.

Compared to Scenario 3, which only uses reflective surfaces, Scenario 4's integration of vegetation leads to more significant reductions in UTCI and CDD (Table 14 and Figure 58). This approach offers enhanced insulation and cooling, resulting in greater mitigation of UHI effects and improved urban thermal comfort.

Table 14: Simulation Results for Scenario 4

<i>KPIs</i>	<i>Current</i>	<i>2050</i>	<i>2080</i>
<i>UTCI Annual [°C]</i>	14.946	17.414 (+16.51%)	19.509 (+30.53%)
<i>Temp Annual[°C]</i>	14.44	16.37 (+13.37%)	18.343 (+27.03%)
<i>UTCI Summer Day[°C]</i>	25.575	30.602 (+19.66%)	33.851 (+32.36%)
<i>UTCI Summer Night[°C]</i>	23.789	26.313 (+10.61%)	29.137 (+22.48%)
<i>UTCI Winter Day[°C]</i>	2.942	5.33 (+81.17%)	6.831 (+132.19%)
<i>UTCI Winter Night[°C]</i>	2.105	2.761 (+31.16%)	4.275 (+103.09%)
<i>Heating Degree-Days [°C-days]</i>	1948.329	1667.158 (+-14.43%)	1358.471 (+-30.28%)
<i>Cooling Degree-Days[°C-days]</i>	165.754	461.55 (+178.45%)	758.525 (+357.62%)

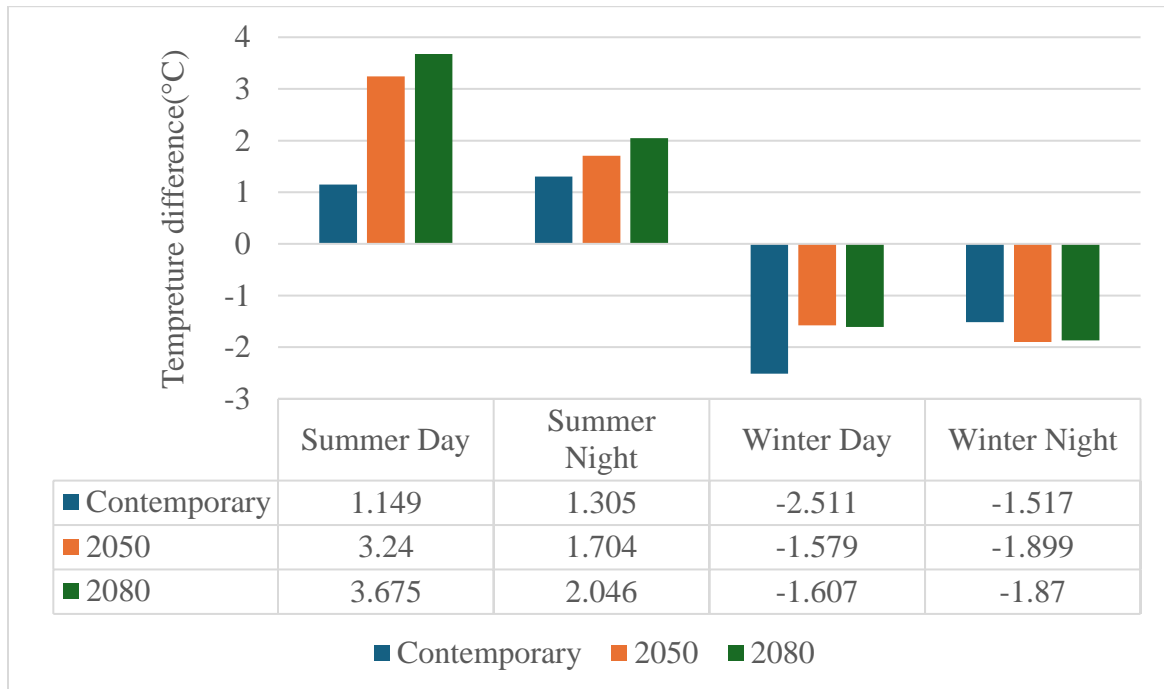


Figure 58: UHI intensity for scenario 4

## 6.2.5 Scenario 5

Scenario 5 evaluates a mixed urban cooling strategy featuring 50% roof vegetation and high-albedo materials (90% reflectivity). Ground surfaces are covered with grass, and trees are planted around buildings. This approach effectively reduces summer heat, achieving slightly lower temperatures during summer days (33.83°C) and nights (29.12°C) in 2080 (Table 15). It balances cooling impacts, mitigates the UHIs effect, and enhances thermal comfort. Practical for urban implementation, it provides long-term benefits in managing temperatures and improving climate resilience.

Also based on Figure 59, The most significant difference in Scenario 5 lies in its adaptability across different seasons. Whereas other scenarios exhibit stronger impacts either in summer or winter, Scenario 5 offers a more balanced solution across both seasons, providing substantial cooling in summer without overcooling in winter.

*Table 15: Simulation Results for Scenario 5*

<b>KPIs</b>	<b>Current</b>	<b>2050</b>	<b>2080</b>
<i>UTCI Annual [°C]</i>	14.939	17.404 (+16.50%)	19.498 (+30.52%)
<i>Temp Annual[°C]</i>	14.429	16.355 (+13.35%)	18.328 (+27.02%)
<i>UTCI Summer Day[°C]</i>	25.555	30.579 (+19.66%)	33.827 (+32.37%)
<i>UTCI Summer Night[°C]</i>	23.775	26.295 (+10.60%)	29.118 (+22.47%)
<i>UTCI Winter Day[°C]</i>	2.942	5.324 (+80.97%)	6.818 (+131.75%)
<i>UTCI Winter Night[°C]</i>	2.108	2.747 (+30.31%)	4.261 (+102.13%)
<i>Heating Degree-Days [°C-days]</i>	1950.438	1669.575 (+-14.40%)	1360.704 (+-30.24%)
<i>Cooling Degree-Days[°C-days]</i>	164.9	459.5 (+178.65%)	756.108 (+358.53%)

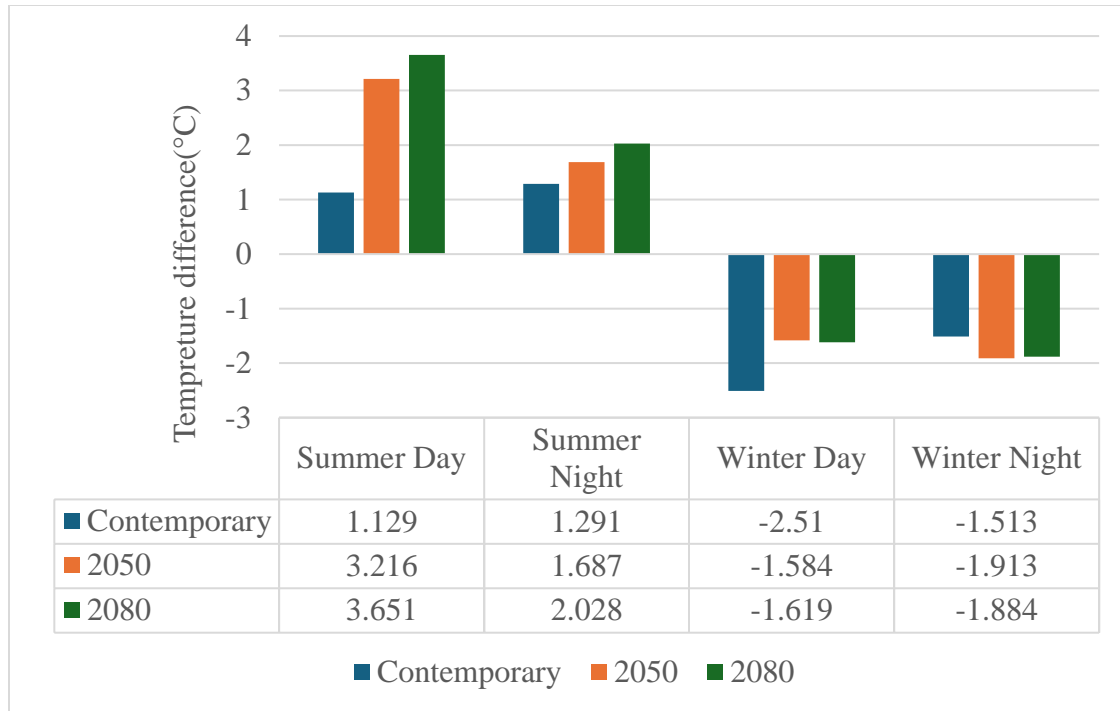


Figure 59: UHI intensity for scenario 5

## 6.3 Compare and define best scenario

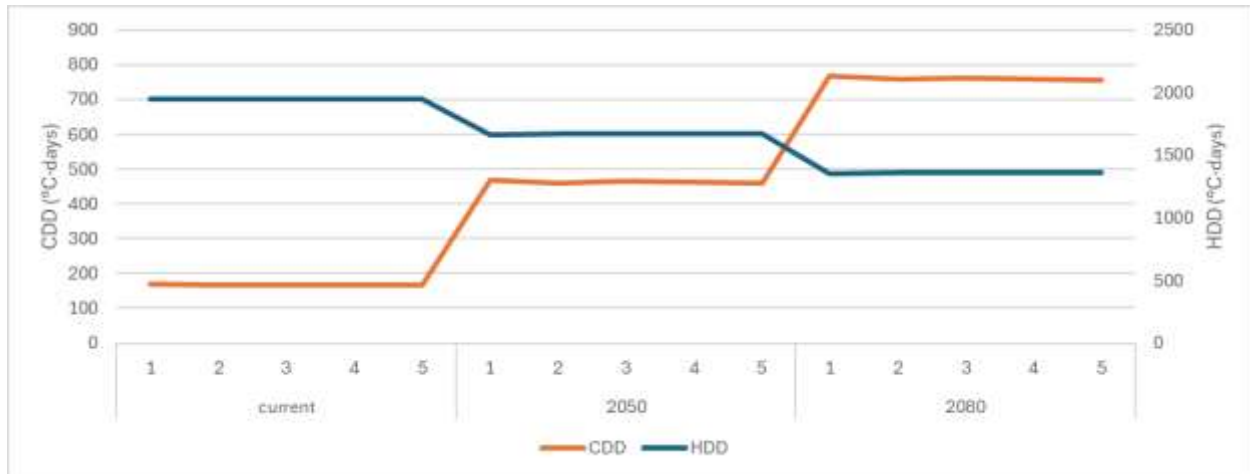
The Table 16 compares scenarios across current, 2050, and 2080, focusing on UTCI, CDD, and HDD. **Scenario 5** consistently performs best, with the **lowest UTCI** and **CDD** values in all periods, indicating it effectively minimizes cooling needs and enhances urban heat mitigation. In the current period, Scenario 5 shows a lower cooling demand but a higher heating requirement. By 2050 and 2080, it maintains its effectiveness with reduced cooling needs, despite a gradual decrease in heating demand. Overall, Scenario 5 is the most balanced and effective strategy for reducing both heating and cooling requirements, optimizing urban resilience to future climate conditions.

Table 16: Comparative Analysis of UHI Mitigation Scenarios for Current, 2050, and 2080 – Evaluating UTCI, CDD, and HDD

		UTCI Annual (°C)	Temp Annual (°C)	UTCI summer day (°C)	UTCI summer night (°C)	UTCI Winter day(°C)	UTCI Winter night(°C)	CDD(°C·day)	HDD(°C·day)
current	1	14.97	14.47	25.70	23.77	3.01	2.12	169.69	1943.38
	2	14.94	14.43	25.59	23.77	2.94	2.10	165.05	1950.48
	3	14.95	14.45	25.62	23.78	2.96	2.12	167.43	1947.49
	4	14.95	14.44	25.58	23.79	2.94	2.11	165.75	1948.33
	5	14.94	14.43	25.56	23.78	2.94	2.11	164.90	1950.44
2050	1	17.44	16.41	30.75	26.30	5.41	2.76	468.45	1662.68
	2	17.41	16.36	30.62	26.30	5.35	2.75	460.45	1668.53
	3	17.42	16.38	30.66	26.31	5.34	2.75	464.77	1666.58
	4	17.41	16.37	30.60	26.31	5.33	2.76	461.55	1667.16
	5	17.40	16.36	30.58	26.30	5.32	2.75	459.50	1669.58
2080	1	19.54	18.38	34.01	29.13	6.92	4.27	766.60	1355.03
	2	19.50	18.33	33.87	29.12	6.85	4.26	757.27	1359.77
	3	19.52	18.35	33.91	29.14	6.85	4.27	762.17	1358.60
	4	19.51	18.34	33.85	29.14	6.83	4.28	758.53	1358.47
	5	19.50	18.33	33.83	29.12	6.82	4.26	756.11	1360.70

Overall, the Figure 60 suggests a warming trend from the "current" period through "2050" and into "2080." As time progresses, the demand for cooling (represented by CDD) increases significantly, while the demand for heating (represented by HDD) decreases. This reflects a shift towards a warmer climate scenario, where cooling becomes more critical than heating. The optimal scenario is determined based on the 2080 data, which offers a future-oriented perspective. This remains consistent even when considering the 2050 scenario.





*Figure 60: HDD and CDD over time*

In 2080, to highlight the changes in CDD and HDD, the data indicates a decrease in HDD by approximately 36% from the current scenario to 2080, reflecting a reduced need for heating. Conversely, CDD increases by about 430%, signifying a substantial rise in cooling demand. This sharp increase in CDD emphasizes the need to prioritize strategies for managing future urban heat stress during summer months (Figure 61).

To explain the performance differences, Scenario 2 (extensive vegetation) shows better cooling compared to Scenarios 3 and 4 due to its effective use of shade and evapotranspiration, which actively lowers ambient temperatures. Scenario 3's reliance on high albedo surfaces reflects heat but doesn't cool the air as effectively, while Scenario 4's mixed approach balances both strategies, resulting in moderate performance. Scenario 5, which combines 50% vegetation with high albedo surfaces, shows a balanced outcome but doesn't reach the cooling efficiency of full vegetation (Scenario 2) due to reduced evapotranspiration benefits (Figure 61).

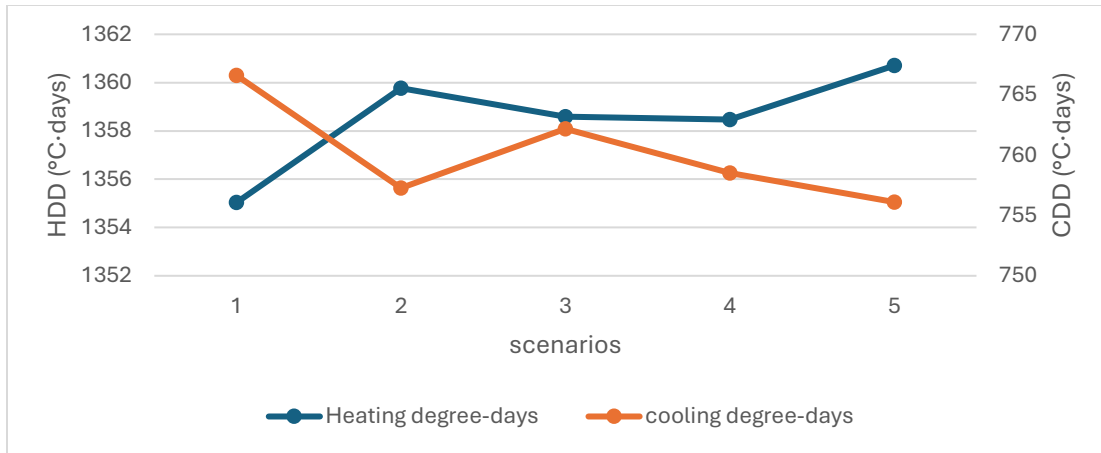


Figure 61: HDD and CDD in 2080

From a temperature perspective, it is better to consider the UTCI, especially on summer days.

Scenarios 4 and 5 show better performance under these conditions (Figure 62).

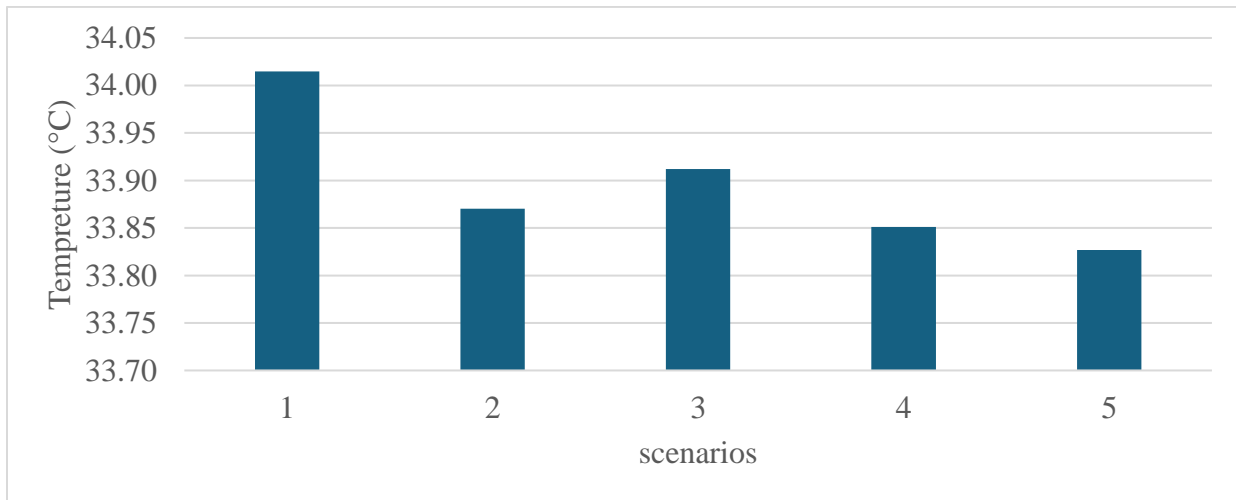


Figure 62: UTCI in summer day comparison

Table 17 presents the UHI intensity across various scenarios for summer and winter days and nights. Scenario 1 exhibits the highest UHI intensity during summer days by 2080, indicating significant urban heat accumulation. In contrast, Scenario 2 demonstrates a slight reduction in UHI intensity due to increased vegetation. Scenarios 3 and 4 show similar trends, with minor variations in UHI intensity, while Scenario 5 provides a balanced approach with relatively lower summer

night UHI intensity by 2080. Winter UHI intensities are generally negative across all scenarios, reflecting a cooling effect, with Scenario 5 showing the most significant reduction in winter daytime UHI intensity by 2080. These variations emphasize the different impacts of each mitigation strategy on urban thermal comfort and UHI effects.

*Table 17: UHI intensity across all scenarios*

scenarios		summer day	summer night	Winter day	Winter night
1	current	1.276	1.283	-2.439	-1.502
	2050	3.389	1.696	-1.501	-1.902
	2080	3.839	2.040	-1.518	-1.875
2	current	1.160	1.290	-2.510	-1.520
	2050	3.250	1.690	-1.560	-1.910
	2080	3.690	2.030	-1.590	-1.880
3	current	1.190	1.300	-2.490	-1.500
	2050	3.290	1.700	-1.570	-1.910
	2080	3.740	2.050	-1.590	-1.870
4	current	1.149	1.305	-2.511	-1.517
	2050	3.240	1.704	-1.579	-1.899
	2080	3.675	2.046	-1.607	-1.870
5	current	1.129	1.291	-2.510	-1.513
	2050	3.216	1.687	-1.584	-1.913
	2080	3.651	2.028	-1.619	-1.884

### 6.3.1 Sensitivity analysis

The chart provided in Figure 63 and Figure 64 demonstrates the sensitivity analysis results, offering a detailed comparison of the impact of various mitigation scenarios on the primary KPIs

for the year 2080. The sensitivity analysis highlights how each scenario influences these KPIs, offering insights into their effectiveness in mitigating urban heat and optimizing thermal comfort.

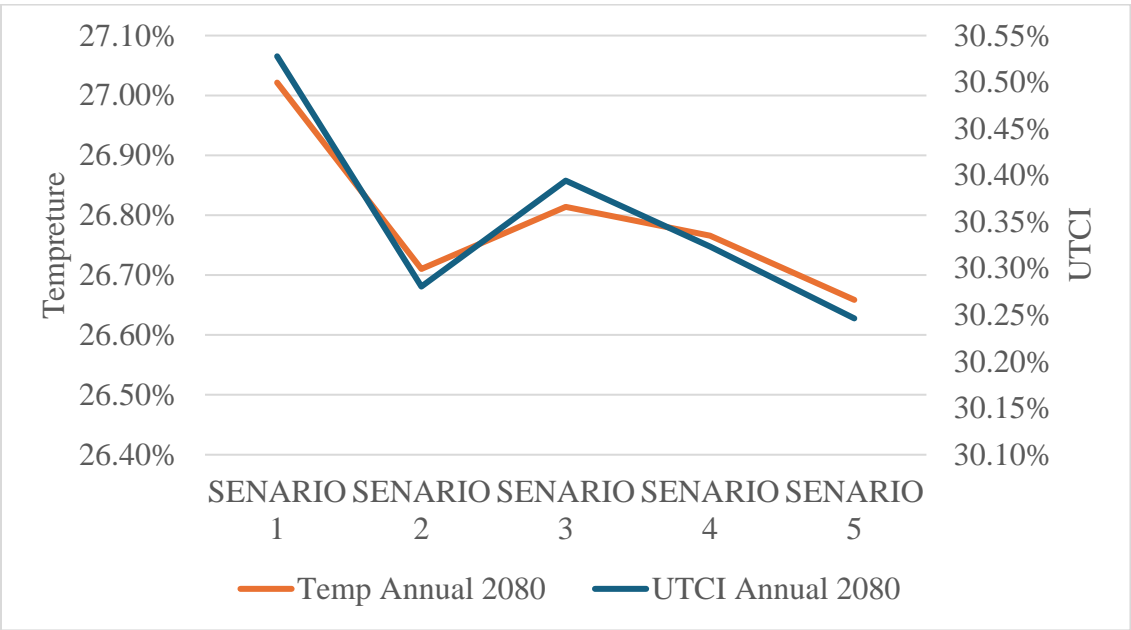


Figure 63: Sensitivity analysis of mitigation scenarios: Annual temperature and UTCI reduction for 2080

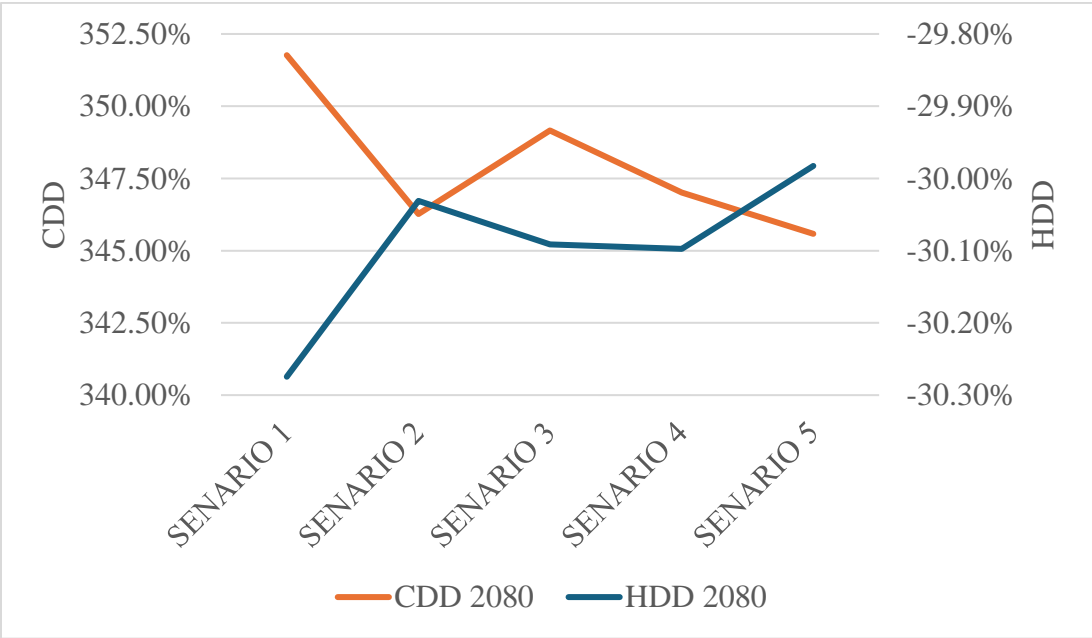


Figure 64 Sensitivity analysis of mitigation scenarios: HDD and CDD for 2080

1. **Scenario 2 (Vegetation implementation):**

- This scenario significantly improves both **Temp Annual** and **UTCI Annual**, reducing temperatures and thermal discomfort by around **1.2%** compared to Scenario 1.
- **CDD** drops by approximately **1.3%**, reflecting the cooling benefits of vegetation, while **HDD** remains almost the same as Scenario 1.
- This makes Scenario 2 an efficient cooling strategy with moderate heating demands.

## 2. Scenario 3 (High albedo implementation):

- The use of reflective surfaces shows moderate reductions in **UTCI Annual** and **Temp Annual** compared to Scenario 2 but still falls short of the benefits seen in full vegetation strategies. The impact is **approximately 0.8%** better than Scenario 1.
- **CDD** drops compared to Scenario 1 by around **1.1%**, but **HDD** shows only a marginal improvement over the vegetation-focused Scenario 2.

## 3. Scenario 4 (Mixed strategy with vegetation and high albedo):

- Combining vegetation with high albedo shows a balanced performance. The **UTCI Annual** improves by **1%**, and **Temp Annual** remains low, almost identical to Scenario 2.
- **CDD** is slightly better than Scenario 3 by **0.5%**, but **HDD** performance is still not as optimal as Scenario 5.

## 4. Scenario 5 (50% roof vegetation and high albedo surfaces):

- Scenario 5 performs the best overall, with further reductions in **Temp Annual** and **UTCI Annual** by around **1.7%** compared to Scenario 1.
- **CDD** is reduced by **1.5%**, and **HDD** decreases by **1.2%**, reflecting the scenario's balance in reducing cooling needs and enhancing urban heat mitigation.

These percentages indicate that Scenario 5, which combines both vegetation and high albedo, provides the best balance in mitigating urban heat stress, optimizing thermal comfort, and minimizing both cooling and heating needs.

The graphs visually highlight that both **Temp Annual** and **UTCI Annual** steadily decrease from Scenario 1 to Scenario 5, while **CDD** and **HDD** follow a similar trend, with CDD showing the most substantial decrease in Scenario 5.

### 6.3.2 Design explorer tool result

To facilitate a comprehensive comparison and analysis of different UHI mitigation scenarios, the Design Explorer website was utilized. In Figure 65 this webpage is shown with its default data just to represent the tool in website. This tool is particularly useful because it allows for the easy upload and visualization of CSV data, providing a clear, interactive representation of multiple variables and outcome.

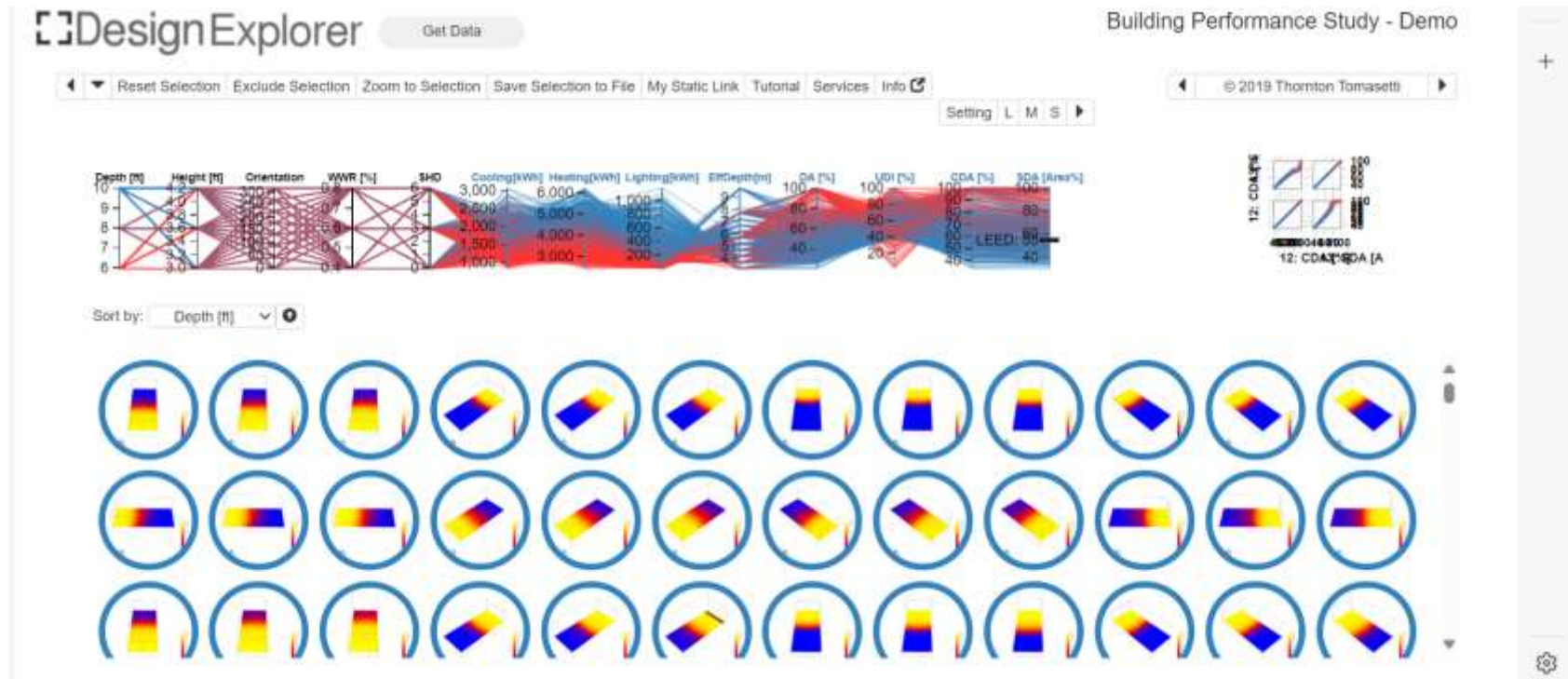
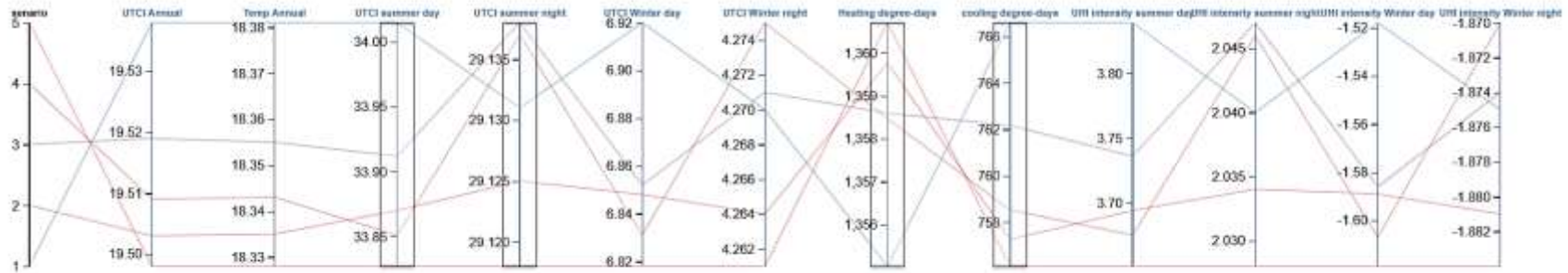


Figure 65: Design explorer 2 website homepage with default value

By using Design Explorer, we can effectively compare different scenarios side by side, identifying trends and relationships between KPIs such as UTCI, UHI intensity, HDD, and CDD (Figure 66). This approach enables a more informed decision-making process, allowing us to select the most suitable mitigation strategy based on specific data ranges and desired outcomes.



senario	UTCI Annual	Temp Annual	UTCI summer ...	UTCI summer ...	UTCI Winter day	UTCI Winter ni...	Heating degre...	cooling degre...	UHI intensity s...	UHI intensity s...	UHI intensity ...	UHI intensity ...	Rating
1	19.538	18.381	34.015	29.131	6.820	4.270	1355.033	766.506	3.630	2.040	-1.518	-1.875	0
2	19.503	18.335	33.870	29.125	6.848	4.264	1359.767	757.271	3.604	2.034	-1.589	-1.881	0
3	19.519	18.355	33.912	29.138	6.852	4.271	1358.506	762.171	3.736	2.047	-1.586	-1.874	0
4	19.509	18.343	33.851	29.137	6.831	4.275	1358.471	758.525	3.675	2.046	-1.607	-1.87	0
5	19.498	18.328	33.827	29.118	6.818	4.261	1360.704	756.108	3.651	2.028	-1.619	-1.884	0

Figure 66: Design explorer presenting all data of scenarios

With this methodology, we identified the optimal solution by examining the data ranges that best meet our criteria for each scenario, as illustrated in Figure 67. This figure demonstrates how the selected ranges were used to pinpoint the most effective strategy for urban heat management.



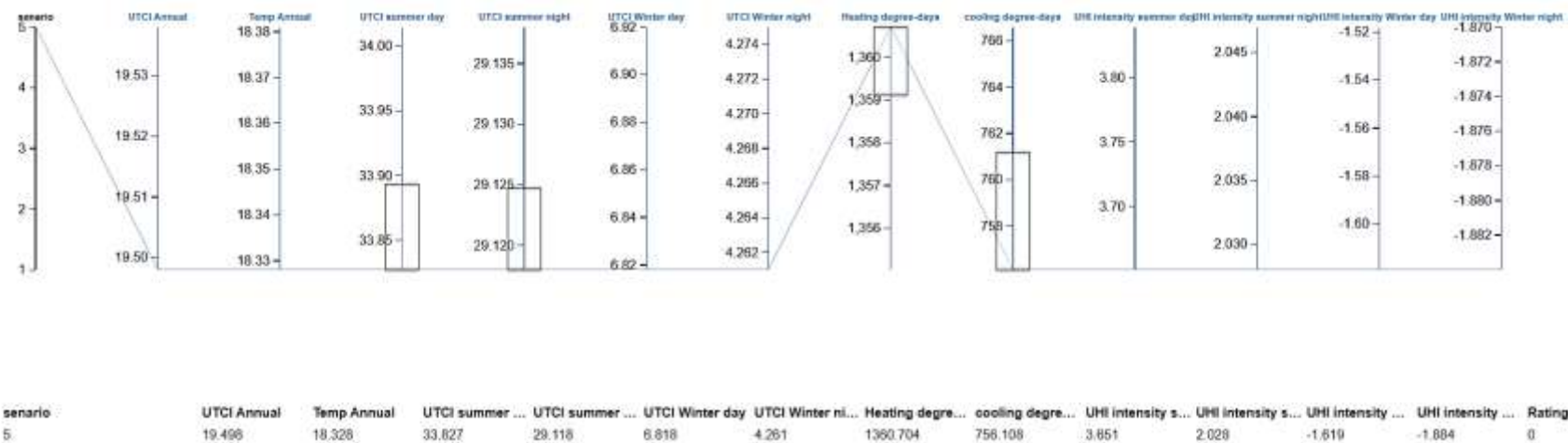


Figure 67: selecting range of suitable result to find best solution in design explorer

As it is evident in Figure 67, a lower summer temperature and lower CDD have been selected, making Scenario 5 the optimal choice based on these criteria

## 6.4 Conclusion

In this chapter, we explored various UHIs mitigation strategies tailored to the urban environment of Turin, examining their effectiveness through simulations for the present and future scenarios (2050 and 2080). Five mitigation scenarios were assessed, with a focus on different combinations of high albedo surfaces and vegetation to manage UHI intensity and improve thermal comfort. Using simulation tools like Dragonfly, we analyzed the performance of each scenario against key performance indicators (UTCI, UHI intensity, Heating Degree Days (HDD), and Cooling Degree Days (CDD)).

The findings of this analysis reveal a clear trend of rising temperatures and cooling demands as we approach 2080. Scenario 1, representing the baseline with no mitigation, demonstrated the highest temperature increases and UHI intensity, particularly during summer months. Conversely, Scenario 2, which emphasized extensive vegetation, effectively mitigated UHI effects, providing significant cooling benefits through increased shading and evapotranspiration. However, its reliance solely on vegetation limited its impact on annual cooling demands.

Scenarios 3 and 4, focusing on high-albedo surfaces with varying degrees of vegetation, showed moderate improvements. Scenario 3 reduced heat absorption but was less effective than vegetation-based strategies in enhancing overall thermal comfort. Scenario 4 offered a more balanced approach by integrating reflective surfaces and greenery, reducing both summer and winter UHI effects more effectively than Scenario 3.

Scenario 5 emerged as the most effective mitigation strategy. Its balanced approach—combining vegetation and high albedo surfaces—showed the greatest reduction in UTCI, CDD, and UHI intensity. This scenario outperformed the others in managing both current and future thermal

stresses, offering long-term resilience by significantly lowering cooling demands while maintaining a relatively moderate heating requirement. Sensitivity analyses further confirmed that Scenario 5 consistently reduced both temperatures and cooling needs, making it the optimal strategy for mitigating UHI effects in Turin by 2080.

Overall, this chapter underscores the importance of adopting a multifaceted approach in UHI mitigation. Scenario 5, with its combination of vegetation and reflective surfaces, presents a robust and scalable solution for future urban planning. It offers a practical, long-term strategy for enhancing climate resilience, mitigating UHI intensity, and improving thermal comfort in rapidly warming urban environments like Turin.

# 7 Conclusion

This thesis presents a comprehensive study on the UHIs phenomenon in Turin, Italy, leveraging advanced geospatial analysis, remote sensing, and 3D modeling techniques. The research aimed to understand UHI dynamics in Turin, predict future scenarios under different climate conditions, and propose effective mitigation strategies to enhance urban resilience.

## 7.1 Summary of key findings

This research employed a structured methodology to meet its objectives. First, areas prone to the UHI effect were identified through the use of remote sensing data and land surface temperature analysis. Subsequently, Dragonfly software, integrated with Rhino, was utilized to construct a 3D urban environment model, simulating UHI effects under various future climate change scenarios. Finally, the study tested multiple mitigation strategies, including the use of high-albedo surfaces and increased vegetation coverage, to assess their effectiveness in reducing UHI impacts.

**Identification of UHI-Prone Areas:** By using remote sensing data from Google Earth Engine, the study accurately mapped UHI-prone areas in Turin, revealing significant temperature variations between urban and rural zones. The analysis highlighted that areas with dense infrastructure and limited vegetation, such as the Mirafiori complex, are more susceptible to higher temperatures, emphasizing the role of urban morphology in UHI formation.

**Impact of Urban Configuration and Climate Change on UHI Intensity:** The study demonstrated that urban materials, reduced vegetation, and anthropogenic heat sources are critical factors contributing to UHI effects. Projections using the HadCM3 A2 climate change scenarios from the Intergovernmental Panel on Climate Change (IPCC) Third Assessment Report indicated

a significant intensification of UHI effects by 2050 and 2080, with urban areas expected to experience greater increases in temperature compared to rural areas. These findings underscore the escalating challenge of managing heat stress in urban settings under future climate conditions.

**Effectiveness of Mitigation Strategies:** The research explored various mitigation strategies, including increasing vegetation, applying high-albedo materials, and implementing mixed strategies. The results showed that a combination of vegetation and reflective surfaces is most effective in reducing UHI impacts, leading to lower urban temperatures and improved thermal comfort. These strategies are crucial for reducing energy demand for cooling and enhancing the livability of urban environments.

**Policy Implications for UHI Mitigation:** Given the demonstrated effectiveness of a mixed strategy, these findings offer practical guidance for policymakers in Turin and similar cities to tackle the UHI effect effectively. By identifying UHI-prone areas and testing mitigation strategies such as high-albedo materials and increased vegetation, this study provides a robust framework for implementing targeted interventions. These data-driven insights enable urban planners to prioritize areas for cooling initiatives, adjust building regulations, and integrate UHI mitigation into broader climate adaptation policies. Such actions are crucial for reducing energy consumption, enhancing thermal comfort, and improving the overall climate resilience of urban environments.

## 7.2 Addressing research questions

The research successfully addressed the key research questions outlined in Section 1.2:

**Which areas in Turin are most susceptible to UHIs formation, and what are the key parameters contributing to this susceptibility?**

The study identified specific zones in Turin, such as the Mirafiori complex and other densely built-up areas, as being most susceptible to UHI formation. These areas were characterized by a high concentration of impervious surfaces, reduced vegetation cover, and extensive use of heat-retaining materials like concrete and asphalt. Key parameters contributing to UHI susceptibility included urban morphology, land use patterns, and anthropogenic heat sources, such as traffic and industrial activities. The findings underscore the importance of urban design and infrastructure in influencing local microclimates.

**How can remote sensing technology and land cover analysis be effectively utilized to identify and characterize UHI-prone regions in Turin?**

Remote sensing technology, particularly the use of thermal infrared data from satellites, proved to be a powerful tool in identifying and characterizing UHI-prone regions. The study utilized data from Google Earth Engine to detect temperature anomalies and assess land cover characteristics that contribute to UHI effects. This approach enabled a detailed spatial analysis of temperature variations across Turin, highlighting areas with significant heat accumulation. By integrating land cover data, the study effectively mapped the spatial extent and intensity of UHIs, providing valuable insights for targeted mitigation efforts.

**How does Dragonfly software, integrated within the Rhino environment, enhance the analysis of UHI effects and inform mitigation strategies in urban areas?**

Dragonfly software, integrated within the Rhino environment, allowed for detailed 3D modeling of urban areas in Turin, incorporating various parameters such as building heights, materials, land cover characteristics, and anthropogenic heat sources. This enhanced analysis facilitated a comprehensive understanding of the microclimatic conditions contributing to UHI formation. The software's simulation capabilities enabled the testing of different mitigation strategies, providing

critical insights into their potential effectiveness. This approach proved instrumental in identifying optimal strategies for reducing UHI effects and improving thermal comfort in urban environments.

**What are the projected impacts of climate change on UHI intensity in Turin, specifically under the HadCM3 A2 climate change scenarios for the years 2050 and 2080?**

Under the HadCM3 A2 climate change scenarios, UHI intensity in Turin is projected to increase significantly by 2050 and further intensify by 2080. The simulations indicated that urban areas would experience more substantial temperature increases than rural areas, particularly during the summer months. This projected intensification of UHI effects is attributed to rising global temperatures and the continued development of urban infrastructure that retains heat. The findings highlight the growing need for adaptive urban planning and mitigation strategies to cope with the anticipated increase in urban heat stress.

**Which mitigation strategies are most effective in reducing UHI effects in Turin under current and future climate conditions, and what practical insights can this research provide to urban planners and policymakers?**

The most effective strategy for mitigating UHI effects in Turin, under both current and future climate conditions, is a combination of increased vegetation (such as green roofs and tree cover) and high-albedo materials (like reflective surfaces). This mixed approach significantly reduces temperatures, lowers energy consumption for cooling, and improves thermal comfort in urban areas. The research provides practical insights for urban planners and policymakers, emphasizing the importance of integrating these strategies into urban design and tailoring interventions to specific urban zones. Utilizing advanced modeling tools like Dragonfly can also aid in evidence-based decision-making for enhancing urban sustainability and resilience.

## 7.3 Future research directions

While this study has provided valuable insights into UHI dynamics and effective mitigation strategies, it opens the door for further exploration in several key areas:

- **Enhanced Modeling Techniques:** Future research could benefit from incorporating more granular data on building materials, surface albedo, and human activity patterns. This would improve the precision of temperature predictions and enhance the effectiveness of UHI mitigation strategies.
- **Broader Geographic Application:** Expanding this research to other cities with similar climates could provide a more comprehensive understanding of UHI dynamics and help assess the applicability of various mitigation strategies in diverse urban environments.
- **Long-Term Monitoring and Adaptation:** Continuous monitoring of UHI-prone areas and validating models with real-time data will improve the understanding of UHI trends and aid in developing adaptive urban planning strategies to address the growing challenges posed by climate change.

## 7.4 Limitations of the study

This study has several limitations that need to be acknowledged:

**Uncertainty in future weather data:** The research utilized future weather data generated from climate change models, specifically the HadCM3 A2 experiment ensemble from the IPCC Third Assessment Report. While these models offer valuable projections, they inherently involve some inaccuracies and uncertainties due to the complexity of climate systems and the assumptions made



during modeling. These uncertainties could impact the accuracy of the projected UHI intensities for 2050 and 2080, thereby influencing the results of the mitigation strategies evaluated.

**Simplified 3D modeling approach:** The study employed a simplified 3D modeling approach due to the capabilities of the Dragonfly plugin within the Rhino environment. The Dragonfly plugin operates on an urban scale and utilizes generalized inputs, such as the percentage of ground covered by grass or the proportion of surfaces with high albedo. Consequently, the model does not account for finer details, such as the precise height of buildings or shading effects, which are important in smaller-scale studies. This limitation affects the model's ability to capture detailed microclimatic variations, potentially impacting the precision of the analysis. While the approach provides a useful overview of UHI dynamics, it may not fully represent all the complexities of the urban environment, especially in areas with varied building heights and shading. Future studies could benefit from more detailed modeling to capture these finer-scale urban features.

## 7.5 Final remarks

This research has provided a comprehensive analysis of the UHIs phenomenon in Turin, using a combination of remote sensing, 3D modeling, and climate change projections. By identifying UHI-prone areas, analyzing the contributing factors, and evaluating various mitigation strategies, the study offers valuable insights into managing urban heat in a changing climate.

The findings underscore the importance of adopting a multi-faceted approach to UHI mitigation, combining increased vegetation, high-albedo materials, and strategic urban planning. Such strategies not only help reduce urban temperatures but also improve thermal comfort and reduce energy demands, contributing to more sustainable and resilient urban environments.

Despite its limitations, this research provides a solid foundation for future studies and offers practical guidance for urban planners and policymakers. Continued innovation in modeling techniques, data integration, and adaptive urban planning will be essential to addressing the growing challenges of urban heat in the face of ongoing climate change.

By advancing our understanding of UHI dynamics and developing effective mitigation strategies, this study aims to foster a more livable and sustainable future for cities like Turin and beyond. Future research should build on these findings, exploring new technologies and methods to further refine our approach to urban climate resilience.

## 8 Appendix 1 – Script for GEE

The provided code snippet demonstrates the methodology for calculating Land Surface Temperature (LST) in Turin and its surrounding areas using Landsat-8 satellite data within Google Earth Engine (GEE). The script selects satellite imagery over a defined period, utilizes the Split-Window Algorithm to compute LST, and visualizes the results through a color-coded map indicating different temperature ranges. By specifying parameters such as the region of interest, date range, and vegetation indices, the code effectively highlights spatial temperature variations, helping to identify UHIs effects by pinpointing areas with elevated surface temperatures compared to cooler, vegetated regions.

```
var LandsatLST = require('users/sofiaermida/landsat_smw_lst:modules/Landsat_LST.js');
```

```
// Define the region of interest
```

```
var geometry = ee.Geometry.Rectangle([5.5, 43.8, 6.5, 45.1]);
```

```
// Define the Landsat satellite, date range, and NDVI usage
```

```
var satellite = 'L8';
```

```
var date_start = '2022-08-01';
```

```
var date_end = '2024-05-01';
```

```
var use_ndvi = true;
```

```
// Get the Landsat collection within the specified date range and region
```

```
var LandsatColl = LandsatLST.collection(satellite, date_start, date_end, geometry, use_ndvi);
```

```
print('Landsat Collection:', LandsatColl);
```

```
// Calculate the mean LST over the specified date range
```

```
var meanLST = LandsatColl.select('LST').mean();
```

```

// Define color map for visualization, adjusted for 17-35 Celsius range
var cmap1 = ['blue', 'lightblue', 'green', 'yellow', 'orange', 'red'];

// Define legend labels based on the new color map
var labels = ['<17 °C', '17-21 °C', '21-26 °C', '26-31 °C', '31-35 °C', '>35 °C'];

// Center the map on the region of interest
Map.centerObject(geometry);

// Add the average LST layer to the map with adjusted min/max for Celsius
Map.addLayer(meanLST, {min: 273.15 + 17, max: 273.15 + 35, palette: cmap1}, 'Average LST
(°C)');

// Create legend entries with colored boxes and labels
var legendEntries = [];
for (var i = 0; i < cmap1.length; i++) {
  var color = cmap1[i];
  var label = labels[i];
  legendEntries.push(ui.Panel([
    // Set fixed width and height for colored box
    ui.Label({style: {backgroundColor: color, width: '20px', height: '15px', margin: '1px 2px'}}),
    ui.Label(label, {margin: '2px'})
  ]));
}

// Create legend title
var legendTitle = ui.Label('Average LST (°C)');

// Combine legend entries and title in a vertical layout
var legendPanel = ui.Panel({

```

```
widgets: [legendTitle].concat(legendEntries),  
layout: ui.Panel.Layout.flow('vertical'),  
style: {padding: '5px', position: 'bottom-left'} // Set position to bottom-left  
});  
  
// Add legend panel to the map  
Map.add(legendPanel);
```

## 9 Appendix 2 – Algorithm file of grasshopper

The algorithm file of grasshopper and dragonfly for download is provided in following link:

<https://tinyurl.com/UHITHESIS>

# 11 References

- Abshaev, M. T., Abshaev, A. M., Aksenov, A. A., Fisher, J. V., Shchelyaev, A. E., Al Mandous, A., Al Yazeedi, O., Wehbe, Y., Sîrbu, E., Sîrbu, D. A., & Eremeico, S. (2023). Results of Field Experiments for the Creation of Artificial Updrafts and Clouds. *Atmosphere*, 14(1), 136. <https://doi.org/10.3390/atmos14010136>
- Abu Bakar, N. N., Hassan, M. Y., Abdullah, H., Rahman, H. A., Abdullah, M. P., Hussin, F., & Bandi, M. (2015). Energy efficiency index as an indicator for measuring building energy performance: A review. *Renewable and Sustainable Energy Reviews*, 44, 1–11. <https://doi.org/10.1016/j.rser.2014.12.018>
- Al-Kayiem, H. H., Koh, K., Riyadi, T. W. B., & Effendy, M. (2020). A Comparative Review on Greenery Ecosystems and Their Impacts on Sustainability of Building Environment. *Sustainability*, 12(20), 8529. <https://doi.org/10.3390/su12208529>
- Andoni, H., & Wonorahardjo, S. (2018). A Review on Mitigation Technologies for Controlling Urban Heat Island Effect in Housing and Settlement Areas. *IOP Conference Series: Earth and Environmental Science*, 152, 012027. <https://doi.org/10.1088/1755-1315/152/1/012027>
- Aram, F., Higuera García, E., Solgi, E., & Mansournia, S. (2019). Urban green space cooling effect in cities. *Heliyon*, 5(4), e01339. <https://doi.org/10.1016/j.heliyon.2019.e01339>
- Bahi, H., Mastouri, H., & Radoine, H. (2020). Review of methods for retrieving urban heat islands. *Materials Today: Proceedings*, 27, 3004–3009. <https://doi.org/10.1016/j.matpr.2020.03.272>

- Bandara, J. S., & Cai, Y. (2014). The impact of climate change on food crop productivity, food prices and food security in South Asia. *Economic Analysis and Policy*, 44(4), 451–465. <https://doi.org/10.1016/j.eap.2014.09.005>
- Battista, G., Evangelisti, L., Guattari, C., De Lieto Vollaro, E., De Lieto Vollaro, R., & Asdrubali, F. (2020). Urban Heat Island Mitigation Strategies: Experimental and Numerical Analysis of a University Campus in Rome (Italy). *Sustainability*, 12(19), 7971. <https://doi.org/10.3390/su12197971>
- Bayulken, B., Huisingh, D., & Fisher, P. M. J. (2021). How are nature based solutions helping in the greening of cities in the context of crises such as climate change and pandemics? A comprehensive review. *Journal of Cleaner Production*, 288, 125569. <https://doi.org/10.1016/j.jclepro.2020.125569>
- Beck, H. E., Zimmermann, N. E., McVicar, T. R., Vergopolan, N., Berg, A., & Wood, E. F. (2018). Present and future Köppen-Geiger climate classification maps at 1-km resolution. *Scientific Data*, 5(1), 180214. <https://doi.org/10.1038/sdata.2018.214>
- Belda, M., Holtanová, E., Halenka, T., & Kalvová, J. (2014). Climate classification revisited: from Köppen to Trewartha. *Climate Research*, 59(1), 1–13. <https://doi.org/10.3354/cr01204>
- Biasin, A., Masiero, M., Amato, G., & Pettenella, D. (2023). Nature-Based Solutions Modeling and Cost-Benefit Analysis to Face Climate Change Risks in an Urban Area: The Case of Turin (Italy). *Land*, 12(2), 280. <https://doi.org/10.3390/land12020280>
- Bonetto, C., Garwood, D., Hardy, P., Wheeler, D. (Travel writer), Williams, N., & Lonely Planet Publications (Firm). (n.d.). *Grand tour of Italy : road trips*. 135.



- Bornstein, R., Styrbicki-Imamura, R., González, J. E., & Lebassi, B. (2012). *Interactions of Global-Warming and Urban Heat Islands in Different Climate-Zones* (pp. 49–60). [https://doi.org/10.1007/978-94-007-2430-3\\_5](https://doi.org/10.1007/978-94-007-2430-3_5)
- Campbell-Lendrum, D., Manga, L., Bagayoko, M., & Sommerfeld, J. (2015). Climate change and vector-borne diseases: what are the implications for public health research and policy? *Philosophical Transactions of the Royal Society B: Biological Sciences*, 370(1665), 20130552. <https://doi.org/10.1098/rstb.2013.0552>
- Cao, C., Lee, X., Liu, S., Schultz, N., Xiao, W., Zhang, M., & Zhao, L. (2016). Urban heat islands in China enhanced by haze pollution. *Nature Communications*, 7(1), 12509. <https://doi.org/10.1038/ncomms12509>
- Chatfield, C. (1977). Some Recent Developments in Time-Series Analysis. *Journal of the Royal Statistical Society. Series A (General)*, 140(4), 492. <https://doi.org/10.2307/2345281>
- Chui, A. C., Gittelsohn, A., Sebastian, E., Stamler, N., & Gaffin, S. R. (2018). Urban heat islands and cooler infrastructure – Measuring near-surface temperatures with hand-held infrared cameras. *Urban Climate*, 24, 51–62. <https://doi.org/10.1016/j.uclim.2017.12.009>
- Corrales-Suastegui, A., Ruiz-Alvarez, O., Torres-Alavez, J. A., & Pavia, E. G. (2021). Analysis of Cooling and Heating Degree Days over Mexico in Present and Future Climate. *Atmosphere*, 12(9), 1131. <https://doi.org/10.3390/atmos12091131>
- David Thorpe. (2024). *The World's Most Successful Model for Sustainable Urban Development?* <https://www.smartcitiesdive.com/ex/sustainablecitiescollective/words-most-successful-model-sustainable-urban-development/229316/>

- Degirmenci, K., Desouza, K. C., Fieuw, W., Watson, R. T., & Yigitcanlar, T. (2021). Understanding policy and technology responses in mitigating urban heat islands: A literature review and directions for future research. *Sustainable Cities and Society*, 70, 102873. <https://doi.org/10.1016/j.scs.2021.102873>
- Deilami, K., Kamruzzaman, Md., & Liu, Y. (2018). Urban heat island effect: A systematic review of spatio-temporal factors, data, methods, and mitigation measures. *International Journal of Applied Earth Observation and Geoinformation*, 67, 30–42. <https://doi.org/10.1016/j.jag.2017.12.009>
- Di Sabatino, S., Barbano, F., Brattich, E., & Pulvirenti, B. (2020). The Multiple-Scale Nature of Urban Heat Island and Its Footprint on Air Quality in Real Urban Environment. *Atmosphere*, 11(11), 1186. <https://doi.org/10.3390/atmos11111186>
- Dong, J., Peng, J., He, X., Corcoran, J., Qiu, S., & Wang, X. (2020). Heatwave-induced human health risk assessment in megacities based on heat stress-social vulnerability-human exposure framework. *Landscape and Urban Planning*, 203, 103907. <https://doi.org/10.1016/j.landurbplan.2020.103907>
- EBERT, J. I. (1984). Remote Sensing Applications in Archaeology. In *Advances in Archaeological Method and Theory* (pp. 293–362). Elsevier. <https://doi.org/10.1016/B978-0-12-003107-8.50010-4>
- Ellena, M., Melis, G., Zengarini, N., Di Gangi, E., Ricciardi, G., Mercogliano, P., & Costa, G. (2023). Micro-scale UHI risk assessment on the heat-health nexus within cities by looking at socio-economic factors and built environment characteristics: The Turin case study (Italy). *Urban Climate*, 49, 101514. <https://doi.org/10.1016/J.UCLIM.2023.101514>

- Ermida, S. L., Soares, P., Mantas, V., Göttsche, F.-M., & Trigo, I. F. (2020). Google Earth Engine Open-Source Code for Land Surface Temperature Estimation from the Landsat Series. *Remote Sensing*, *12*(9), 1471. <https://doi.org/10.3390/rs12091471>
- Falco, N., Benediktsson, J. A., & Bruzzone, L. (2015). Spectral and Spatial Classification of Hyperspectral Images Based on ICA and Reduced Morphological Attribute Profiles. *IEEE Transactions on Geoscience and Remote Sensing*, *53*(11), 6223–6240. <https://doi.org/10.1109/TGRS.2015.2436335>
- Feinberg, A. (2022). A re-radiation model for the earth’s energy budget and the albedo advantage in global warming mitigation. *Dynamics of Atmospheres and Oceans*, *97*, 101267. <https://doi.org/10.1016/j.dynatmoce.2021.101267>
- Feliciano, R. J., Boué, G., & Membré, J.-M. (2020). Overview of the Potential Impacts of Climate Change on the Microbial Safety of the Dairy Industry. *Foods*, *9*(12), 1794. <https://doi.org/10.3390/foods9121794>
- Feng, Y., Du, S., Myint, S. W., & Shu, M. (2019). Do Urban Functional Zones Affect Land Surface Temperature Differently? A Case Study of Beijing, China. *Remote Sensing*, *11*(15), 1802. <https://doi.org/10.3390/rs11151802>
- Founda, D., & Santamouris, M. (2017). Synergies between Urban Heat Island and Heat Waves in Athens (Greece), during an extremely hot summer (2012). *Scientific Reports*, *7*(1), 10973. <https://doi.org/10.1038/s41598-017-11407-6>
- Gao, Y., Zhang, M., Wang, J., & Li, W. (2023). Cross-Scale Mixing Attention for Multisource Remote Sensing Data Fusion and Classification. *IEEE Transactions on Geoscience and Remote Sensing*, *61*, 1–15. <https://doi.org/10.1109/TGRS.2023.3263362>

- Garzena, D., Acquaotta, F., & Fratianni, S. (2019a). Analysis of the long-time climate data series for Turin and assessment of the city's urban heat island. *Weather*, 74(10), 353–359. <https://doi.org/10.1002/wea.3292>
- Garzena, D., Acquaotta, F., & Fratianni, S. (2019b). Analysis of the long-time climate data series for Turin and assessment of the city's urban heat island. *Weather*, 74(10), 353–359. <https://doi.org/10.1002/wea.3292>
- Ghaderpour, E., Pagiatakis, S. D., & Hassan, Q. K. (2021). A Survey on Change Detection and Time Series Analysis with Applications. *Applied Sciences*, 11(13), 6141. <https://doi.org/10.3390/app11136141>
- Gregório, V., & Seixas, J. (2017). Energy savings potential in urban rehabilitation: A spatial-based methodology applied to historic centres. *Energy and Buildings*, 152, 11–23. <https://doi.org/10.1016/j.enbuild.2017.06.024>
- Guattari, C., Evangelisti, L., & Balaras, C. A. (2018). On the assessment of urban heat island phenomenon and its effects on building energy performance: A case study of Rome (Italy). *Energy and Buildings*, 158, 605–615. <https://doi.org/10.1016/j.enbuild.2017.10.050>
- Gunawardena, K. R., Wells, M. J., & Kershaw, T. (2017). Utilising green and bluespace to mitigate urban heat island intensity. *Science of The Total Environment*, 584–585, 1040–1055. <https://doi.org/10.1016/j.scitotenv.2017.01.158>
- Haines, A., Kovats, R. S., Campbell-Lendrum, D., & Corvalan, C. (2006). Climate change and human health: Impacts, vulnerability and public health. *Public Health*, 120(7), 585–596. <https://doi.org/10.1016/j.puhe.2006.01.002>

- He, B. (2019). Towards the next generation of green building for urban heat island mitigation: Zero UHI impact building. *Sustainable Cities and Society*.  
<https://api.semanticscholar.org/CorpusID:195415615>
- He, B.-J. (2019). Towards the next generation of green building for urban heat island mitigation: Zero UHI impact building. *Sustainable Cities and Society*, 50, 101647.  
<https://doi.org/10.1016/j.scs.2019.101647>
- He, B.-J., Ding, L., & Prasad, D. (2020). Urban ventilation and its potential for local warming mitigation: A field experiment in an open low-rise gridiron precinct. *Sustainable Cities and Society*, 55, 102028. <https://doi.org/10.1016/j.scs.2020.102028>
- Heaviside, C., Macintyre, H., & Vardoulakis, S. (2017). The Urban Heat Island: Implications for Health in a Changing Environment. *Current Environmental Health Reports*, 4(3), 296–305.  
<https://doi.org/10.1007/s40572-017-0150-3>
- Howden, S. M., Soussana, J.-F., Tubiello, F. N., Chhetri, N., Dunlop, M., & Meinke, H. (2007). Adapting agriculture to climate change. *Proceedings of the National Academy of Sciences*, 104(50), 19691–19696. <https://doi.org/10.1073/pnas.0701890104>
- Ibrahim, Y. I., Kershaw, T., & Shepherd, P. (2020). A methodology for modelling microclimate: a Ladybug-tools and ENVI-met verification study. *35th PLEA Conference Sustainable Architecture and Urban Design: Planning Post Carbon Cities*.
- Jänicke, B., Milošević, D., & Manavvi, S. (2021). Review of User-Friendly Models to Improve the Urban Micro-Climate. *Atmosphere*, 12(10), 1291.  
<https://doi.org/10.3390/atmos12101291>

- Jentsch, M. F., James, P. A. B., Bourikas, L., & Bahaj, A. S. (2013). Transforming existing weather data for worldwide locations to enable energy and building performance simulation under future climates. *Renewable Energy*, 55, 514–524.  
<https://doi.org/10.1016/j.renene.2012.12.049>
- Kandya, A., & Mohan, M. (2018). Mitigating the Urban Heat Island effect through building envelope modifications. *Energy and Buildings*, 164, 266–277.  
<https://doi.org/10.1016/j.enbuild.2018.01.014>
- Kaya, S., Basar, U. G., Karaca, M., & Seker, D. Z. (2012). Assessment of Urban Heat Islands Using Remotely Sensed Data. *Ekoloji*, 21(84), 107–113.  
<https://doi.org/10.5053/ekoloji.2012.8412>
- Keramitsoglou, I., Kiranoudis, C. T., Ceriola, G., Weng, Q., & Rajasekar, U. (2011). Identification and analysis of urban surface temperature patterns in Greater Athens, Greece, using MODIS imagery. *Remote Sensing of Environment*, 115(12), 3080–3090.  
<https://doi.org/10.1016/j.rse.2011.06.014>
- Kong, J., Zhao, Y., Carmeliet, J., & Lei, C. (2021). Urban Heat Island and Its Interaction with Heatwaves: A Review of Studies on Mesoscale. *Sustainability*, 13(19), 10923.  
<https://doi.org/10.3390/su131910923>
- Kwofie, S., Nyamekye, C., Appiah Boamah, L., Owusu Adjei, F., Arthur, R., & Agyapong, E. (2022). Urban growth nexus to land surface temperature in Ghana. *Cogent Engineering*, 9(1).  
<https://doi.org/10.1080/23311916.2022.2143045>
- Ladybug Tools / Dragonfly*. (n.d.). Retrieved April 19, 2024, from  
<https://www.ladybug.tools/dragonfly.html>

- Leal Filho, W., Echevarria Icaza, L., Emanche, V., & Quasem Al-Amin, A. (2017). An Evidence-Based Review of Impacts, Strategies and Tools to Mitigate Urban Heat Islands. *International Journal of Environmental Research and Public Health*, 14(12), 1600. <https://doi.org/10.3390/ijerph14121600>
- Leal Filho, W., Echevarria Icaza, L., Neht, A., Klavins, M., & Morgan, E. A. (2018). Coping with the impacts of urban heat islands. A literature based study on understanding urban heat vulnerability and the need for resilience in cities in a global climate change context. *Journal of Cleaner Production*, 171, 1140–1149. <https://doi.org/10.1016/j.jclepro.2017.10.086>
- Lee, J. S., Kim, J. T., & Lee, M. G. (2014). Mitigation of urban heat island effect and greenroofs. *Indoor and Built Environment*, 23(1), 62–69. <https://doi.org/10.1177/1420326X12474483>
- Li, H., Zhou, Y., Li, X., Meng, L., Wang, X., Wu, S., & Sodoudi, S. (2018). A new method to quantify surface urban heat island intensity. *Science of The Total Environment*, 624, 262–272. <https://doi.org/10.1016/j.scitotenv.2017.11.360>
- Li, J., & Donn, M. (2017, August 7). *The Influence of Building Height Variability on Natural Ventilation and Neighbor Buildings in Dense Urban Areas*. <https://doi.org/10.26868/25222708.2017.671>
- Li, Z.-L., Si, M., & Leng, P. (2020). A REVIEW OF REMOTELY SENSED SURFACE URBAN HEAT ISLANDS FROM THE FRESH PERSPECTIVE OF COMPARISONS AMONG DIFFERENT REGIONS (INVITED REVIEW). *Progress In Electromagnetics Research C*, 102, 31–46. <https://doi.org/10.2528/PIERC20020403>

- Liu, H., Kong, F., Yin, H., Middel, A., Zheng, X., Huang, J., Xu, H., Wang, D., & Wen, Z. (2021). Impacts of green roofs on water, temperature, and air quality: A bibliometric review. *Building and Environment*, 196, 107794. <https://doi.org/10.1016/j.buildenv.2021.107794>
- Lo Scalzo, A., Donatini, A., Orzella, L., Cicchetti, A., Profili, S., Maresso, A., & Organization, W. H. (2009). *Italy: Health system review*.
- Loh, N., & Bhiwapurkar, P. (2022). Urban heat-mitigating building form and façade framework. *Architectural Science Review*, 65(1), 57–71. <https://doi.org/10.1080/00038628.2021.1924610>
- Louis, V. R., & Phalkey, R. K. (2016). Health Impacts in a Changing Climate – An Overview. *The European Physical Journal Special Topics*, 225(3), 429–441. <https://doi.org/10.1140/epjst/e2016-60073-9>
- Maggiotto, G., Miani, A., Rizzo, E., Castellone, M. D., & Piscitelli, P. (2021). Heat waves and adaptation strategies in a mediterranean urban context. *Environmental Research*, 197, 111066. <https://doi.org/10.1016/j.envres.2021.111066>
- Makvandi, M., Li, W., Ou, X., Chai, H., Khodabakhshi, Z., Fu, J., Yuan, P. F., & Horimbere, E. de la J. (2023). Urban Heat Mitigation towards Climate Change Adaptation: An Eco-Sustainable Design Strategy to Improve Environmental Performance under Rapid Urbanization. *Atmosphere*, 14(4), 638. <https://doi.org/10.3390/atmos14040638>
- Marinoni, A., Heiden, U., & Gamba, P. (2019). Human settlement and infrastructure monitoring with hyperspectral imaging. *2019 Joint Urban Remote Sensing Event (JURSE)*, 1–4. <https://doi.org/10.1109/JURSE.2019.8809062>



- Martin, M., Chong, A., Biljecki, F., & Miller, C. (2022). Infrared thermography in the built environment: A multi-scale review. *Renewable and Sustainable Energy Reviews*, 165, 112540. <https://doi.org/10.1016/j.rser.2022.112540>
- Masson, V., Lemonsu, A., Hidalgo, J., & Voogt, J. (2020). Urban Climates and Climate Change. *Annual Review of Environment and Resources*, 45(1), 411–444. <https://doi.org/10.1146/annurev-environ-012320-083623>
- Medaiyese, O. . O., Ezuma, M., Lauf, A. P., & Guvenc, I. (2022). Wavelet transform analytics for RF-based UAV detection and identification system using machine learning. *Pervasive and Mobile Computing*, 82, 101569. <https://doi.org/10.1016/j.pmcj.2022.101569>
- Meola, C., Boccardi, S., & Carlomagno, G. (2016). An Excursus on Infrared Thermography Imaging. *Journal of Imaging*, 2(4), 36. <https://doi.org/10.3390/jimaging2040036>
- Mertikas, S. P., Partsinevelos, P., Mavrocordatos, C., & Maximenko, N. A. (2021). Environmental applications of remote sensing. In *Pollution Assessment for Sustainable Practices in Applied Sciences and Engineering* (pp. 107–163). Elsevier. <https://doi.org/10.1016/B978-0-12-809582-9.00003-7>
- Milelli, M., Bassani, F., Garbero, V., Poggi, D., von Hardenberg, J., & Ridolfi, L. (2023). Characterization of the Urban Heat and Dry Island effects in the Turin metropolitan area. *Urban Climate*, 47, 101397. <https://doi.org/10.1016/j.uclim.2022.101397>
- Mirzaei, P. A., & Haghighat, F. (2010). Approaches to study Urban Heat Island – Abilities and limitations. *Building and Environment*, 45(10), 2192–2201. <https://doi.org/10.1016/j.buildenv.2010.04.001>

- Mohajerani, A., Bakaric, J., & Jeffrey-Bailey, T. (2017). The urban heat island effect, its causes, and mitigation, with reference to the thermal properties of asphalt concrete. *Journal of Environmental Management*, 197, 522–538. <https://doi.org/10.1016/j.jenvman.2017.03.095>
- Mokhtari, A., Noory, H., Pourshakouri, F., Haghighatmehr, P., Afrasiabian, Y., Razavi, M., Fereydooni, F., & Sadeghi Naeni, A. (2019). Calculating potential evapotranspiration and single crop coefficient based on energy balance equation using Landsat 8 and Sentinel-2. *ISPRS Journal of Photogrammetry and Remote Sensing*, 154, 231–245. <https://doi.org/10.1016/J.ISPRSJPRS.2019.06.011>
- Morabito, M., Crisci, A., Gioli, B., Gualtieri, G., Toscano, P., Di Stefano, V., Orlandini, S., & Gensini, G. F. (2015). Urban-Hazard Risk Analysis: Mapping of Heat-Related Risks in the Elderly in Major Italian Cities. *PLOS ONE*, 10(5), e0127277. <https://doi.org/10.1371/JOURNAL.PONE.0127277>
- Morais, M. V. B. de, Urbina Guerrero, V. V., Rudke, A. P., Fujita, T., Martins, L. D., Reboita, M. S., & Martins, J. A. (2020). EVALUATION OF FUTURE CLIMATE CHANGE SCENARIOS IN URBAN HEAT ISLAND AND ITS NEIGHBORHOOD USING DYNAMICAL DOWNSCALING. *Journal of Urban and Environmental Engineering*, 110–118. <https://doi.org/10.4090/juee.2020.v14n1.110118>
- Munafò, M. (2019). *Consumo di suolo, dinamiche territoriali e servizi ecosistemici*. Ispra Roma, Italy.
- Mutani, G., Cristino, V., & Bullita, M. (2018). Associazione Italiana Proprietà Termofisiche) tenutosi a Torino nel 21-22 Settembre. *XXIII Convegno A.I.P.T*, 105–123. [www.polito.it](http://www.polito.it)

- Nakicenovic, N., Alcamo, J., Davis, G., Vries, B. de, Fenhann, J., Gaffin, S., Gregory, K., Grubler, A., Jung, T. Y., & Kram, T. (2000). *Special report on emissions scenarios*.
- Nardi, I., Lucchi, E., de Rubeis, T., & Ambrosini, D. (2018). Quantification of heat energy losses through the building envelope: A state-of-the-art analysis with critical and comprehensive review on infrared thermography. *Building and Environment*, 146, 190–205. <https://doi.org/10.1016/j.buildenv.2018.09.050>
- Nifatova, O. (2022). IMPROVING THE ENERGY EFFICIENCY OF BUILDINGS BY PROVIDING BETTER PROTECTIVE STRUCTURES BASED ON THE UNIVERSITY’S KNOWLEDGE HUB. *Management*, 34(2), 26–34. <https://doi.org/10.30857/2415-3206.2021.2.3>
- Noro, M., & Lazzarin, R. (2015a). Urban heat island in Padua, Italy: Simulation analysis and mitigation strategies. *Urban Climate*, 14, 187–196. <https://doi.org/10.1016/j.uclim.2015.04.004>
- Noro, M., & Lazzarin, R. (2015b). Urban heat island in Padua, Italy: Simulation analysis and mitigation strategies. *Urban Climate*, 14, 187–196. <https://api.semanticscholar.org/CorpusID:107982801>
- Okada, T., Fukuhara, T., Tanaka, S., Taguchi, M., Arai, T., Senshu, H., Sakatani, N., Shimaki, Y., Demura, H., Ogawa, Y., Suko, K., Sekiguchi, T., Kouyama, T., Takita, J., Matsunaga, T., Imamura, T., Wada, T., Hasegawa, S., Helbert, J., ... Tsuda, Y. (2020). Highly porous nature of a primitive asteroid revealed by thermal imaging. *Nature*, 579(7800), 518–522. <https://doi.org/10.1038/s41586-020-2102-6>
- OneBuilding. (2023, July). *Repository of free climate data for building performance simulation*.

- Park, S., Tuller, S. E., & Jo, M. (2014). Application of Universal Thermal Climate Index (UTCI) for microclimatic analysis in urban thermal environments. *Landscape and Urban Planning*, *125*, 146–155. <https://doi.org/10.1016/j.landurbplan.2014.02.014>
- Parsaee, M., Joybari, M. M., Mirzaei, P. A., & Haghighat, F. (2019). Urban heat island, urban climate maps and urban development policies and action plans. *Environmental Technology & Innovation*, *14*, 100341. <https://doi.org/10.1016/j.eti.2019.100341>
- Patz, J. A., Grabow, M. L., & Limaye, V. S. (2014). When It Rains, It Pours: Future Climate Extremes and Health. *Annals of Global Health*, *80*(4), 332. <https://doi.org/10.1016/j.aogh.2014.09.007>
- Paulina, W., Poh-Chin, L., & Melissa, H. (2015). Temporal Statistical Analysis of Urban Heat Islands at the Microclimate Level. *Procedia Environmental Sciences*, *26*, 91–94. <https://doi.org/10.1016/j.proenv.2015.05.006>
- Pauly, L., Canonico, M., & Ferrero, E. (2024). Numerical investigation of thermal patterns and local wind circulations to characterize Urban Heat Island during a heatwave in Turin. *Urban Climate*, *54*, 101847. <https://doi.org/10.1016/j.uclim.2024.101847>
- Phelan, P. E., Kaloush, K., Miner, M., Golden, J., Phelan, B., Silva, H., & Taylor, R. A. (2015a). Urban Heat Island: Mechanisms, Implications, and Possible Remedies. *Annual Review of Environment and Resources*, *40*(1), 285–307. <https://doi.org/10.1146/annurev-environ-102014-021155>
- Phelan, P. E., Kaloush, K., Miner, M., Golden, J., Phelan, B., Silva, H., & Taylor, R. A. (2015b). Urban Heat Island: Mechanisms, Implications, and Possible Remedies. *Annual Review of*

*Environment and Resources*, 40(1), 285–307. <https://doi.org/10.1146/annurev-environ-102014-021155>

Piemonte, A. (2020). Analisi di Vulnerabilità Climatica della Città di Torino. *Torino, IT: Dipartimento Rischi Naturali e Ambientali Arpa Piemonte. Disponibile Online All'indirizzo: Www. Comune. Torino. It/Torinosostenibile/Documenti/200806\_analisi\_Vulnerabilita\_climatica. Pdf (Ultimo Accesso Il 9 Giugno 2021).*

Pioppi, B., Pigliautile, I., & Pisello, A. L. (2020). Human-centric microclimate analysis of Urban Heat Island: Wearable sensing and data-driven techniques for identifying mitigation strategies in New York City. *Urban Climate*, 34, 100716. <https://doi.org/10.1016/j.uclim.2020.100716>

Pongrácz, R., Bartholy, J., & Dezső, Z. (2010). Application of remotely sensed thermal information to urban climatology of Central European cities. *Physics and Chemistry of the Earth, Parts A/B/C*, 35(1–2), 95–99. <https://doi.org/10.1016/j.pce.2010.03.004>

Price, A., Jones, E. C., & Jefferson, F. (2015). Vertical Greenery Systems as a Strategy in Urban Heat Island Mitigation. *Water, Air, & Soil Pollution*, 226(8), 247. <https://doi.org/10.1007/s11270-015-2464-9>

Qin, Y. (2015). A review on the development of cool pavements to mitigate urban heat island effect. *Renewable and Sustainable Energy Reviews*, 52, 445–459. <https://doi.org/10.1016/j.rser.2015.07.177>

RIZWAN, A. M., DENNIS, L. Y. C., & LIU, C. (2008a). A review on the generation, determination and mitigation of Urban Heat Island. *Journal of Environmental Sciences*, 20(1), 120–128. [https://doi.org/10.1016/S1001-0742\(08\)60019-4](https://doi.org/10.1016/S1001-0742(08)60019-4)

- RIZWAN, A. M., DENNIS, L. Y. C., & LIU, C. (2008b). A review on the generation, determination and mitigation of Urban Heat Island. *Journal of Environmental Sciences*, 20(1), 120–128. [https://doi.org/10.1016/S1001-0742\(08\)60019-4](https://doi.org/10.1016/S1001-0742(08)60019-4)
- Roessner, S., Segl, K., Bochow, M., Heiden, U., Heldens, W., & Kaufmann, H. (2011). Potential of Hyperspectral Remote Sensing for Analyzing the Urban Environment. In *Urban Remote Sensing* (pp. 49–61). Wiley. <https://doi.org/10.1002/9780470979563.ch4>
- Rossi, F., Castellani, B., Presciutti, A., Morini, E., Filipponi, M., Nicolini, A., & Santamouris, M. (2015). Retroreflective façades for urban heat island mitigation: Experimental investigation and energy evaluations. *Applied Energy*, 145, 8–20. <https://doi.org/10.1016/j.apenergy.2015.01.129>
- Russell, B. J., Soffer, R. J., Ientilucci, E. J., Kuester, M. A., Conran, D. N., Arroyo-Mora, J. P., Ochoa, T., Durell, C., & Holt, J. (2023). The Ground to Space CALibration Experiment (G-SCALE): Simultaneous Validation of UAV, Airborne, and Satellite Imagers for Earth Observation Using Specular Targets. *Remote Sensing*, 15(2), 294. <https://doi.org/10.3390/rs15020294>
- SADEGHIPOUR ROUDSARI, M., PAK, M., & VIOLA, A. (2013, August 28). *Ladybug: A Parametric Environmental Plugin For Grasshopper To Help Designers Create An Environmentally-conscious Design*. <https://doi.org/10.26868/25222708.2013.2499>
- Saibi, H., Bersi, M., Mia, M. B., Saadi, N. M., Bloushi, K. M. S. Al, & Avakian, R. W. (2018). Applications of Remote Sensing in Geoscience. In *Recent Advances and Applications in Remote Sensing*. InTech. <https://doi.org/10.5772/intechopen.75995>

- Sailor, D. J. (2011). A review of methods for estimating anthropogenic heat and moisture emissions in the urban environment. *International Journal of Climatology*, 31(2), 189–199. <https://doi.org/10.1002/joc.2106>
- Sangiorgio, V., Fiorito, F., & Santamouris, M. (2020). Development of a holistic urban heat island evaluation methodology. *Scientific Reports*, 10(1), 17913. <https://doi.org/10.1038/s41598-020-75018-4>
- SARRAT, C., LEMONSU, A., MASSON, V., & GUEDALIA, D. (2006). Impact of urban heat island on regional atmospheric pollution. *Atmospheric Environment*, 40(10), 1743–1758. <https://doi.org/10.1016/j.atmosenv.2005.11.037>
- Short, C. A., Lomas, K. J., & Woods, A. (2004). Design strategy for low-energy ventilation and cooling within an urban heat island. *Building Research & Information*, 32(3), 187–206. <https://doi.org/10.1080/09613210410001679875>
- Sidiqui, P., Roös, P. B., Herron, M., Jones, D. S., Duncan, E., Jalali, A., Allam, Z., Roberts, B. J., Schmidt, A., Tariq, M. A. U. R., Shah, A. A., Khan, N. A., & Irshad, M. (2022). Urban Heat Island vulnerability mapping using advanced GIS data and tools. *Journal of Earth System Science*, 131(4), 266. <https://doi.org/10.1007/s12040-022-02005-w>
- Solecki, W. D., Rosenzweig, C., Parshall, L., Pope, G., Clark, M., Cox, J., & Wiencke, M. (2005). Mitigation of the heat island effect in urban New Jersey. *Environmental Hazards*, 6(1), 39–49. <https://doi.org/10.1016/j.hazards.2004.12.002>
- Sreedhar, S., & Biligiri, K. P. (2016). Comprehensive Laboratory Evaluation of Thermophysical Properties of Pavement Materials: Effects on Urban Heat Island. *Journal of Materials in Civil Engineering*, 28(7). [https://doi.org/10.1061/\(ASCE\)MT.1943-5533.0001531](https://doi.org/10.1061/(ASCE)MT.1943-5533.0001531)

- Stolz, C. J. (2012). The National Ignition Facility: the path to a carbon-free energy future. *Philosophical Transactions of the Royal Society A: Mathematical, Physical and Engineering Sciences*, 370(1973), 4115–4129. <https://doi.org/10.1098/rsta.2011.0260>
- Straffelini, E., & Tarolli, P. (2023). Climate change-induced aridity is affecting agriculture in Northeast Italy. *Agricultural Systems*, 208, 103647. <https://doi.org/10.1016/j.agry.2023.103647>
- Sturiale, & Scuderi. (2019). The Role of Green Infrastructures in Urban Planning for Climate Change Adaptation. *Climate*, 7(10), 119. <https://doi.org/10.3390/cli7100119>
- Superficie di Comuni Province e Regioni italiane al 9 ottobre 2011*. (n.d.). Italian National Institute of Statistics. Retrieved April 19, 2024, from <https://www.istat.it/it/archivio/156224>
- Susca, T., Zanghirella, F., & Del Fatto, V. (2023). Building integrated vegetation effect on micro-climate conditions for urban heat island adaptation. Lesson learned from Turin and Rome case studies. *Energy and Buildings*, 295, 113233. <https://doi.org/10.1016/j.enbuild.2023.113233>
- Taha, H. (1997). Urban climates and heat islands: albedo, evapotranspiration, and anthropogenic heat. *Energy and Buildings*, 25(2), 99–103. [https://doi.org/10.1016/S0378-7788\(96\)00999-1](https://doi.org/10.1016/S0378-7788(96)00999-1)
- Tan, J., Zheng, Y., Tang, X., Guo, C., Li, L., Song, G., Zhen, X., Yuan, D., Kalkstein, A. J., Li, F., & Chen, H. (2010). The urban heat island and its impact on heat waves and human health in Shanghai. *International Journal of Biometeorology*, 54(1), 75–84. <https://doi.org/10.1007/s00484-009-0256-x>



- Theeuwes, N. E., Steeneveld, G., Ronda, R. J., Heusinkveld, B. G., & Holtslag, A. A. M. (2012). *197: Mitigation of the urban heat island effect using vegetation and water bodies*. <https://api.semanticscholar.org/CorpusID:202690832>
- Torino Turistica - Servizio Telematico Pubblico - Città di Torino. (n.d.). Retrieved April 19, 2024, from <https://web.archive.org/web/20090429121444/http://www.comune.torino.it/canaleturismo/en/clima.htm>
- Tsoka, S., Tsikaloudaki, A., & Theodosiou, T. (2018). Analyzing the ENVI-met microclimate model's performance and assessing cool materials and urban vegetation applications—A review. *Sustainable Cities and Society*, 43, 55–76. <https://doi.org/10.1016/j.scs.2018.08.009>
- Ulpiani, G. (2021). On the linkage between urban heat island and urban pollution island: Three-decade literature review towards a conceptual framework. *The Science of the Total Environment*, 751, 141727. <https://doi.org/10.1016/j.scitotenv.2020.141727>
- Voogt, J. A., & Oke, T. R. (2003). Thermal remote sensing of urban climates. *Remote Sensing of Environment*, 86(3), 370–384. [https://doi.org/10.1016/S0034-4257\(03\)00079-8](https://doi.org/10.1016/S0034-4257(03)00079-8)
- Wang, Y., Long, D., & Li, X. (2023). High-temporal-resolution monitoring of reservoir water storage of the Lancang-Mekong River. *Remote Sensing of Environment*, 292, 113575. <https://doi.org/10.1016/j.rse.2023.113575>
- Weber, C., Aguejidad, R., Briottet, X., Avala, J., Fabre, S., Demuynck, J., Zenou, E., Deville, Y., Karoui, M. S., Benhalouche, F. Z., Gadai, S., Ourghemmi, W., Mallet, C., Bris, A. Le, & Chehata, N. (2018). Hyperspectral Imagery for Environmental Urban Planning. *IGARSS 2018*

- 2018 *IEEE International Geoscience and Remote Sensing Symposium*, 1628–1631.  
<https://doi.org/10.1109/IGARSS.2018.8519085>
- Weng, Q. (2009). Thermal infrared remote sensing for urban climate and environmental studies: Methods, applications, and trends. *ISPRS Journal of Photogrammetry and Remote Sensing*, 64(4), 335–344. <https://doi.org/10.1016/j.isprsjprs.2009.03.007>
- Weng, Q., Lu, D., & Schubring, J. (2004). Estimation of land surface temperature–vegetation abundance relationship for urban heat island studies. *Remote Sensing of Environment*, 89(4), 467–483. <https://doi.org/10.1016/j.rse.2003.11.005>
- Wong, N. H., Tan, C. L., Kolokotsa, D. D., & Takebayashi, H. (2021). Greenery as a mitigation and adaptation strategy to urban heat. *Nature Reviews Earth & Environment*, 2(3), 166–181. <https://doi.org/10.1038/s43017-020-00129-5>
- Xiao, J., Aggarwal, A. K., Duc, N. H., Arya, A., Rage, U. K., & Avtar, R. (2023). A review of remote sensing image spatiotemporal fusion: Challenges, applications and recent trends. *Remote Sensing Applications: Society and Environment*, 32, 101005. <https://doi.org/10.1016/j.rsase.2023.101005>
- Yang, J., Wang, Z.-H., & Kaloush, K. E. (2015). Environmental impacts of reflective materials: Is high albedo a ‘silver bullet’ for mitigating urban heat island? *Renewable and Sustainable Energy Reviews*, 47, 830–843. <https://doi.org/10.1016/j.rser.2015.03.092>
- Yaoyu Lin, Jingjing Dong, & Yu Ding. (2009a). RS and urban heat island: From ecological health to public health on the application of remote sensing technique to healthy urban design in the course of sustainable urbanization. *2009 Joint Urban Remote Sensing Event*, 1–6. <https://doi.org/10.1109/URS.2009.5137706>

- Yaoyu Lin, Jingjing Dong, & Yu Ding. (2009b). RS and urban heat island: From ecological health to public health on the application of remote sensing technique to healthy urban design in the course of sustainable urbanization. *2009 Joint Urban Remote Sensing Event*, 1–6. <https://doi.org/10.1109/URS.2009.5137706>
- Zhang, Y., Jiang, P., Zhang, H., & Cheng, P. (2018). Study on Urban Heat Island Intensity Level Identification Based on an Improved Restricted Boltzmann Machine. *International Journal of Environmental Research and Public Health*, 15(2), 186. <https://doi.org/10.3390/ijerph15020186>
- Zhao, L., Oppenheimer, M., Zhu, Q., Baldwin, J. W., Ebi, K. L., Bou-Zeid, E., Guan, K., & Liu, X. (2018). Interactions between urban heat islands and heat waves. *Environmental Research Letters*, 13(3), 034003. <https://doi.org/10.1088/1748-9326/aa9f73>
- Zhou, D., Xiao, J., Bonafoni, S., Berger, C., Deilami, K., Zhou, Y., Frolking, S., Yao, R., Qiao, Z., & Sobrino, J. (2018). Satellite Remote Sensing of Surface Urban Heat Islands: Progress, Challenges, and Perspectives. *Remote Sensing*, 11(1), 48. <https://doi.org/10.3390/rs11010048>
- Zhou, Q. (2023). Application of Remote Sensing Technologies in Environmental Monitoring and Geological Surveys. *Applied and Computational Engineering*, 3(1), 178–185. <https://doi.org/10.54254/2755-2721/3/20230403>
- Ziaemehr, B., Jandaghian, Z., Ge, H., Lacasse, M., & Moore, T. (2023). Increasing Solar Reflectivity of Building Envelope Materials to Mitigate Urban Heat Islands: State-of-the-Art Review. *Buildings*, 13(11), 2868. <https://doi.org/10.3390/buildings13112868>

